Synthesis and characterisation of organic-inorganic hybrid block copolymers of polydimethylsiloxane and polystyrene

by

Gareth Michael Bayley

Thesis presented in partial fulfilment of the requirements for the degree of Master of Science at the University of Stellenbosch

Study leader

Dr. PE Mallon

Stellenbosch

March 2007

I, the undersigned, hereby declare that the work contained in this thesis is my own original work and that I have not previously in its entirety or in part submitted it at any university for a degree.

Signature:…………….
Date:…………………..

Abstract

Hybrid A-B type block copolymers of polydimethylsiloxane (PDMS) and polystyrene (PS) were synthesised. Three different synthetic routes, which allowed control over polymer structure, were chosen to synthesise these block copolymers. The first technique, coupling of functional prepolymers, involved using anionic polymerisation to produce PDMS and PS functional prepolymers of controlled structure. These prepolymers were functionalised with either silane or allyl functionality and then coupled using a hydrosilylation reaction with Karstetds platinum catalyst. This technique was the least efficient in block synthesis due to the incompatibility of the disparate prepolymers. The second technique under study, sequential anionic polymerisation, gave excellent block copolymer formation with good control over the chain architecture. The final technique employed atom transfer radical polymerisation (ATRP) of styrene using a bromoisobutyrate functionalised PDMS macroinitiator. Silane functional PDMS molecules underwent a hydrosilylation reaction with allyl-2-bromo-2-methyl-propionate to produce the bromoisobutyrate functionalised polymer in excellent yields. Subsequent ATRP with styrene allowed the successful synthesis of block copolymers of controlled structure. Chromatographic systems that allowed liquid chromatography at the critical conditions (LC-CC) of PS and gradient elution chromatography (GEC) of the products were developed. GEC was used successfully in the monitoring of the presence and removal of PDMS homopolymer present in the block copolymer products. LC-CC at the critical point of PS allowed successful chromatographic separation of PS homopolymer from the block material, as well as, the molecular weight distribution of the block material according to the segmental length of the PDMS component. LC-CC coupled to FT-IR using a LC-transform device allowed successful characterisation of the block copolymer chemical composition. Corona treatment was used to modify the surface structure of the block copolymer films. Optical microscopy and slow positron beam studies highlighted the formation of a thin silica like layer on the surface of the films after corona. The positron studies enabled determination of the silica like layer's thickness. Contact angle studies provided the first evidence of hydrophobic loss and recovery for these PDMS containing hybrid polymer materials after corona treatment. A novel offline coupling technique was developed between LC-CC separation and transmission electron microscopy (TEM) analysis. This allowed easy sample preparation without the difficult bulk extraction procedures needed to remove homo-PS contaminants from the block copolymer. This technique also provided morphological information as a function of PDMS segmental length.

Opsomming

Hibried A-B tipe blok kopolimere van polydimetielsiloksaan (PDMS) en polystireen (PS) is gesintetiseer. Drie verskillende sintese roetes is gevolg ten einde blok kopolimere van die verlangde struktuur te verkry. Die eerste tegniek behels die vervaardiging van PDMS en PS pre-polimere deur middel van anioniese polimerisasie. In die volgende stap is die betrokke pre-polimere gefunksionaliseer met 'of silaan 'of alliel groepe en daarvolgens gekoppel deur middel van 'n hidrosililasie reaksie met 'n Karstetd platinum katalis. Blok sintese deur middel van hierdie tegniek was die minste doeltreffend as gevolg van die onmengbaarheid van die afsonderlike pre-polimere. Die tweede tegniek, agtereenvolgende anioniese polimerisasie het goeie blok kopolimeer formasie getoon met uitstekende beheer oor kettingargitektuur. Die finale tegniek, het atoom oordrag radikaal polimerisasie (AORP) van stireen met 'n bromo-isobutiraat gefunksionaliseerde PDMS makro-inisieerder behels. Silaan-gefunksioneerde PDMS molekules het 'n hidrosililasie reaksie met alliel-2-bromo-2-metiel-propionaat ondergaan ten einde 'n uitstekende opbrengs van die bromo-isobutiraat gefunksioneerde polimeer te lewer. Daaropvolgende AORP met stireen het die suksesvolle sintese van blok kopolimere met gekontroleerde struktuur gelewer. Vloeistof chromatografie by die kritiese kondisies (VC-KK) van PS en gradiënt-vloeistof chromatografie (GVC) is geoptimiseer ten einde die gesintetiseerde kopolimere te analiseer. GVC kon suksesvol aandui hoe PDMS homopolimeer uit die blok kopolimeer produkte verwyder is. VC-KK by die kritiese punt van PS kon PS homopolimeer suksesvol skei van die blok kopolimere, en terselfdertyd die molekulere massa verspreiding van die PDMS segmente lewer. VC-KK gekoppel aan fourier transform infrarooispektroskopie deur middel van 'n VC-transform tussenfase, is aangewend ten einde die chemise samestelling van die blok kopolimeer te bepaal. Die oppervlak struktuur van films van die kopolimere is gemodifiseer deur middel van corona behandeling. Optiese mikroskopie en stadige positroonstraal studies het die formasie van 'n dun silica-tipe laag op die films uitgewys na corona behandeling. Die dikte van die silica-tipe lagie is bepaal deur middel van positroon studies. Kontakhoek eksperimente het die eerste bewyse van hidrofobiese verlies en herwinning van hierdie PDMS bevattende hibried polimer materiale na corona behandeling bevestig. 'n Innoverende koppelingstegniek tussen VC-KK en transmissie elektronmikroskopie (TEM) is ontwikkel ten einde monster voorbereiding te vergemaklik, aangesien moeilike ekstraksieprosedures gewoonlik benodig word om homo-PS onsuiwerhede vanuit die blok kopolimere te verwyder. Hierdie tegniek het ook waardevolle morfologiese informasie van die blok kopolimere verskaf as 'n funksie van PDMS segment lengte.

Dedicated to my parents

Acknowledgements

List of Contents

Chapter 3: Experimental 46

Chapter 4: Results and discussion

Glossary

Notations

$[I]_0$	Initial initiator concentration
$[M]$	Monomer concentration
$[M^-]$	Active propagating anion concentration
$[M]_0$	Initial monomer concentration
χ	Flory-Huggins parameter
δ	Chemical shift in NMR
ΔH	Change in enthalpy
DP_n	Degree of polymerisation
E_+	Incident energy
f	Volume fraction segment A
H	Height
k_{act}	Activation rate constant
k_{deact}	Deactivation rate constant
K_{ex}	Equilibrium constant
K_{lac}	Distribution coefficient for LAC
k_p	Propagation constant
k_p^{app}	Apparent propagation rate constant
K_{sec}	Distribution coefficient for SEC
k_t	Termination rate constant
M	Metal counterion
M^*	Active monomer at the end of a growing chain
M_n	Number average molecular weight
m_t^n	Metal catalyst in ATRP
m_t^{n+1}	Metal catalyst in ATRP after oxidation
M_w	Weight average molecular weight
N	Overall degree of polymerisation
n	Chain architectural constraints
P_m	Active propagating radical species
P_n	Active propagating radical species
θ	Contact angle
R	Radius
r	Density
R_p	Rate of propagation

S	S parameter
TΔS	Entropy
V_i	Interstitial volume
V_p	Pore volume
V_R	Retention volume
V_{stat}	Stationary phase volume
Z	Depth penetration

Abbreviations

AFM	Atomic force microscopy
AIBN	Azobisisobutyronitrile
ATRP	Atom transfer radical polymerisation
ATRP #	ATRP reaction code
BP	Benzophenone
BPO	Benzoyl peroxide
BuLi	Butyllithium
CCD	Chemical composition distribution
CDMS	Chlorodimethylsilane
CuCl	Copper(I) chloride
D_3	Hexamethylcyclotrisiloxane
D_4	Octamethyltetrasiloxane
dNbipy	4,4'-di-(5-nonyl)-2,2'-bipyridine
DRI	Differential refractive index
ELSD	Evaporative light scattering detector
FTIR	Fourier transform infra-red
GEC	Gradient elution chromatography
homo-PDMS	Polydimethylsiloxane homopolymer
homo-PS	Polystyrene homopolymer
HS #	Hydrosilylation reaction code
KOH	Potassium hydroxide
LAC	Liquid adsorption chromatography
LC-CAP	Liquid chromatography at critical adsorption point
LC-CC	Liquid chromatography at critical conditions
LC-LCA	Liquid chromatography under limiting conditions of adsorption
LC-LCD	Liquid chromatography under limiting conditions of desorption
LiCl	Lithium chloride salt
LS #	Sequential anionic reaction code

MENQ	2-Methyl-1,4-naphthoquinone
MeOH	Methanol
$MgSO_4$	Magnesium Sulphate
MMA	Methyl methacrylate
MMP-PDMS	mono methacryloxy propyl terminal PDMS
MW	Molecular weight
N_2	Nitrogen
NMP	Nitroxide mediated polymerisation
NMR	Nuclear magnetic resonance
NP	Normal phase column
Nu	Nucleophile
OBDD	Ordered bicontinuous double diamond
PDI	Polydispersity index
PDMS	Polydimethylsiloxane
PI	Polyisoprene
PMMA	Polymethylmethacrylate
PstLi	Polystyrillithium anion
RAFT	Reversible addition fragmentation chain transfer polymerisation
RI	Refractive index
RP	Reversed phase column
RT	Room temperature
SAXS	Small angle X-ray scattering
SEC	Size exclusion chromatography
SEM	Scanning electron microscopy
SSIP	Solvent separated ion pairs
SSL	Strong segregation limit
Sty	Styrene
TEM	Transmission electron microscopy
TEMPO	2,2,6,6-teteramethylpiperidinyl-1-oxy
THF	Tetrahydrofuran
TPEN	N,N,N',N'-tetrakis (2-pyridylmethyl) - ethylenediamine
URP	Conventional/uncontrolled radical polymerisation
UV	Ultra violet
v/v	Volume/volume
v/w	Volume/weight
VD_2	2-vinyl-2,4,4,6,6-pentamethylcyclotrisiloxane
WSL	Weak segregation limit
X	Halogen

List of Figures

Chapter 2

Chapter 3

Chapter 4

List of Schemes

Chapter 2

Chapter 3

Chapter 4

List of Tables

Chapter 2

Chapter 4

-1-

Chapter 1

General introduction and objectives

This chapter gives a brief introduction to the field of hybrid materials with regards to synthesis, characterisation and applications. A list of the objectives of this study is also presented.

1.1   General introduction

Hybrid materials are gaining interest in the scientific world owing to their ability to combine the properties of their disparate components. For example the hybrid polymers under study in this project, namely, polydimethylsiloxane-block-polystyrene (PDMS-b-PS) copolymers have hugely dissimilar physical properties. At room temperature PDMS is a viscous liquid, even at high molecular weight, while PS is a brittle and glassy material. In the polymer field typical hybrid materials consist of organic and inorganic segments. These segments can be joined to give a wide variety of different architectural structures, namely, block copolymers (di-blocks and tri-blocks), star copolymers, mikto-arm star block copolymers and graft copolymers. In creating such complex molecular architectures, polymerisation reactions that allow control over these factors need to be utilised. These techniques range from anionic polymerisation[1], the first living polymerisation technique, to the more recently developed controlled radical polymerisation techniques. These include such techniques as atom transfer radical polymerisation (ATRP)[2], reversible addition fragmentation chain transfer (RAFT)[3] polymerisation and nitroxide mediated polymerisation (NMP)[4]. Without these polymerisation techniques at our disposal synthesis of complex polymers with controlled structure would not be possible.

In recent years a field that has grabbed the attention of the scientific community is that of nanotechnology. Advancing technology is leading to the development of smaller and more efficient devices especially in the electronics world. Hybrid copolymers are finding a niche in this field. PDMS containing hybrids have been widely studied due to the selective etching capabilities this material affords. PDMS-PS copolymers, under study in this project, are known to form nano phase segregated morphologies, due to the incompatibility of the two materials. By controlling the structure of the block copolymer segments, it is possible to control theses phase segregated morphologies on a nano-scale.

When it comes to analysis, complex polymers call for advanced analytical techniques. Chromatography has been used as a primary technique to study and characterise polymeric materials for many years[5]. Advances in this field have lead to gradient elution chromatography and the development of liquid chromatography at critical conditions. These techniques allow characterisation of the chemical composition distribution of complex polymers. When coupled to other analytical techniques such as Fourier transform infrared (FT-IR), atomic force microscopy (AFM), nuclear magnetic resonance (NMR) and differential scanning calorimetry (DSC) it is possible to gain a wealth of information.

1.2   Objectives

The main objectives of this research endeavour were as follows.

- The evaluation of three different synthetic methods to prepare block copolymers of PDMS and PS.
  - Evaluation of the hydrosilylation coupling method using allyl and silane functional prepolymer of PDMS and PS together with Karstedts platinum catalyst.
  - Evaluation of sequential anionic polymerisation to synthesise block copolymers of PDMS and PS
  - Evaluation of PDMS the macroinitiator technique for the ATRP of styrene to synthesise PDMS block PS copolymers.
- Development of a chromatographic system that allows LC-CC analysis at the critical point of PS for CCD distribution analysis.
- Development of a GEC profile to allow monitoring of the presence and removal of PDMS homopolymer
- Evaluation of PDMS surface segregation studies before and after corona modification using various analytical techniques.
- Evaluation of the surface modification after corona treatment using the slow positron beam.
- The development of a novel analytical technique to study the morphological features of PDMS-b-PS block copolymers.

1.3   References

(1)   Szwarc, M., Levy, M., Milkovich, R. *J. Am. Chem. Soc.* **1956**, *78*, 2656-2657.

(2)   Greszta, D., Mardare, D., Matyjaszewski, K. *Macromolecules* **1994**, *27*, 638-644.

(3)   Chiefari, J., Chong, Y.K., Ercole, F., Krstina, J., Jeffery, J., Le, T.P.T., Mayadunne, R.T.A., Meijs, G.F., Moad, C.L., Moad, G., Rizzardo, E., Thang, S.H. *Macromolecules* **1998**, *31*, 5559-5562.

(4)   George, M. K., Veregin, R.P.N., Kazmaier, P.M., Hamer, G.K. *Macromolecules* **1993**, *26*, 2987-2988.

(5)   Pasch, H. *Chapter 1: Introduction*. In: Pasch, H., Trathnigg, B. editors, *HPLC of Polymers*; Springer-Verlag: Berlin, 1998.

Chapter 2

Historical and literature review

This chapter gives a general overview of the block copolymers synthesised and characterised in this project. Emphasis is placed on the synthetic techniques, morphological investigations and chromatographic fractionation used to prepare and study this block copolymer.

_____

2.1   Hybrid materials

Hybrid materials are gaining importance in modern day applications. This is because many scientists are investigating new ways of synthesising high performance materials from existing monomers and materials[1]. Hybrid polymers are polymer chains that consist of organic and inorganic segments.

2.1.1   General overview

The synthesis of organic/inorganic hybrid materials is an area of growing interest as the useful properties of disparate components can be combined into a single material. The fact that the inorganic polymers have totally different properties to their organic counterparts, lends these materials interesting properties. The opposing properties of most hybrid materials lead to block immiscibility within the material substrate. This leads to the formation of nanophase segregated morphologies[1-3]. One can also control these morphologies to a certain extent using "living" anionic polymerisation methods to produce these block copolymers. A review by Matyjaszewski *et al.*[1] covered the synthesis of hybrid materials with varying chain architectures. Polydimethylsiloxane-block-polystyrene copolymers (PDMS-b-PS), where synthesised and studied in this project. The distinctly different properties of the constituent groups lead to microphase segregated morphologies. The first major difference between the two materials is their glass transition temperatures (Tg). PS, with a Tg of 100°C, is a glassy brittle material at room temperature. PDMS, with a Tg of -127°C, is in fact a viscous liquid at room temperature, even at high molecular weights. The difference in surface energy also plays a dominating role, where PDMS preferentially surface segregates. PDMS also has interesting properties when exposed to corona discharges as shown in work by Mallon *et al.*[4] with the formation of a nano thick glass-like layer. Combining these distinct materials allows the synthesis of complex materials with very interesting properties and possible applications. A brief overview of the possible applications of general hybrid materials and the hybrid material under study will be discussed in the following section.

2.1.2   PDMS block copolymers and possible applications

Much of the research today in polymer hybrid materials is focused on using hybrid polymers to produce new materials used in the electronics industry. Ro and co-

_____

workers[2] studied hybrids of polysilsesquioxanes (PSSQs) and polymethylmethacrylate (PMMA) to make low dielectric constant (low-k) thin films, to reduce the interconnect delay times in next-generation microelectronic devices. The idea is to incorporate air, by removing the PMMA inclusions in the material. Utilisation of the mesomorphic porous structures derived from selective etching of the polydimethylsiloxane blocks also lend applications to electronic templating, special dielectric materials, catalyst substrates, nanoreactors and microfiltration membranes[5]. Work done by Ndoni *et al.*[5] studied the removal of PDMS segments via a reaction with excess hydrogen fluoride. Results indicated successful removal of PDMS segments and the preparation of bulk nanoporous material. The field of membranes is another possible application of these block-copolymers. Miyata *et al.*[6] studied the permselectivity of PDMS-b-PMMA membrane films in relation to their fractal microphase separation. Raising PDMS content increased ethanol permeation by lowering the fractal dimensions of the PDMS components. The effect of annealing these films was also studied, and the results indicated that the annealing produced a smoother interface between the PDMS and PMMA phases lowering interfacial free energy. A review by Barton and co-workers[7] studied various porous materials made from hybrid materials and their adsorption properties. Han *et al.*[8] produced materials with superhydrophobic properties using block copolymers of polybutylacrylate (PBA) and PDMS to form micelles stabilised by silica nano-particles. These are just a few of the possible applications afforded by hybrid materials, mainly related to electronics, filtration and adsorption.

As can be seen, there is a wide spectrum of possible applications for these specialised materials. Before one can study these applications, however, the materials have to be synthesised. The synthesis of polymers with complex architectures and compositions require synthetic routes that allow control over these parameters. The following section focuses on the theory behind these techniques.

_____

2.2   Polymerisation techniques

There are various ways to synthesise block copolymers. A few of the different techniques will be discussed in the following section of work. A few of these techniques, including the methods used to produce the polymers in this study, involve anionic polymerisation. It is thus essential that we take a look at this technique itself, before moving on and explaining how it can be used to prepare block copolymers.

2.2.1   Anionic polymerisation

The first paper on anionic polymerisation was published in 1956 by Michael Szwarc[9], entitled, "Polymerisation initiated by electron transfer to monomer, a new method of formation of block polymers". This revolutionary discovery facilitated the synthesis of materials of controlled structure, chain morphology and architecture[10]. This breakthrough has recently been celebrated in a series of review articles based on Szwarc's contribution to the field of controlled "living" polymerisation[10-13]. Anionic polymerisation is a reaction, where the propagating species or active end-group of the growing polymer chain is an anion[14]. Monomers susceptible to anionic polymerization can be divided into two main classes, namely, the vinyl (olefin) type monomers and the cyclic monomers. The vast majority of the olefin monomers have groups that can stabilise the anion at the propagating centre of the growing chain[14,15]. These groups tend to be electron withdrawing and a few examples are given below in scheme 2.1. The combinations of certain initiators and solvent systems with specific monomers are very important in this polymerisation technique. Detailed information on these different systems is reviewed in work by Morton[14].
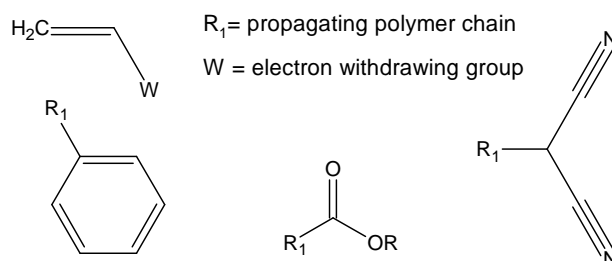
Scheme 2.1 Examples of possible olefin substituent groups able to stabilise anions.

_____

The propagating species can be stabilised by the inductive effect of the group or by the delocalisation of charge, which is illustrated in scheme 2.2. The aromatic ring of the styrene monomer and its ability to delocalise the anion and spread the charge over the entire ring makes this monomer highly suited to anionic polymerisation.
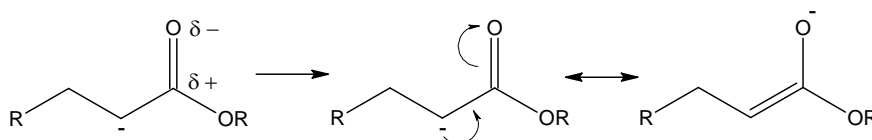
Scheme 2.2   Resonance stabilisation of the carbanion propagating species by charge delocalisation.

The presence of polar substituents on the olefin monomers lead to problems involving the carbanionic reactivity towards these polar groups, causing unwanted side reactions[14]. This is illustrated in the scheme 2.3 below, where we have a chlorine atom as substituent. It seems to be a good choice at first due to the electron withdrawing capability of the chlorine, which can stabilise the anion, but we see undesirable side reactions occurring. That is why halogenated monomers tend to be polymerised free radically.
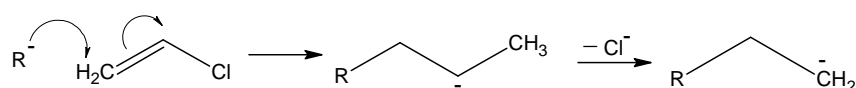
Scheme 2.3   Unwanted side reaction when using halogenated monomers.

We also see problems with methyl methacrylate (MMA). This widely used monomer is more reactive than styrene due to the stabilising effect of the polar group on the anion, however, the polar substituents are more reactive to nucleophiles and we get termination and side reactions occurring[15]. The anionic polymerisation of MMA was studied in an extensive review by Vlcek *et al*[16]. In scheme 2.4 one can see what happens upon attack of initiator to monomer. The formation of cyclics due to backbiting is also a problem. The alkyl-lithium is converted to a less reactive alkoxide initiator and the MMA monomer is converted to isopropenyl alkyl ketone[15,16].

_____
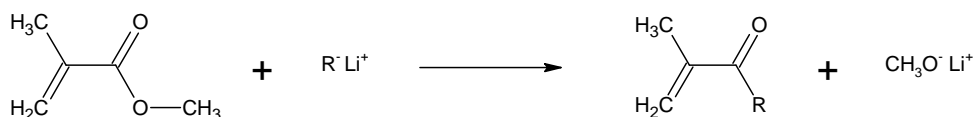
Scheme 2.4   Anionic side reaction of a typical polar monomer, MMA.

The new carbanion is not as reactive as the MMA resulting in a slower polymerisation rate and the resulting polymerisation is also a copolymerisation of the two monomers. Minimising these side reactions involve temperature and solvent control as well as addition of ligands to modify the anionic initiators. Ligand modified initiators studied in the review by Vlcek *et al.*[16] included alkali metal halides, bidentate lithium alkoxides, alkylaluminiums and alkali metal ester enolates.

2.2.1.1   Initiation

Before chain propagation the anion must first be generated by some initiation step. This can be achieved using highly electropositive elements such as the alkaline metals[14,17]. Lithium alkyls are widely used as initiating agents[15,16,18-22]. These reagents also have the advantage of being commercially available and soluble in hydrocarbons. This is very important as solvents suitable for anionic polymerisation are restricted to hydrocarbons and ethers. Other solvents (halogenated, ketones, aldehydes, alcohols) tend to react with the propagating species[15]. Solvents with easily removable protons should also be avoided. The general initiation step can be seen in scheme 2.5, where Nu is the nucleophile (eg: anionically charged alkyl) and M is the associated metal counterion (eg: lithium cation).
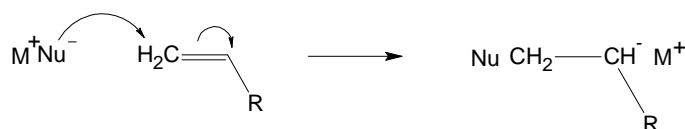
Scheme 2.5   Initiation step for anionic polymerisation of olefin using a lithium- alkyl as initiator.

Depending on the reactivity of the monomer we can vary the strength of the initiator. This means that the more stable the monomer propagating center system the weaker the initiator may be[15]. An example is vinylidine cyanide, which may be initiated by water, which is a very weak base[14].

_____

The initiation of cyclic monomers can differ from that of olefinic monomers in some cases, however, with hexamethylcyclotrisiloxane (D_3) to produce PDMS it appears to be the same. Initiation is also achieved by electron transfer to the silicon atom[14,15], opening of the ring and formation of a silanolate anion which is illustrated in scheme 2.6.
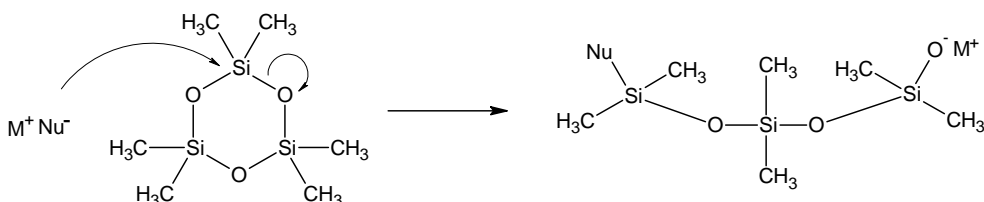
Scheme 2.6   The anionic ring opening initiation of D_3 cyclic monomer to produce PDMS

It must also be noted that ring strain plays an important role. Comparing octamethyltetrasiloxane (D_4) to D_3[18], we see that the latter is more reactive due to the presence of ring strain. The free energy of the linear polymer is similar to that of the cyclic monomer in the case of D_4.

Initiation can be complicated by the aggregation of initiators[14,15,17] in the solvent, leading to a decrease in active initiator concentration. These aggregates tend to form in non-polar solvents, owing to lower solvent interactions. They can, however, also form in polar solvents such as tetrahydrofurane (THF). The lithium atoms tend to aggregate[14,15] in the centre, while the alkyl groups surround them to form a reversed micelle like structure. We can also get dimerisation[14] of the initiator molecules which is illustrated in scheme 2.7.
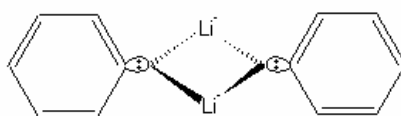
Scheme 2.7   Dimerisation at low temperatures leads to inactive initiator.

_____

2.2.1.2 Propagation

The anionic active centre formed in the initiation step is a strong base in itself, and can incorporate further monomer by nucleophyllic attack as illustrated in the following mechanism in scheme 2.8. The chain propagates further as more monomers are attacked and added to the growing chain.
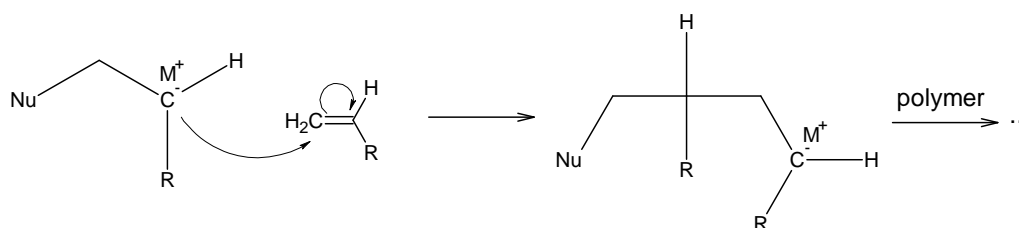
Scheme 2.8 Propagation mechanism for anionic polymerisation with counterion.

The rate of propagation in polar solvents where the initiation rate is higher than propagation rate is shown in equation 2.1[15], where [M] is the monomer concentration, [M⁻] is the total concentration of anionic propagating centres and k_p^{app} is the apparent propagation rate constant.

$$R_p = k_p^{app}[M^-][M] \qquad\qquad 2.1$$

The reason for the much higher polymerisation rates in anionic methods as opposed to free radical methods, is owing to the higher concentration of propagating species [M⁻] and the lack of termination reactions[15]. It must be noted that the metal cation of the initiator is always associated with the anionic active end-group. This association is very important as it regulates polymerisation rate, as well as affecting undesirable side reactions. If the association between anion and metal counterion is too strong, the counter ion will block further monomer from adding to the growing chain end[14]. If the counterion is too loosely associated with the anion, we can get adverse side reactions occurring, such as various transfer reactions[14]. There is always a mixture of free or solvent separated ion pair (SSIP) active centres and contact ion pairs. Both contribute to propagation, but the SSIP's are far more reactive and a small increase in their relative concentrations causes a large increase in propagation rates[11]. Scheme 2.9, shows the different ion pair associations using an alkyl-lithium as example. The aim is to have a SSIP, where the solvent molecules insert themselves between the anion active centre and its' counterion. This enables monomer to add

_____

more easily to the growing chain end, thus increasing activity and decreasing the time to full conversion of the monomer.
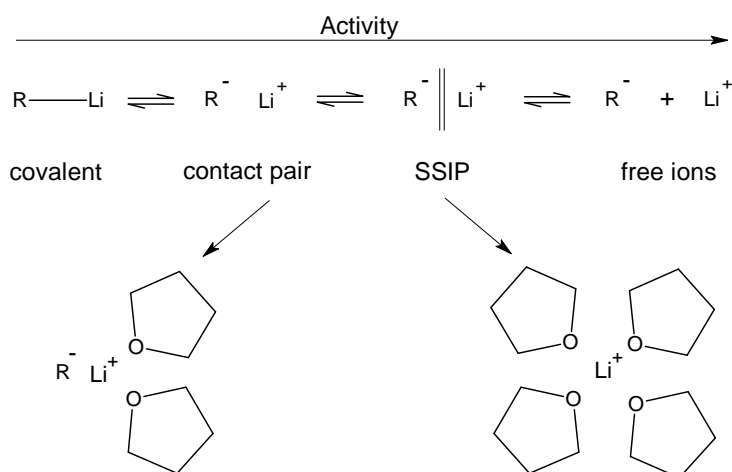
Scheme 2.9 Possible ion pair associations with alkyl-lithium initiators in THF.

In the book by Odian[15] as well as the review by Smid *et al.*[11] there is a comprehensive evaluation of the propagation rate constants for free living anions and anion-counterion pairs. The nature of the counterion also plays a role in the propagation rate. In polar solvents (eg: THF), there is an increase in free ion concentration as we move in the following series: $Cs^+ < Rb^+ < K^+ < Na^+ < Li^+$. This is because the smaller Li^+ anions are solvated more easily than the larger Cs^+ counterparts[11,15]. Further, when we move to non-polar solvents where the solvation effect does not play a role we have a different phenomenon occurring. There is a reverse in the series with an increased activity as follows: $Cs^+ > Rb^+ > K^+ > Na^+ > Li^+$. The propagation activity is now dependant on the species with the weakest bond between the anion and counterion, not solvation power[11,15]. The larger the counterion the weaker the bond, although this effect levels off as we reach K^+, Rb^+ and Cs^+.

Interesting work by Verheyden *et al.*[23] studied the effect of lithium chloride (LiCl) on the polymerisation rate of a styrene polymerisation. It was shown that when the polystyryllithium (PstLi) anion (active anion centre) was present in low concentration in THF solvent, the LiCl reduced the rate of propagation. At higher concentrations of PstLi, however, the presence of LiCl increased the rate of propagation. This phenomenon was due to a common ion effect between the Li^+ ions of the PstLi and the LiCl salt.

_____

Owing to the lack (limited number) of side reactions, one can easily manipulate the degree of polymerisation by varying the ratio of initiator to monomer concentration. In the case of alkyl-lithium initiators, where we have initiation by addition, each initiator molecule initiates the growth of a polymer chain[11,14,15]. Thus we can calculate the degree of polymerisation by dividing the concentration of monomer before reaction $[M]_0$ by the concentration of initiator $[I]_0$ at time zero, as shown in equation 2.2. In the case of initiation by electron transfer we have two polymer chains growing from one initiator and the degree of polymerisation changes to that shown in equation 2.3.

$$DP_n = [M]_o/[I]_o \qquad\qquad 2.2$$

$$DP_n = 2[M]_o/[I]_o \qquad\qquad 2.3$$

If the rate of chain initiation is rapid compared to that of chain propagation, we have a situation, where all the chains start growing at roughly the same time. This means that they will tend to add monomer equally, giving us a small distribution of chain lengths. A measure of this broadness, the polydispersity index (PDI) of the molecules, can be calculated from equation 2.4, where PDI is equal to the weighted average molecular weight (M_w) divided by the number average molecular weight (M_n).

$$PDI = M_w/M_n = 1 + 1/M_n \qquad\qquad 2.4$$

2.2.1.3 Termination

Finally we get to the termination step. This is where the most useful property of anionic polymerisation comes to light. There are no inherent chemical termination steps. Anionic polymerisation is a living system, even after all the monomer has been consumed, the chain end anions still remain active. This enables one to grow the chain further by adding more monomer, or even create blocks by adding other suitable monomer. It is extremely important to work as cleanly as possible, under moisture and oxygen free environments to achieve an anionic living system. Presence of contaminants is detrimental to the activity of this system. Due to the living nature of this polymerisation technique, all the chains should be of similar length (low PDI) and all the chains should have active anionic end-groups (vast

_____

majority). This enables facile routes to end-group functionalisation of the synthesised polymer chains.

Functionally terminated polymers are valuable intermediates. This is especially true in the area of combining anionic polymerisation with controlled radical techniques. The living nature of anionic polymerisation can be used to prepare blocks[19-21,24], couple with other chemical species enabling further reactions[24,25] and graft copolymerisation[26,27] among others. A recent review by Yagci and Tasdelen[13] highlights some of the techniques combining terminated anionically synthesised chains with another form of polymerisation. Morgan et al.[28] created PDMS-PS blocks by terminating the anionically grown PDMS with an alkoxyamine to form a 2,2,6,6-teteramethylpiperidinyl-1-oxy (TEMPO) functionalised macro-initiator. Nitroxide mediated radical polymerisation (NMP) was then used in the controlled synthesis of the PS segment. Similar work by Yoshida and Tanimoto[29] also used NMP to synthesise the PS block, but a macroazoinitiator was used. Lu et al.[30] synthesised novel block copolymers of ethylene oxide and 4-vinyl pyridine using anionic ring opening polymerisation terminated with TEMPO and then growing the 4-vinyl pyridine segment using NMP. Matyjaszewski, Miller and Pyun[24,25] have combined anionic polymerisation with atom transfer radical polymerisation (ATRP) to synthesise block copolymers. Terminating the anionically grown segment with a functional halide to create the macroinitiator is the first step in this technique. A similar method was used in this project and is discussed in more detail later. Another controlled technique combined with anionic polymerisation is reversible addition chain transfer polymerisation (RAFT). Pyun and Matyjaszewski[24] show how terminating the anionically grown segment with thioester functionality allows controlled polymerisation of a subsequent segment using RAFT. As mentioned the synthesis of graft copolymers also utilises the combination of anionic polymerisation and other controlled radical techniques. Work by Shinoda et al.[31] compared grafting reactions using uncontrolled radical polymerisation, ATRP controlled polymerisation and RAFT controlled polymerisation. In this case the PDMS was terminated with a methacrylate moiety. They were then copolymerised with MMA to prepare chains with MMA backbones and PDMS pendant chains. The uncontrolled polymerisation gave randomly distributed pendant chains, RAFT gave gradient distribution of the chains and ATRP gave uniform distribution of the PDMS pendant chains. Further reactions include the synthesis of star and miktoarm-star block polymers. Zhao et al.[32] combined anionic ring opening polymerisation with ATRP to synthesise "dendrimer-

_____

like" star block copolymers. These are just a few of the synthetic possibilities afforded by anionic polymerisation combined with controlled polymerisation. These examples, however, emphasise the usefulness of being able to terminate a polymerisation with functionality to a high degree. The controlled radical polymerisations mentioned previously (RAFT, NMP and ATRP) will be discussed later in this chapter.

There are of course many different ways to deactivate the living chains with suitable functionality, and the deactivator used depends on the desired end functionality, required functionalisation efficiency and reaction conditions. A few more methods are discussed by Bywater.[17]

2.2.1.4 Summation

In summary, anionic polymerisation techniques present excellent control over polymer structure and functionality. They are relatively fast reactions with limited side reactions and no inherent chemical termination steps, allowing a living system of growing chains. The ability to calculate and synthesise molecules of desired molecular weight by simply varying the ratio of monomer to initiator allows easy access to molecules of controlled length and structure. The ability to end functionalise these living chains also opens up doors to various copolymerisation and grafting reactions that can be used to create molecules of varying chemical compositions, structures and morphologies.

2.2.2 Controlled Polymerisation Techniques

In industry free radical polymerisation is one of the most widely used synthetic routes to producing high molecular weight polymers[15,33]. This is due to the wide variety of monomers that can be polymerised, as well as the fact that water can be used as solvent in many cases. These reactions also tend to be more robust when it comes to the presence of impurities such as oxygen and monomer stabilisers[15,33], however, one of the disadvantages of this technique is the lack of control leading to polymers of uncontrolled molecular weight and broad PDI's[34]. The synthesis of well defined materials with complex architectures is not possible. Therefore it became increasingly important to develop techniques that made controlled free radical polymerisation possible. The main techniques[34] developed to allow controlled radical polymerisation are NMP, RAFT and ATRP. A brief overview of controlled radical polymerisation using the NMP and RAFT processes will be given. A more in depth

_____

look at ATRP will be presented as this technique was employed in this project. Firstly we will discuss some of the fundamental aspects of conventional/uncontrolled radical polymerisation (URP) to better understand the controlled processes.

2.2.2.1   Conventional radical polymerisation

The three major processes of URP are illustrated in scheme 2.10[33,34] below. There are of course other mechanisms involved such as transfer reactions (eg: to solvent, transfer agent, monomer or impurities) [33,34], but that is beyond the scope of this introduction. The main obstacle with free radical polymerisations is the inevitable interaction between the active radical centres, leading to termination via radical coupling or disproportionation[34]. In URP it must be noted that all three processes occur concurrently and polymerisation is extremely fast. That is to say that during initiation chains are propagating and terminating all at once. This process continues so long as there are free radicals in the system. This is achieved by adding an initiator source that decomposes with time. The net result of this is that we have a wide spread of chains of varying molecular weight. High molecular weight chains tend to form early in the reaction and other chains initiated later tend to have lower degrees of polymerisation as the monomer is consumed and reaction rates change[34]. This leads to materials with very high PDI's. As mentioned earlier, this PDI ratio gives the statistical broadness of the molecular weight distribution. The closer to unity this value is the more monodisperse the chain lengths are. The termination and transfer reactions also result in a variety of chain end-groups being present.

Initiation:
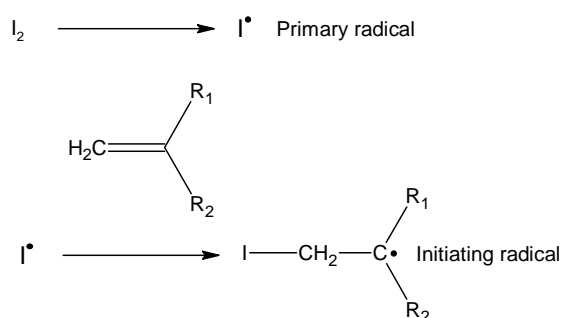
Propagation:

Termination:
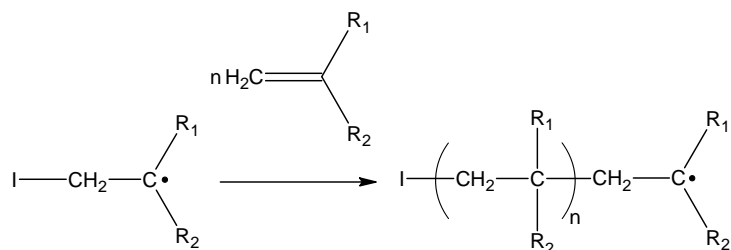
Radical Coupling   Disproportionation
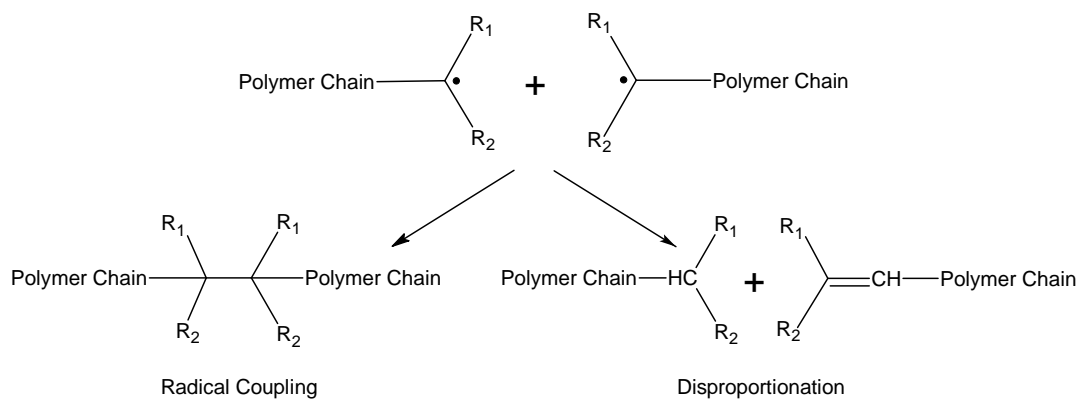
Scheme 2.10   Illustration of the three main processes in URP, namely, initiation, propagation and termination.

2.2.2.2   Reversible addition fragmentation chain transfer (RAFT)

RAFT was first reported in 1998 by Chiefari *et al.*[35], and subsequently patented[36]. The general structure of a RAFT agent is presented in scheme 2.11.
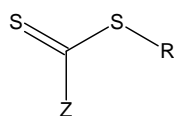
Scheme 2.11 General thiocarbonylthio RAFT agent structure with Z and R groups.

The RAFT agent is named according to the structure of the Z and R groups[37]. Table 2.1 summarises the main classes of RAFT agents according to Z group structure.

Table 2.1   The four main classes of RAFT agents according to Z group structure[37].

Group	Dithioester	Trithiocarbonate	Dithiocarbamate	Xanthate
Z Group	-C-R'	-S-R''	-N-R'''	-O-R''''

_____

Requirements for a good R group, are that it should be a good homolytic leaving group and R• should be able to initiate polymerisation.[37] A good Z group is one that modifies the reactivity of the RAFT moiety to support radical addition.[37] In RAFT, initiation and termination occurs as with URP. As seen in scheme 2.12, for a general thiocarbonylthio RAFT agent, we have an active propagating radical ($Pm^•$) which adds to the thiocarbonylthio compound followed by fragmentation of the intermediate radical to give a new polymeric thiocarbonylthio capped species and an active propagating radical ($Pn^•$). When the propagating radicals are free (uncapped), they can add monomer and grow. When added to the thiocarbonylthio compound (capped) they remain in a dormant state.
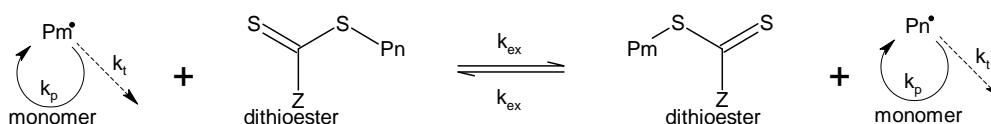
Scheme 2.12   Simplified RAFT mechanism involving dithioester moieties.[37]

Rapid equilibrium between the active propagating radicals and the dormant thiocarbonylthio compounds, allows equal probability for the molecules to grow.[37] This leads to materials with lower PDI's and equivalent end group functionality, as most of the chains retain their thiocarbonylthio "caps" once polymerisation is completed. These functional chains remain stable and can later be used to react with other monomer to prepare di-blocks[38], tri-blocks[39], stars[40] and graft/brush[41] copolymers.

2.2.2.3   Nitroxide mediated polymerisation

Alkoxyamine nitroxides are efficient in the scavenging of carbon centered radicals, which have made them useful as trapping agents in the study of radical initiation mechanisms[33,34]. Early work by Solomon *et al.* in 1982[42] showed the use of 1,1,3,3-tetramethylindolinyl-2-oxy as a trapping agent in the initiator studies of styrene polymerisation. These radical trapping studies led to the development of NMP as a controlled polymerisation technique.

As can be seen in scheme 2.13 this technique follows similar principles to RAFT.

_____
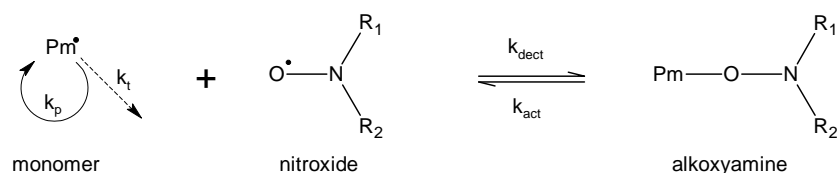
Scheme 2.13 Simplified NMP mechanism using a general nitroxide moiety.

We once again have the radical propagating center ($Pm^\bullet$) which adds monomer and can terminate as with URP. We do, however, have deactivation of the active radical by addition of the nitroxide moiety forming a polymeric alkoxyamine. This deactivation reaction is reversible and we have regeneration of the active radical to add more monomer, hence growing the chain[37,43]. It was not until 1993 when George *et al.*[44] demonstrated the use of 2,2,6,6-tetramethylpiperidinyl-1-oxy (TEMPO) as the stable nitroxide radical in the polymerisation of styrene using benzoyl peroxide (BPO) initiator. This development allowed synthesis of PS of low PDI with a linear increase of conversion with monomer consumption. Since then many different nitroxides have been developed and studied. Effects of substituents on the nitroxide as well as nitroxide ring size have been investigated. The presence of electron donating groups on the nitroxide lowers k_{act}, the reverse is also true[37]. It was also shown as we move from 5 to 6 membered rings k_{act} increases.[37] There are many effects coming into play, but are outside the scope of this brief introduction. Unfortunately, most of these reactions must be performed at high temperatures ($>100^{o}C$) owing to the stability of the C-O bond, to allow for reactivation. A review by Hawker *et al.*[45] takes a look at the progress in NMP. In a recent study by Tang *et al.*[46] a new highly effective and versatile catalyst system was developed, CuBr / N,N,N',N'-tetrakis (2-pyridylmethyl) - ethylenediamine (TPEN), for the polymerisation of acrylic, methacrylic, and styrenic monomers.

2.2.2.4   Atom transfer radical polymerisation

ATRP, developed by Matyjaszewski[47] and Sawamoto[48] in the early 1990's, has become an extensively studied field and only a brief outline will be presented in this section. Similarly to the other controlled radical polymerisation methods, ATRP is based on an equilibrium between a large amount of dormant radical species to a minuscule amount of active/growing radical species. The general scheme is shown in scheme 2.14 and is explained below [15,33,49,50].

_____
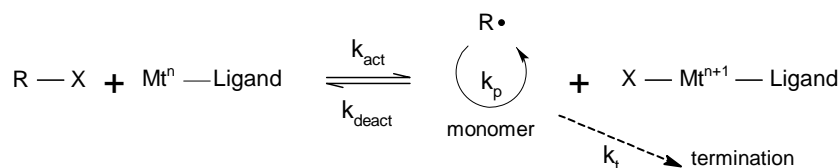
Scheme 2.14   Basic mechanism for ATRP showing dynamic equilibrium between active and dormant species.

In the above diagram X represents a halogen (Br, Cl, I), R is the growing radical chain and Mt^n-Ligand is the transition metal complex which catalyses the reaction. The activation step involves a reversible redox reaction between the polymer endgroup and the metal complex where the metal complex undergoes a one electron oxidation with abstraction of the halogen atom. At this stage the dormant growing radical becomes active and we have addition of these dormant radicals to monomer as with URP. The persistent radical ($X-Mt^{n+1}$-Ligand) ensures a decrease in the steady state concentration of radicals and thus decreases termination. Then in the deactivation process the radicals are trapped by atom transfer (halogen) from the higher oxidation state metal. Termination usually occurs via radical coupling or disproportionation, so by ensuring that the k_{deact} is larger than k_{act} we get a shift in equilibrium to the dormant side, decreasing the amount of active radicals that could terminate. By rapidly deactivating the active radical, we limit the ability to terminate with neighbouring radicals. Another important factor is that the initiation should be fast so that all chains start growing simultaneously. Through this fast initiation and rapid deactivation process we have uniform growth of the polymer chains as well as a small contribution of terminated species. In the initial stages of polymerisation (up to 5% conversion) we do find termination occurring, until the concentration of the deactivator or persistent radical ($X-Mt^{n+1}$-Ligand) is large enough to suppress normal termination.

There are many important factors when developing an ATRP system and these include monomers, initiators, catalysts, solvents, additives, temperature and reaction time. These factors have been extensively studied and published in books[15,33] and reviews[51], only a brief outline of these factors will be discussed, with close reference to the reagents used in this project.

(i) *Initiators*

These are typically alkyl halides (R-X) where the halide group (X) must be able to migrate between the growing chain and the transition metal complex rapidly and

_____

selectively. It is also found that tertiary alkyl halides are more active than secondary alkyl halides which are more active than primary alkyl halides.[33] Bromine and chlorine tend to give excellent control. Iodine is used less extensively, but has been found to work in controlled polymerisation of styrene in ruthenium- and rhenium-based ATRP.[52] Fluorine is not used because the C-F bond is too strong to undergo homolytic cleavage. A tertiary halide (bromoisobutyrate) macroinitiator was used in this project as shown in scheme 2.15, where R represents the polymer chain.
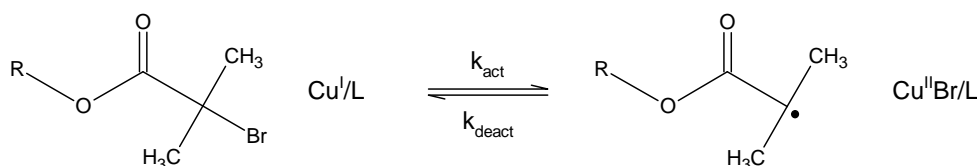
Scheme 2.15   Initiation using a bromoisobutyrate initiator and copper catalyst.

(ii)   *Catalysts and ligands*

As shown in scheme 2.15 above we see that a copper complex was used as transition metal catalyst in this project. Catalysts used vary, but can all be considered as one electron oxidants/reductants. The main prerequisites for a suitable catalyst include, having a metal center with at least two accessible oxidation states separated by one electron and an affinity for halogens. Also the coordination sphere around the metal should be able to accommodate a halogen upon oxidation[33,51]. We will focus on the copper[33,49,53,54] complex catalyst in this project, but many other metals have been used for ATRP. Much of the work studied by Matyjaszewski *et al.* and Sawamoto *et al.* cover ruthenium[33,48,51], iron[33,51,55-57], nickel[33,51,58] palladium[51], rhenium[51,59], rhodium[51,60], molybdenum[51] and chromium[51] complexes.

The ligand complexes with the transition metal salt to solubilise it in the organic reaction system. It also plays a crucial role in adjusting the redox potential of the metal center for appropriate activity. Nitrogen ligands have been used widely in copper mediated ATRP[46,49,53,61]. Bidentate and multidentate nitrogen ligands work best. Bridged and cyclic ligands yield more active catalysts than do simple linear ligands. The general order of activities of Cu ligand complexes is related to their structure and follows the following order; tetradentate (cyclic-bridged) > tetradentate (branched) > tetradentate (cyclic) > tridentate > tetradentate (linear) > bidentate ligands as shown in work by Tang *et al.*[61] In this project a simple bidentate ligand was

_____

used 4,4'-di-(5-nonyl)-2,2'-bipyridine (dNbipy) studied by Matyjaszewski *et al.*[49] and shown to be effective in the polymerisation of styrene.

(iii)   *Solvents, monomers and reaction temperature*

A variety of monomers including styrenes, (meth)acrylates, (meth)acryl-amides, and acrylonitrile have been successfully polymerised using ATRP[51]. Most monomers which contain substituents that can stabilise the propagating radicals are polymerisable using this technique[15]. A variety of solvents has also been used for solution polymerisation such as toluene, ethyl acetate, alcohols, water, dimethyl-formamide and THF.[15] Several factors affect the solvent choice. Chain transfer to solvent should be minimal. Interactions between the solvent and catalyst causing poisoning[62] or displacement of ligands must be avoided. Certain polymer endgroups (eg: polystyrol halides) can also undergo substitution or elimination reactions, particularly in polar solvents[63]. Reaction temperatures are generally in the range of 60-120°C. The higher the temperature the faster the reaction rate, because both k_p and k_{act}/k_{deact} increase with temperature[15]. This can lead to a better "living system", but it may also cause decomposition of catalyst or increase chain transfer and other side reactions[51]. It must also be noted that in many cases, such as styrene, we have thermally initiated auto-polymerisation occurring[64]. A balance must be found, as lowering the temperature too much can lead to impractical reaction durations.

2.3 Synthesis of block copolymers

There are a number of synthetic approaches that can be used to synthesise block copolymers. A brief review of the techniques relative to this study is given below.

2.3.1 Sequential polymerisation using living polymerisation techniques

As the name implies, these living techniques employ anionic or living radical polymerisation methods. As discussed previously, anionic polymerisation is living, even after all the monomer is consumed. This suggests that if one were to add monomer of another type to the living reaction one could produce a linear block copolymer. This is indeed the case, but many factors must be taken into consideration. These include the reaction conditions, miscibility of the newly introduced monomer with the system, as well as relative reactivity ratios of the monomers used. It can be seen that there are clear limitations as to the type of

_____

monomers that can be used in this block polymerisation method. For example, work done by Saam et al.[65] showed that living PstLi obtained from anionic polymerisation of styrene was able to initiate ring opening polymerisation of D_3. However, the lithium silanolate was not sufficiently reactive enough to initiate further anionic polymerisation of styrene to produce PS-b-PDMS-b-PS triblock copolymers. Other routes have to be used to synthesise this type of triblock copolymer[25]. In work done by Tezuka et al.[66] PS-b-PDMS macromonomers were prepared using sequential anionic polymerisation. These macromonomers were then functionalised with silane or diol moieties and used in free radical reactions with AIBN to synthesis three component polymers having PS-b-PDMS graft segments. Bellas et al.[67] also used this sequential anionic polymerisation technique to synthesise linear and star copolymers of PS, PDMS and polyisoprene. Similarly to Tezuka et al., PS-b-PDMS blocks were anionically synthesised followed by functionalisation to form macro-"block"-monomers. Sequential polymerisation using controlled free radical methods are also possible. Work done by Bernard et al.[68] used the RAFT process to synthesise linear poly(acryloyl glucosamine) molecules. The "livingness" of the reaction was shown by chain extending the molecules with N-isopropylacrylamide monomer to form well defined block copolymers with narrow PDI's. Although there are limitations on possible chain architectures as well as monomers that can be used, this method still provides a feasible route to the synthesis of block copolymers of controlled structure.

2.3.2 Functionalised macroinitiator technique

This technique, when combined with controlled polymerisation methods, yields polymers of controlled composition and architecture. This method requires initial synthesis of macroinitiators. As the name suggests, "large" initiators that consist of one of the polymer blocks in the copolymer. Anionic polymerisation as described earlier presents a facile route for macroinitiator synthesis, due to the ease of chain end capping with a variety of functionalities. Depending on the chosen end cap functionality a variety of different methods can be used to produce the final block copolymer. Figure 2.1 illustrates the general mechanism of this type of block copolymer synthesis.

Much work has been carried out on using this technique to produce block copolymers. Miller and Matyjaszewski[25] combined the macroinitiator technique with ATRP to synthesise block copolymers of PDMS and poly(methylmethacrylate)

_____

(PMMA). Hydrosilyl functionalised PDMS macroinitiator was converted to a macroinitiator for ATRP of methacrylate monomers. ATRP allowed good control over the synthesis of the methacrylate blocks from the macroinitiator. Coca and coworkers[69] used ring opening polymerisation of norbornene to produce poly(dicyclopentadiene) macroinitiators for ATRP.
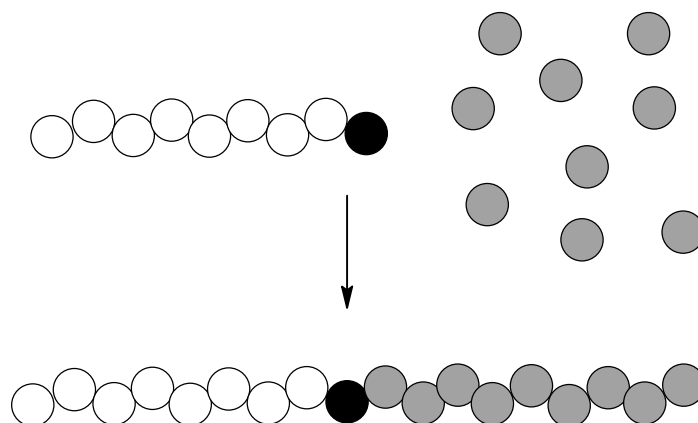
Figure 2.1   Functionalised macroinitiator used to produce the block copolymers.

These were then used to polymerise styrene to make block copolymers. Work by Bielawski *et al.*[70] used a difunctional polybutadiene (PB) macroinitiator, prepared by the ring opening polymerisation of 1,5,cyclooctadiene, to polymerise PS and PMMA using ATRP. This method produced PS-b-PB-b-PS and PMMA-PB-PMMA triblock copolymers. A very recent article by Liu and Wang[71] showed how the hydroxyl groups on attapulgite clay surfaces can be modified to macroinitiators for ATRP. MMA was then grown from the clay surfaces via ATRP. Essentialy this method created a star polymer from a hyper branched macroinitiator. Controlled radical techniques[24] are receiving much attention due to their robust nature and compatibility with a wide range of monomers, compared to that of anionic polymerisation methods. It can be seen that by combining anionic methods to produce macroinitiator blocks of controlled structure and functionality with controlled radical polymerisation techniques to produce supplementary blocks, offers the ability to synthesise polymers with a broad spectrum of compositional and architectural complexity.

_____

2.3.3 Coupling of prepolymers to synthesise blocks

This technique involves the synthesis of prepolymers of different structures that are subsequently joined via their functional end-groups using a coupling reaction. Figure 2.2 illustrates this block synthesis technique. This technique shows promise due to the fact that anionic techniques to prepare the prepolymers together with this coupling mechanism can yield block copolymers of well controlled structure. In literature a well known reaction type called click chemistry[72,73] is used as a means of joining two complementary functional groups. In this case, modification of polymeric endgroups by a low molecular weight compound is used, as opposed to the coupling of two large molecular weight species. The coupling reaction used in this project was the hydrosilylation reaction between vinyl and silane terminal moieties. There are other methods available but we will restrict this section to the coupling reaction used in this project.
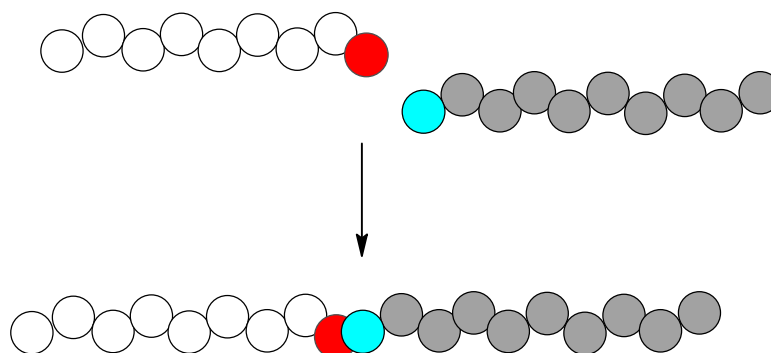
Figure 2.2   The coupling of functionalised prepolymers to synthesise block copolymers.

The hydrosilylation reaction is a widely used industrial reaction for the synthesis of silane coupling agents and crosslinking reactions, like those used in the formation of silicone rubber. The reaction occurs readily upon addition of a suitable catalyst such as Karstedts catalyst. Karstedts catalyst is a divinyl-platinum complex shown in Scheme 2.16.

The most commonly accepted mechanism for the hydrosilylation reaction is the Chalk-Harrod mechanism[74] developed in 1964, or the modified Chalk-Harrod mechanism[75], illustrated in scheme 2.17. What we see is the silane oxidative addition to the metal and alkene insertion into the metal-hydride bond followed by Si-C reductive elimination.

_____
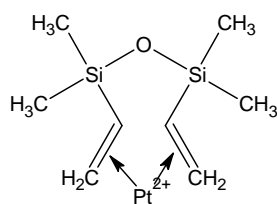
Scheme 2.16 Karstedts catalyst structure showing Pt coordination with the divinyl compound.

There are many phenomenon occurring during this reaction that are not fully explained by the Chalk-Harrod mechanism which lead to the development of the similar Lewis mechanism[76,77]. This mechanism helps describe the colloid formation found at the end of the reaction. There is still much debate on the exact mechanism and research in this specific field still continues[78,79]. New work in this field shows that the undesired colloidal formation occurring as explained by the Lewis mechanism leading to discolouration, can be exploited to form platinum nanoparticles[80].

$R_2 = SiMe_2OR_b$

$R_1 = SiCH_2Me_2OR_a$
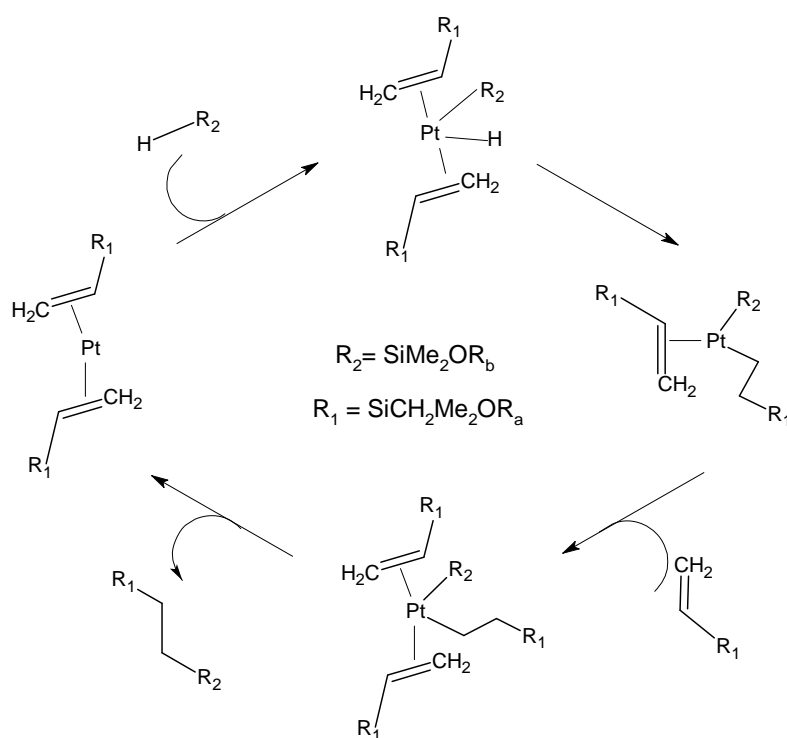
Scheme 2.17: The Chalk-Harrod mechanism for the platinum catalysed hydrosilylation reaction[74].

_____

2.3.4 Reactivity ratio and block synthesis

This technique will be the final technique to synthesise block copolymers discussed in this chapter. When synthesising a linear di-block copolymer using this technique, both monomers are added simultaneously. Depending on the relative reactivity ratios of each monomer type, preferential incorporation of the monomers into the growing chain occurs. The active monomer sites have different polarities and resonance stabilisation characteristics and thus different relative reactivities. A brief overview of reactivity ratios and how they affect polymerisation will be presented to further understand this technique.

We will look at the first order Markov (terminal model) of copolymerisation. This is valid for radical, carbocation and carbanion active centers. It must be noted that in this model, it is solely the last incorporated monomer unit that determines which monomer unit will be added next. There are four fundamental equations:

$$M_1^* + M_1 \xrightarrow{k_{11}} M_1^* \qquad\qquad 2.4$$

$$M_1^* + M_2 \xrightarrow{k_{12}} M_2^* \qquad\qquad 2.5$$

$$M_2^* + M_1 \xrightarrow{k_{21}} M_1^* \qquad\qquad 2.6$$

$$M_2^* + M_2 \xrightarrow{k_{22}} M_2^* \qquad\qquad 2.7$$

where M^* indicates the monomer at the end of a growing polymer chain, and the footnote denotes whether it is monomer one or monomer two. Now the reactivity ratios of each monomer can be written as follows:

$$r_1 = k_{11}/k_{12} \qquad\qquad 2.8$$

$$r_2 = k_{22}/k_{21} \qquad\qquad 2.9$$

It can be seen from equations 2.8 and 2.9 that the reactivity ratio of each monomer is the likelihood that the same monomers will be incorporated consecutively as opposed to incorporation of a different monomer each time. If r_1 were to be larger than unity, then monomer one would be preferentially incorporated after the addition of monomer one. If r_1 was smaller than unity then monomer two would be preferentially incorporated after the addition of monomer one. The same can be said

_____

for monomer two and its reactivity. From this information it is apparent that if $r_1 > 1$ and $r_2 < 1$, then monomer one will be incorporated preferentially until the monomer is exhausted before monomer two is incorporated. This would then yield a linear block copolymer of polymer one block polymer two. Due to the factors mentioned earlier which affect the reactivity ratios, it is extremely difficult to find two monomers that can undergo such a polymerisation, and there are invariably mistakes along the length of the chain, or the synthesis of gradient block copolymers.

An article by Chonjnowski et al.[22] used the idea of reactivity ratios to prepare gradient block copolymers of vinylmethylsiloxane and dimethylsiloxane. The monomers used were D_3 along with 2-vinyl-2,4,4,6,6-pentamethylcyclotrisiloxane (VD_2), with reactivity ratios of 0.22 and 8.1 respectively. After anionic polymerisation of these monomers, it was found that the first section of the chains were majority VD_2, but as the VD_2 monomer headed for exhaustion there was an increase in D_3 incorporation. The last sections of the chains were mainly D_3 units. This gave a gradient distribution of monomer incorporation. Williamson et al.[81] copolymerised 1,3-cyclohexadiene and styrene with reactivity ratios of 0.022 and 0.024, respectively. This gave alternating block copolymers as $r_1 = r_2$. They determined the reactivity ratios using Fourier transform infra-red spectroscopy (FTIR) combined with Mayo-Lewis graphical plots.

2.4   Morphology of block copolymers

The development of living anionic polymerisation as well as the other controlled polymerisation techniques discussed earlier in this work, has lead to the ability to produce a variety of block copolymer architectures[24,31,38-40]. These include diblocks, triblocks, and multi-arm star copolymers. This section will focus on simple $(A-B)_n$ diblock copolymers, where A and B are different monomer segments.

2.4.1   Bulk morphology

In the equilibrium state these copolymers can exhibit a variety of morphological configurations depending on a number of factors[82]. Firstly (N), the overall degree of polymerisation, secondly architectural constraints (n) and (f), (the volume fraction of component A). Lastly we have the A-B segment to segment interaction parameter (χ) which is also known as the Flory-Huggins interaction parameter. As stated

_____

previously, this section will deal with diblock copolymers, therefore (n) is unity. The other factors can be divided into two competing phenomena, namely entropic and enthalpic effects[82-84]. The entropic effects consist of N, n and f, which describe the configurational and steric effects of the block copolymer. The segmental interaction parameter χ is an enthalpic effect and relies on the choice of monomer pairs. This parameter is temperature dependant as shown in equation 2.10[82], where $\alpha > 0$ and β are constants dependant on f and n.

$$\chi = \alpha T^{-1} + \beta \qquad\qquad 2.10$$

Therefore, if the temperature is decreased we have an increase in χ. If N is also increased these factors override the lowest energy equilibrium configuration with an accompanying loss in entropy. This results in an ordering of the disparate segments into microphase separated domains[82-84], as illustrated in figure 2.3 (b). A lowering in N and χ cause the entropic effects to dominate resulting in disordered phases, shown in figure 2.3 (a). By combining the entropic and enthalpic effects of N and χ we have the product χN which can be used to derive the copolymer phase state. When $\chi N < 10$ we have weak segregation and this is referred to as the weak segregation limit (WSL)[82,83]. Alternately, when $\chi N \gg 10$ we have strong segregation and this system is known as the strong segregation limit (SSL)[82,84].
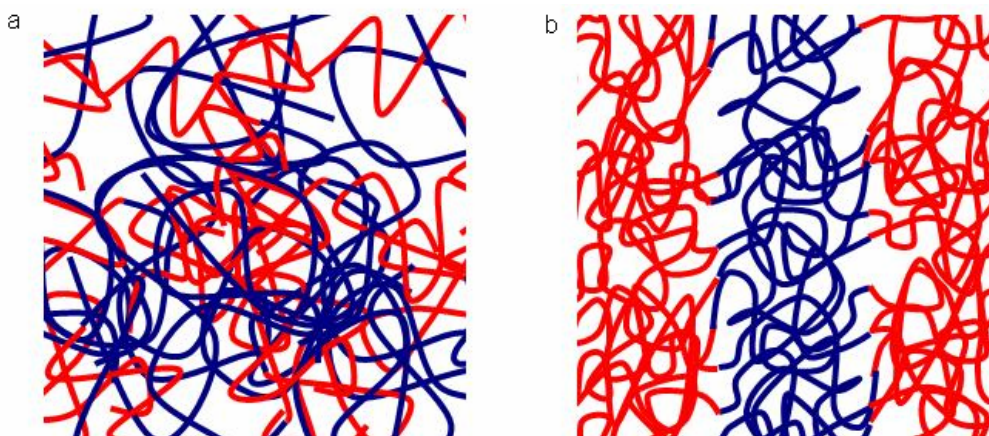
Figure 2.3 Illustration of (a) disordered phase and (b) ordered phase morphology.

As previously stated, the A-B segments used in this project are PDMS and PS. It has been shown in literature that these polymers are extremely immiscible[85], resulting in a high χ parameter of approximately 0.3, as shown in work by Chu *et al.*[86] With the

_____

chain lengths used in this project the product χN ranges from 50 to 300. This is far above 10, which infers that the SSL applies in all instances. Emphasis will thus be placed on this regime as the WSL is outside the scope of this work.

In the SSL regime the fundamental characteristic is that the "opposing" monomer segments segregate into distinct morphological configurations to minimise the interfacial contact between the disparate components. The advent of transmission electron microscopy (TEM) allowed in depth characterisation of copolymer morphologies. It was, however, not until Fujimura et al.[87] combined small angle x-ray scattering (SAXS) investigation with TEM that detailed investigations of block copolymer thermodynamics became possible. The first complete theory on ordered phases was developed by Leibler[83] in 1980 and expanded on by Otha[88] and co-workers. The ordered phases proposed in these works were defined as either spheres, lamellae or cylinders. As shown in figure 2.4 (a) to (e). Depending on the volume fraction f of each segment, we get inverted morphologies. Figure 2.4 (a) and (e) are both spherical morphologies, but in the case of (a) we have a larger volume fraction of segment A, in a typical ratio of 80:20. The inverse morphology is true for (e) with the opposing segmental ratio. In this case segment B constitutes the matrix.
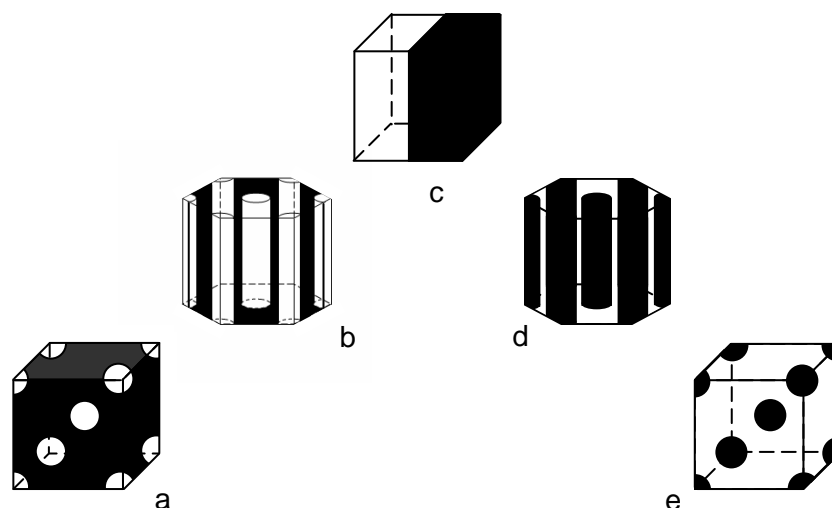
Figure 2.4   The six classical strong segregation limit morphologies (a-e), where the polymer segment A is coloured black and segment B is clear.

Figure 2.4 (b) and (d) have the same relationship. In this case the volume fraction ratio of (b) is approximately 70:30 with segment A being the larger volume fraction. In this range of volume fractions cylindrical morphologies persist. When the volume fractions of each segment tend towards a 1:1 ratio, lamellar type morphology is

_____

formed as shown in (c). The ratios mentioned above are for ideal cases as presented in work by Bates and Fredrickson[82], and differ from experimentally obtained results. They vary from polymer to polymer and also tend to be skewed[86], where the inverse morphology does not occur at exactly the opposite ratio. These values do however help elucidate how the morphologies change with volume fraction changes of the copolymers segments.

Continued research in this field, by Anderson *et al.*[89], lead to the discovery of a new morphology which became known as the ordered bicontinuous double diamond (OBDD) morphology. This phase consisted of two continuous interpenetrating diamond networks of PS rods in a polyisoprene (PI) matrix and was determined using TEM combined with SAXS. It was found that this morphology occurred at a block composition between that of the cylindrical and lamellar structures. A further morphological configuration related to this OBDD structure, known as the gyroid was later found to exist. This was investigated in work by Hajduk *et al.*[90] where they studied PS block PI copolymers. This configuration also occurs between the cylindrical and lamellar phases as with OBDD. Recent work is focusing more on developing computer based simulations to describe the phase behaviour of diblocks in the SSL region. Olmsted and Milner[84] computed phase diagrams to calculate which of the bicontinuous phases in the SSL are the most stable. It was found that the gyroid was most stable with the least surface contacts. Work by Grason and Kamien[91] studied the role that the A-B interface has on the phase behaviour of A-B type three armed star polymers. Honda and Kawakatsu[92] have very recently proposed a high-speed and accurate hybrid dynamic density functional theory for the computer simulations of the phase separation processes of polymer melts and blends.

Currently with the advent of techniques such as nuclear magnetic resonance (NMR) and atomic force microscopy (AFM) there are even more possibilities to further understand the behaviour of microscopic phase separated copolymers. Examples of such work are by Soltani *et al.*[93] who used solid state NMR to investigate the existence and extent of interphase regions in PDMS block PS copolymers and their dependence on molecular weight. Simon and co-workers[94] compared the use of TEM (provided by electron holography) and AFM in investigating PS block PI copolymers. The advantage of electron holography over conventional TEM is that film staining is not required which can disrupt the equilibrium morphology by local swelling and induced segregation[82]. After cross sectional cryo-microtoming of the surface of the

_____

films for electron holography analysis, the cut surface underwent AFM analysis. Both techniques gave clear and comparable results highlighting the use of AFM as a new addition to the family of techniques used in morphological characterisation.

2.4.2 Surface segregation and modification with corona

An important property of the block copolymers studied in this project is the ability of PDMS to preferentially surface segregate. PDMS has a lower surface energy compared to that of PS. This combined with the fact that the two components are strongly segregated, leads to PDMS migrating to the air-polymer interface. Much work has been done by Chen and co-workers[95] in studying this phenomenon of PDMS. One of their publications looked at the relationship between molecular weight and surface segregation ability of PDMS-PS diblocks and compared that to the case of PS-PDMS-PS triblocks[96]. They also compared diblocks to star polymers of PDMS and PS[97]. Other work looked at the ability of PDMS blocked with polyurethane[98] and polycarbonate[99] to surface segregate.

In this project, the preferential surface segregation phenomenon was exploited in corona degradation studies. It is known from literature that when undergoing corona degradation, PDMS forms a nano glass-like layer on the outer most surface.[4,100] PDMS which is usually hydrophobic in nature, becomes hydrophilic after corona, but regains its hydrophobicity after a few hours. Work by Zhu and co-workers[100], as well as Mallon *et al.*[4] noticed that the glass layer cracked due to the rubbery nature of the substrate polymer. Mallon *et al.*[4] also employed positron annihilation spectroscopic methods to better understand the formation of the glass layer and the mechanism of hydrophobic loss and recovery. This degradation phenomenon forms part of this study, and the corona procedure is discussed more thoroughly in the experimental chapter.

Once synthesised, advanced analytical techniques are needed to study the chemical composition and molecular weight distributions, of the produced polymers. This brings us to the following section of work.

_____

2.5   Chromatography of polymers

Chromatography is an invaluable technique in the analysis of polymers. It allows one to characterise polymeric materials, through fractionation, according to molecular weight and chemical composition. A short introduction into the heterogeneity of polymers will elucidate the importance and need for chromatographic characterisation of polymers.

2.5.1   Why chromatographic characterisation/separation

Polymer properties can be divided into two groups, namely, simple and distributive properties[101]. Simple properties include the weight of the polymer present and unreacted monomer or additives present in the polymer sample. These properties rely on the conversion of the reaction or percentage additives added to the material. Distributive properties are those which cannot be described by one single value. The molecular weight of a polymer is distributive in nature. In a polymer sample not all the chains are exactly the same length this is indicated by the PDI as stated earlier. In this case a distribution of chain lengths is used to describe the molecular weight of a polymer. The same can be said for chemical composition distribution, sequence length distribution and functionality distribution. It must also be noted that a polymer may be distributive in one property, but homogenous in another, or it may be distributive in more than one property. This necessitates an additional classification of polymers into, monodisperse, polydisperse and complex polymers as indicated in table 2.2.

Table 2.2   The three classes of polymers according to distributive properties[101].

Class	Definition	Example
Monodisperse	All distributive properties of the polymer are homogenous in nature.	A homopolymer with a narrow molecular weight distribution.
Polydisperse	The polymer is heterogeneous in only one of it's distributive property.	A homopolymer with a broad molecular weight distribution.
Complex	The polymer is heterogenous in more than one distributive property.	A diblock copolymer that is distributive in molecular weight and chemical composition.

_____

It is clear that the polymers synthesised and studied in this project fall into the last category of complex polymers. These block copolymers are heterogeneous in molecular weight as well as chemical composition distribution. Advanced chromatographic techniques, gradient elution chromatography (GEC) and liquid chromatography at critical conditions (LC-CC), are needed to characterise these materials. To effectively understand how these advanced techniques work, a brief introduction to size exclusion chromatography (SEC) and liquid adsorption chromatography (LAC) will be presented. The following sections will refer to figure 2.5 which assists in showing the connection between these modes of separation and the elution of molecules of varying molecular weight[101].

2.5.2 Size exclusion chromatography

In this mode separation is achieved according to hydrodynamic volume, or the volume that the molecule assumes in solution. This is of course related to the molecular weight of the sample, so a calibration is needed to convert the hydrodynamic volume separation into a molecular weight distribution.
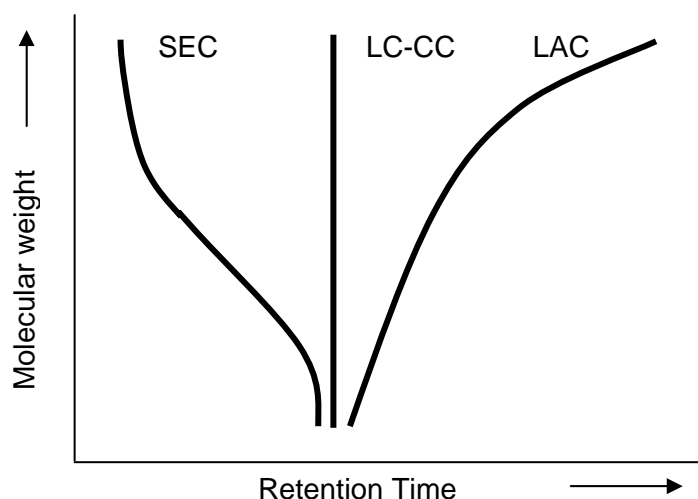
Figure 2.5   Chromatographic behaviour of molecular weight versus retention time in the three modes of separation.

The conformational and steric properties of the molecules lead to molecular separation. The stationery phase is typically a swollen gel with a definite pore size distribution. In this mode entropy effects ($T\Delta S$) are dominant[101]. The distribution coefficient for SEC is given in equation 2.11.

_____

$$K_{SEC} = exp(\Delta S/R) \hspace{4cm} 2.11$$

Conformational entropy decreases as the molecules move through the pores and $\Delta S<0$ so $K_{SEC}<1$. The maximum value $K_{SEC}=1$ is achieved if all the pore sizes are accessible to all of the molecules (separation threshold) and $K_{SEC}=0$ is where the pores are too small for any molecules to penetrate (exclusion limit). When passing through the column, smaller molecules tend to penetrate more of these pores and are thus retained longer. Larger molecules cannot penetrate certain pores due to steric hindrance and thus have a "shorter path" to travel through the column. In this case the molecules elute from largest to smallest as can be seen in figure 2.5. The retention volume (V_R) for ideal SEC is given in equation 2.12, where (V_i) is interstitial volume of the column and (V_p) is the volume of the pores.

$$V_R = V_i + V_p K_{SEC} \hspace{4cm} 2.12$$

This technique is used predominantly as routine analysis in determining molecular weight distributions. Due to the gel nature of the stationary phase, this technique is also known as gel permeation chromatography (GPC).

2.5.3 Liquid adsorption chromatography

Separation in this mode is dependant on enthalpic interactions (ΔH) between the polymer chain and the stationary phase[101]. The distribution coefficient for LAC is shown in equation 2.13.

$$K_{LAC} = exp(-\Delta H/RT) \hspace{4cm} 2.13$$

Interaction with the stationary phase packing material is related to the molecular weight of the molecules. The larger the molecule, the larger the interaction with the packing material. Smaller molecules will thus have a shorter retention time compared to the larger molecules. This is illustrated in figure 2.5 where elution occurs from the lowest molecular weight to the largest. There are two equations describing the retention volume for ideal LAC, given by equations 2.14 and 2.15, where V_{stat} is the volume of the stationary phase.

$$V_R = V_i + V_{stat} K_{LAC} \hspace{4cm} 2.14$$

_____

$$V_R = V_i + V_p + V_{stat}K_{LAC}$$ 2.15

Equation 2.14 describes narrow pore retention, where the molecules interact with the outer surface of the packing material. If the molecules are able to penetrate the pores then the term V_p must be added to the equation as in equation 2.15. It must also be noted that if the interaction between the stationary phase and molecules are too strong, irreversible adsorption could occur. Caution must be used if operating in this region and it is therefore not routinely used for molecular weight determinations.

It must be said that the explanation given here assumes ideal conditions. SEC separation is predominantly due to TΔS, but there is still a small contribution from ΔH due to electrostatic interactions with the packing material[101]. The same is true for LAC, where not all the molecules can pass through all the pores, giving a small ΔS contribution. This is, however, beyond the scope of this chapter.

2.5.4 Liquid chromatography at critical conditions

This chromatographic technique is widely used to characterise polymeric materials according to chemical composition and is unique to macromolecules[101,102]. As stated previously, SEC is predominantly reliant on entropic effects (TΔS>ΔH) and LAC is predominantly reliant on enthalpic interactions (ΔH>TΔS). In the case of LC-CC, we have a mutual compensation phenomenon occurring as shown in equation 2.16. At this point the enthalpic adsorption forces are compensated by entropic losses[101,102]. This is the point where we move from unadsorbed (SEC) to adsorbed (LAC) states.

$$T\Delta S = \Delta H$$ 2.16

At this point, all molecules elute irrespective of molecular weight. The molecules are, in a sense, made "invisible" to the chromatographic system. To achieve this balance, optimisation of the parameters affecting the entropic and enthalpic properties must be attained. This point can be achieved by varying the stationary phase, mobile phase composition or temperature.[101,102] In most cases the simplest way to reach critical conditions is by varying the mobile phase composition. A typical mobile phase composition would include a solvent that easily solvates the chosen polymer (desorli), and a solvent that induces precipitation of the polymer (adsorli)[102]. By varying the solvent combination one reaches a point where the molecules are at the

_____

point of precipitating and adsorbing onto the column, precisely enough, to compensate for their size exclusion behaviour. The close proximity to the point of adsorbtion lends an alternative name to this technique, liquid chromatography at the critical adsorption point (LC-CAP)[101,103,104]. The molecules then elute along with the solvent molecules irrespective of molecular weight. Temperature is usually used to "fine tune" the separation[102,105]. It must also be noted that the solvent in which the sample is dissolved, exactly matches the mobile phase composition. This method can prove tedious, as trial and error must be used to pin-point the precise solvent combination. An alternative method of reaching the critical point, which proved to be successful, was published in work by Bashir and coworkers[106]. They used gradient chromatography to locate the critical point. After comparing the measured solvent combinations to those determined according to conventional methods, they found only a slight deviation. By first using the gradient method to estimate the solvent composition, only a few isocratic experiments are needed to get to the actual critical composition.

As useful as this technique is, it does have its disadvantages. The main disadvantage is the difficulty in applying this technique to high molecular weight polymers as shown in work by Philipson *et al.*[105] There tends to be broadening of the peak at critical conditions which they assumed to be due to differences in diffusion coefficients and the increasing contribution of adsorption to the total retention under critical conditions. Another disadvantage is the severe sensitivity to minute changes in temperature, mobile phase, pore size and pressure[103,104]. New chromatographic techniques related closely to conventional LC-CC have been developed. They also allow elution of molecules irrespective of molecular weight, but prove to be more robust to changes in temperature, pressure, pore size and mobile phase composition. These methods have been published in work by Berek *et al.*[103,104], namely, liquid chromatography under limiting conditions of adsorption (LC-LCA) and liquid chromatography under limiting conditions of desorption (LC-LCD). In LC-LCA[103] the mobile phase promotes adsorption so if a the sample were to be injected it would be retained on the column. The sample is, however, injected in a solvent that strongly promotes desorption. Therefore, the molecules move with the sample solvent. If the molecules exceed the solvent front, they would adsorb due to the mobile phase, and then desorb and move along as the sample solvent passes along. Their experiments showed that the molecules eluted in a narrow band irrespective of molecular weight over quite a broad mobile phase composition range. This is already an advantage as LC-CC is extremely sensitive to solvent composition changes. LC-LCD[104] is basically

_____

the reverse of LC-LCA. In this system, the eluent promotes desorption and the sample is injected in a solvent that promoted adsorption. In this case the molecules travel along the column and cannot exceed the sample solvent zone, as they would adsorb to the column. The desorbing eluent carries along any molecules that may have adsorbed to the column.

2.5.5 Gradient elution chromatography

This technique is widely employed in the separation of polymers according to chemical composition[107]. A good scenario to illustrate the use of this technique, is analysing a polymer sample that contains di-block molecules (A-B), as well as small amounts of the respective constituent homopolymer molecules (A) and (B). These different polymer types will react differently in solutions according to their relative solubilities. They also interact differently with the stationary phase of the column. Depending on the chromatographic system used, analysis can be performed in reversed phase (RP) or normal phase (NP). In NP the stationary phase is polar and the mobile phase is non-polar. In RP the stationary phase is non-polar and the mobile phase is polar. Separation is thus achieved by either the difference in solubility of the disparate components (RP), or by their interaction with the column (NP). A simple RP system will be used to illustrate the point. The solvent will be a mixture of (C) and (D), where D is a good solvent for both components A and B. Solvent C, however, is a poor solvent for component B. Before injection, a 100% solution of solvent C is used as eluent. Upon injection, homopolymer A will remain in solution and move freely through the column. Homopolymer B will precipitate out of solution and be retained on the column. The block copolymer will be partly in solution (segment A) and partly out of solution (segment B). The gradient then starts, where the solvent composition is gradually changed from 100% solvent C to 100% solvent D. As the gradient changes homopolyer A continues eluting, followed by the block copolymer that was already partly in solution. Homopolymer B then elutes last. This is illustrated in figure 2.6.

It must be stressed that this scenario is a very simple example of how GEC is used to characterise polymers according to chemical distribution. The gradients are usually more complicated, involving solvent combinations and steps, where certain solvent compositions are held constant for a certain amount of time before continuing with the gradient. One experiment may contain several gradient of varying steepness to

_____

separate the material. A few typical cases where GEC was put to use are discussed. Work by Graef *et al.*[108] dealt with the development of GEC techniques to analyse graft copolymers of styrene/MMA and epoxidised natural rubber.
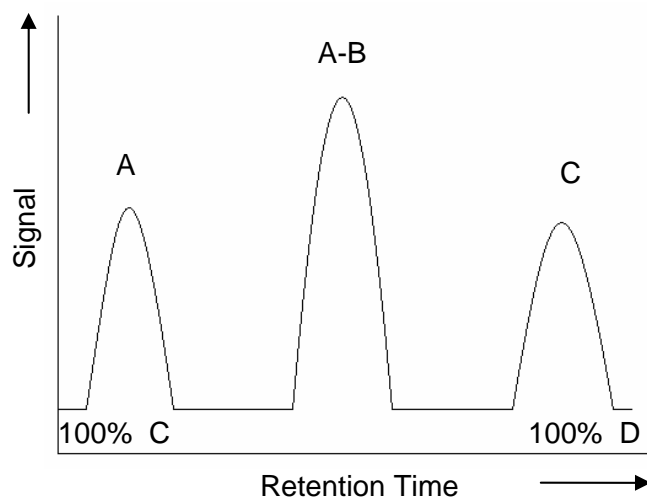
Figure 2.6   Simple GEC elution profile for a mixture of block and homopolymers.

Some examples of the use of GEC follow. Park and co-workers[107] compared the GEC (dichloromethane and acetonitrile) behaviour of triblock copolymers with alternating sequences of segment order. Venkatesh and Klumperman[109] used GEC (THF and n-heptane) to prove the successful formation of block copolymer using a macroinitiator technique. These results allowed separation of the block copolymer from the constituent homopolymers, thus proving successful block copolymer synthesis.

This concludes the literature and historical study presented in this chapter. The following chapter focuses on the experimental and analytical procedures used in this project.

_____

2.6   References

(1)   Matyjaszewski, K., Pyun, J. *Chem. Mater* **2001**, *13*, 3436-3448.

(2)   Ro, H. W., Kim, K.J., Theato, P., Gidley, D.W., Yoon, D.Y. *Macromolecules* **2005**, *38*, 1031-1034.

(3)   Wen, J., Wilkes, G.L. *Chem. Mater.* **1996**, *8*, 1667-1681.

(4)   Mallon, P. E., Greyling, C.J., Vosloo, W., Jean, Y.C. *Radiat. Phys. Chem.* **2003**, *68*, 453-456.

(5)   Ndoni, S., Vigild, M.E., Berg, R.H. *J. Am. Chem. Soc.* **2003**, *125*, 13366-13367.

(6)   Miyata, T., Obata, S., Uragami, T. *J. Polym. Sci., Part B: Polym. Phys.* **2000**, *38*, 584-589.

(7)   Barton, T. J., Bull, L.M., Klemperer, W.G., Loy, D.A., McEnaney, B., Misono, M., Monson, P.A., Pez, G., Scherer, G.W., Vartuli, J.C., Yaghir, O.M. *Chem. Mater.* **1999**, *11*, 2633-2656.

(8)   Han, J. T., Xu, X., Cho, K. *Langmuir* **2005**, *21*, 6662-6665.

(9)   Szwarc, M., Levy, M., Milkovich, R. *J. Am. Chem. Soc.* **1956**, *78*, 2656-2657.

(10)   Matyjaszewski, K., Mu¨ller, A.H.E. *Prog. Polym. Sci.* **2006**, *31*, 1039–1040.

(11)   Smid, J., Van Beylen, M., Hogen-Esch, T.E. *Prog. Polym. Sci.* **2006**, *31*, 1041-1067.

(12)   Hadjichristidisa, N., Iatroua, H., Pitsikalisa, M., Mays, J. *Prog. Polym. Sci.* **2006**, *31*, 1068–1132.

(13)   Yagci, Y., Tasdelen, M.A. *Prog. Polym. Sci.* **2006**, *31*, 1133–1170.

(14)   Morton, M. *Anionic polymerization principles and practice*; London: Academic Press Inc., **1983**.

(15)   Odian, G. *Principles of polymerisation*, 4th ed.; New Jersey: John Wiley and Sons, **2004**.

(16)   Vlcek, P., Lochmann, L. *Prog. Polym. Sci.* **1999**, *24*, 793–873.

(17)   Bywater, S. *Prog. Polym. Sci.* **1975**, *4*, 27-69.

(18)   Mark, H. F., Bikales, N.M., Overberger, C.G., Menges, G. *Encyclopedia of polymer science and engineering*, 2nd ed.; John Wiley & Sons, 1985; Vol. 2.

(19)   Hong, K., Uhrig, D., Mays, J.W. *Curr. Opin. Solid State Mater. Sci.* **1999**, *4*, 531-538.

(20)   Lee, J., Hogebn-Esch, T.E. *Macromolecules* **2001**, *34*, 2095-2100.

(21)   Zilliox, J. G., Roovers, J.E.L., Bywater, S. *Macromolecules* **1975**, *8*, 573-578.

_____

(22)   Chonnowski, J., Cypryk, M., Fortuniak, W., Rozga-Wijas, K., Scibiorek, M. *Polymer* **2002**, *43*, 1993-2001.

(23)   Verheyden, H., Van Lierde, P., Szwarc, M., Litvinenko, G., van Beylen, M. *J. Polym. Sci., Part A: Polym. Chem.* **2002**, *40*, 2148-2157.

(24)   Pyun, J., Matyjaszewski, K. *Chem. Mater.* **2001**, *13*, 3436-3448.

(25)   Miller, P. J.; Matyjaszewski, K. *Macromolecules* **1999**, *32*, 8760-8767.

(26)   Vazaios, A., Lohse, D.J., Hadjichristidis, N. *Macromolecules* **2005**, *38*, 5468-5474.

(27)   Smith, S. D., DeSimone, J.M., Huang, H., York, G., Dwight, D.W., Wilkes, G.L., McGrath, J.E. *Macromolecules* **1992**, *25*, 2575-2581.

(28)   Morgan, A. M., Pollack, S.K., Beshah, K. *Macromolecules* **2002**, *35*, 4238-4246.

(29)   Yoshida, E., Tanimoto, S. *Macromolecules* **1997**, *30*, 4018-4023.

(30)   Lu, G., Jia, Z., Yi, W., Huang, J. *J. Polym. Sci., Part A: Polym. Chem.* **2002**, *40*, 4404-4409.

(31)   Shinoda, H., Matyjaszewski, K. *Macromolecules* **2003**, *36*, 4772-4778.

(32)   Zhao, Y., Shuai, X., Chen, C., Xi, F. *Macromolecules* **2004**, *37*, 8854-8862.

(33)   Moad, G., Solomon, D.H. *The Chemistry of Radical Polymerisation*, 2nd ed.; Heidelberg: Elsevier, 2006.

(34)   Shipp, D. A. *J. Macromol. Sci., Part C: Polym. Rev.* **2005**, *45*, 171–194.

(35)   Chiefari, J., Chong, Y.K., Ercole, F., Krstina, J., Jeffery, J., Le, T.P.T., Mayadunne, R.T.A., Meijs, G.F., Moad, C.L., Moad, G., Rizzardo, E., Thang, S.H. *Macromolecules* **1998**, *31*, 5559-5562.

(36)   Le, T. P., Moad, G., Rizzardo, E., Thang, S.H.: PCT Int. Appl.WO 98/01478, 1998.

(37)   Moad, G., Rizzardo, E., Thang, S.H. *Aust. J. Chem.* **2005**, *58*, 379-410.

(38)   Chong, Y. K., Le, T.P.T., Moad, G., Rizzardo, E., Thang, S.H. *Macromolecules* **1999**, *32*, 2071-2074.

(39)   Mayadunne, R. T. A., Rizzardo, E., Chiefari, J., Krstina, J., Moad, G., Postma, A., Thang, S.H. *Macromolecules* **2000**, *33*, 243-245.

(40)   Mayadunne, R. T. A., Jeffery, J., Moad, G., Rizzardo, E. *Macromolecules* **2003**, *36*, 1505-1513.

(41)   Yu, W. H., Kang, E.T., Neoh, K.G. *Langmuir* **2005**, *21*, 450-456.

(42)   Moad, G., Rizzardo, E., Solomon, D.H. *Macromolecules* **1982**, *15*, 909-914.

(43)   Solomon, D. H. *J. Polym. Sci., Part A: Polym. Chem.* **2005**, *43*, 5748-5764.

(44)   George, M. K., Veregin, R.P.N., Kazmaier, P.M., Hamer, G.K. *Macromolecules* **1993**, *26*, 2987-2988.

_____

(45)   Hawker, C. J., Bosman, A.W., Harth, E. *Chem. Rev.* **2001**, *101*, 3661-3688.

(46)   Tang, H., Arulsamy, N., Radosz, M., Shen,Y., Tsarevsky, N.V., Braunecker,
        W.A., Tang, W., Matyjaszewski, K. *J. Am. Chem. Soc.* **2006**, *128*, 16277-
        16285.

(47)   Greszta, D., Mardare, D., Matyjaszewski, K. *Macromolecules* **1994**, *27*, 638-
        644.

(48)   Kato, M., Kamigaito, M., Sawamoto, M., Higashimura, T. *Macromolecules*
        1995, *28*, 1721-1723.

(49)   Matyjaszewski, K., Patten, E., Xia, J. *J. Am. Chem. Soc.* **1997**, *119*, 674-680.

(50)   Klumperman, B., Chambard, G. *ATRP of Styrene and Butyl Acrylate*. In
        Matyjaszewski, K., editor, *ACS symposium series 768*: *Controlled/living
        Radical Polymerisation: Progress in ATRP,NMP and RAFT*, Washington DC:
        American Chemical Society, **2000**.

(51)   Matyjaszewski, K., Xia, J. *Chem. Rev.* **2001**, *101*, 2921-2990.

(52)   Kotani, Y., Kamigaito, M., Sawamoto, M. *Macromolecules* **2000**, *33*, 6746-
        6751.

(53)   Wang, J., Matyjaszewski, K. *Macromolecules* **1995**, *28*, 7901-7910.

(54)   Wang, J., Matyjaszewski, K. *Macromolecules* **1995**, *117*, 5614-5615.

(55)   Teodorescu, M., Gaynor, S.G., Matyjaszewski, K. *Macromolecules* **2000**, *33*,
        2335-2339.

(56)   Ando, T., Kamigaito, M., Sawamoto, M. *Macromolecules* **1997**, *30*, 4507-
        4510.

(57)   Matyjaszewski, K., Wei, M., Xia, J., McDermott, N.E. *Macromolecules* **1997**,
        30, 8161-8164.

(58)   Uegaki, H., Kotani, Y., Kamigaito, M., Sawamoto, M. *Macromolecules* **1997**,
        30, 2249-2253.

(59)   Kotani, Y., Kamigaito, M., Sawamoto, M. *Macromolecules* **1999**, *32*, 2420-
        2424.

(60)   Moineau, G., Granel, C., Dubois, Ph., Jerome, R., Teyssie, Ph.
        Macromolecules **1998**, *31*, 542-544.

(61)   Tang, W., Matyjaszewski, K. *Macromolecules* **2006**, *39*, 4953-4959.

(62)   Matyjaszewski, K., Patten, E., Xia, J. *J. Am. Chem. Soc.* **1997**, *119*, 674-680.

(63)   Matyjaszewski, K., Davis, K., Patten, T.E., Wei, M. *Tetrahedron* **1997**, *53*,
        15321-15329.

(64)   Parker, J., Jones, R.G., Holder, S.J. *Macromolecules* **2000**, *33*, 9166-9168.

(65)   Saam, J. C., Gordon, D.J., Lindsey, S. *Macromolecules* **1970**, *3*, 1-4.

_____

(66)   Tezuka, Y., Nobe, S., Shiomi, T. *Macromolecules* **1995**, *28*, 8251-8258.

(67)   Bellas, V., Iatrou, H., Hadjichristidis, N. *Macromolecules* **2000**, *33*, 6993-
        6997.

(68)   Bernard, J., Hao, X., Davis, T.P., Barner-Kowollik, C., Stenzel, M.H.
        Biomacromolecules **2006**, *7*, 232-238.

(69)   Coca, S., Paik, H., Matyjaszewski, K. *Macromolecules* **1997**, *30*, 6513-6516.

(70)   Bielawski, C. W., Morita, T., Grubbs, R.H. *Macromolecules* **2000**, *33*, 678-
        680.

(71)   Liu, P., Wang, T. *Ind. Eng. Chem. Res.* **2007**, *46*, 97-102.

(72)   Helms, B., Mynar, J.L., Hawker, C.J., Frechet, J.M.J. *J. Am. Chem. Soc.*
        2004, *126*, 15020-15021.

(73)   Johnson, J. A., Lewis, D.R., Diaz, D.D., Finn, M.G., Koberstein, J.T., Turro,
        N.J. *J. Am. Chem. Soc.* **2006**, *128*, 6564-6565.

(74)   Harrod, J. F., Chalk, A.J. *J. Am. Chem. Soc.* **1964**, *86*, 1779-1779.

(75)   Sakaki, S., Mizoe, N., Sugimoto, M. *Organometallics* **1998**, *17*, 2510-2523.

(76)   Lewis, L. N. *J. Am. Chem. Soc.* **1990**, *112*, 5999-6004.

(77)   Langmuir 2005, 699-704Lewis, L.N., Lewis, N. *J. Am. Chem. Soc.* **1986**, *108*,
        7288-7231.

(78)   Faglioni, F., Blanco, M., Goddard, W.A., Saunders, D. *J. Phys. Chem. B*
        2002, *106*, 1714-1721.

(79)   Stein, J., Lewis, L.N., Gao, Y., Scott, R.A. *J. Am. Chem. Soc.* **1999**, *121*,
        3693-3702.

(80)   Huang, J., Liu, Z., Liu, X., He, C., Chow, S.H., Pan, J. *Langmuir* **2005**, *21*,
        699-704.

(81)   Williamson, D. T., Buchanan, T.D. Elkins, C., Long, T.E. *Macromolecules*
        2004, *37*, 4505-4511.

(82)   Bates, F.S., *Block copolymer thermodynamics.* In Bates, F. S., Fredrickson,
        G.H. editors, *Annual Review of Physical Chemistry*, Vol. 41; California:
        Annual Reviews Inc. **1990**.

(83)   Leibler, L. *Macromolecules* **1980**, *13*, 1602-1617.

(84)   Olmsted, P. D., Milner, S.T. *Macromolecules* **1998**, *31*, 4011-4022.

(85)   Chaumont, P., Beinert, G., Herz, J., Rempp, P. *Polymer* **1981**, *22*, 663-666.

(86)   Chu, J. H., Rangarajan, P., Adams, J.L., Register, R.A. *Polymer* **1994**, *36*,
        1569-1575.

(87)   Fujimura, M., Hashimoto, H., Kurahashi, K., Hashimoto, T., Kawai, H.
        Macromolecules **1981**, *14*, 1196-1202.

(88)   Ohta, T., Kawasaki, K. *Macromolecules* **1986**, *19*, 2621-2632.

_____

(89)   Anderson, D. M., Thomas, E.L. *Macromolecules* **1988**, *21*, 3221-3230.

(90)   Hajduk, D. A., Harper, P.E., Gruner, S.M., Honeker, C.C., Kim, G., Thomas, E.L., Fetters, L.J. *Macromolecules* **1994**, *27*, 4063-4075.

(91)   Grason, G. M., Kamien, R.D. *Macromolecules* **2004**, *37*, 7371-7380.

(92)   Honda, T., Kawakatsu, T. *Macromolecules* **2007**, *40*, 1227-1237.

(93)   Soltani, R., Laupretre, F., Monnerie, L. *Polymer* **1995**, *36*, 275-282.

(94)   Simon, P., Adhikari, R., Lichte, H., Michler, G.H., Langela, M. *J. Appl. Polym. Sci.* **2005**, *96*, 1573-1583.

(95)   Chen, X., Gardella Jr, J.A. *Macromolecules* **1998**, *31*, 9328-9336.

(96)   Chen, X., Gardella Jr, J.A., Kumler, P.L. *Macromolecules* **1992**, *25*, 6631-6637.

(97)   Chen, X., Gardella Jr, J.A., Kumler, P.L. *Macromolecules* **1993**, *26*, 3778-3783.

(98)   Chen, X., Gardella Jr, J.A., Ho, T., Wynne, K.J. *Macromolecules* **1995**, *28*, 1635-1642.

(99)   Chen, X., Lee, H.F., Gardella Jr, J.A. *Macromolecules* **1993**, *26*, 4601-4605.

(100)   Zhu, Y., Otsubo, M., Honda, C. *Polym. Test.* **2006**, *25*, 313-317.

(101)   Pasch, H., *Chapters 1,2 and 3.* In Pasch, H., Trathnigg, B. editors, *HPLC of Polymers*; Springer-Verlag: Berlin, **1998**.

(102)   Macko, T., Hunkeler, D. *Adv. Polym. Sci.* **2003**, *163*, 61-136.

(103)   Berek, D., Hunkeler, D. *J. Liq. Chrom. & Rel. Technol.* **1999**, *22*, 2867-2878.

(104)   Berek, D. *Macromolecules* **1998**, *31*, 8517-8521.

(105)   Phlllpsen, H. J. A., Klumperman, B., van Herk A.M., German, A.L. *J. Chromatogr. A* **1996**, *727*, 13-25.

(106)   Bashir, M. A., Brull, A., Radke, W. *Polymer* **2005**, *46*, 3223-3229.

(107)   Park, I., Park, S., Cho, D., Chang, T., Kim, E., Lee, K., Kim, Y.J. *Macromolecules* **2003**, *36*, 8539-8543.

(108)   Graef, S. M., Van Zyl, A.J.P., Sanderson, R.D., Klumperman, B., Pasch, H. *J. Appl. Polym. Sci.* **2003**, *88*, 2530.

(109)   Venkatesh, R., Klumperman, B. *Macromolecules* **2004**, *37*, 1226-1233.

-46-

Chapter 3

Experimental

This chapter gives a general overview of the experimental procedures followed in the synthesis of the block copolymers, as well as the analytical instrumentation, conditions and sample preparation used.

_____

3.1   Synthesis

All glassware, including reaction vessels and syringes, were dried in an oven at 120°C overnight after rigorous cleaning. Reactions were carried out in a dry-box under high purity argon gas or flushed with argon prior to use.

3.1.1   Materials

Styrene (Plascon, tech. grade) was washed with a 0.3M potassium hydroxide (KOH, Associated Chemical Enterprises, 85%) solution, followed by distillation at reduced pressure to remove inhibitor. The distillate was then dried over excess magnesium sulphate (MgSO$_4$, Riedel-de Haen, 99.5%) then purged and stored under argon (Ar, Afrox Scientific UHP Cyl 17.4kg N5.0, 99.999%) gas in sealed flasks. Monomers were stored at 0°C prior to use. Hexamethylcyclotrisiloxane (D$_3$, 98%); chlorodimethylsilane (CDMS, 98%); allyl-chlorodimethylsilane (ACDMS, 98%); allyl-2-bromo-2-methyl-propionate (ABMP, 98%); 4,4'-dinonyl-2,2'-bipyridyl (dNbipy, 97%); butyllithium (BuLi, 15% in hexane); bromobenzene (Br-benzene, 98%); platinum(0)-1,3-divinyl-1,1,3,3-tetramethyl- disiloxane complex (Karstedts catalyst, 1M in xylene)(all Aldrich), were used as received. Mono-methacryloxypropyl terminated polydimethylsiloxane (MMP-PDMS, Gelest Inc., Mw: 10 000; 5 000; 1 800) were used as received. 2-Methyl-1,4-naphthoquinone (MENQ, Fluka, 97%) was used as received. Solvents toluene (Kimix, 99.8%) and tetrahydrofuran (THF, R&S enterprises, 99.0%) were dried and distilled over sodium metal and benzophenone (BP, Sigma, 98%) under argon (Ar, Afrox Scientific UHP Cyl 17.4kg N5.0, 99.999%) prior to use. 1,4-Dioxane (Dioxane, Saarchem, 95%) was used as received. Styrene polymerisations were preformed under nitrogen (N$_2$, Afrox Scientific UHP Cyl 11kg N5.0, 99.999%). Methanol (MeOH, Sasol, Class 3) was used to precipitate out the synthesised polymer. Solvents for chromatography analysis were tetrahydrofuran (THF, HPLC grade) and n-hexane (Hexane, HPLC grade) both from Sigma-Aldrich.

3.1.2   Purification of monomers

Styrene monomer was washed with a 0.3M KOH solution three times in a 1:1 volume ratio to remove any inhibitor present and separated using a separation funnel. The resultant yellow liquid was then decanted into a round bottomed flask containing glass beads and connected to a condenser and fraction collector. Distillation under

_____

reduced pressure[1] was carried out at 35°C so as to avoid thermal auto-polymerisation of the monomer. The first fraction was collected and discarded followed by collection of the clean purified fraction. The distillate was then dried over anhydrous magnesium sulphate and flushed with argon gas to ensure complete removal of moisture. The monomer mixture was then filtered using a funnel and filter paper under an argon blanket. The filtrate was then sealed and purged with Ar gas for 15 minutes prior to use.

3.1.3 Purification of solvents

Toluene and THF had to be purified and dried to remove all traces of water so as not to contaminate the highly sensitive reactions. This was achieved using a solvent still apparatus. Finely sliced sodium metal pieces, together with benzophenone were used to remove trace amounts of moisture[2]. Once heated the solvents turned a characteristic deep blue colour due to the benzophenone ketyl formation and were allowed to reflux for 2 hours before collection. A connector with a glass tap was used so that the collected solvent could be transferred to the dry-box avoiding atmospheric contamination.

3.1.4 Anionic polymerisation of polystyrene

The following section describes the experimental procedures used to synthesise the polystyrene (PS) polymers and subsequent functionalisation of these molecules. styrene was polymerised using anionic polymerisation to ensure control over the molecular weight and polydispersity of the synthesised PS. This reaction is very straight forward, complicated only by the need to work in extremely clean and dry conditions. A typical procedure used was as follows. Dried toluene and distilled styrene were added via syringe to a 250ml one necked round bottom flask sealed with a rubber septum. The ratio of monomer to solvent was typically 10:1 (toluene:Sty) by volume. Stainless steel needles and glass syringes were used to avoid contamination due to plastic dissolution. These were purged with Ar before use. The flask was then submerged in an oil bath at ambient temperatures. The toluene and styrene solution was stirred for 5 minutes while purging the reaction mixture with Ar. Initiation was achieved by adding sec-BuLi solution to the reaction mixture via syringe. The amount of initiator added to the concentration of monomer

_____

present determines the degree of polymerisation according to the following relationship[3], in equation 3.1.

$$DP_n = [M_o]/[I_o] \qquad\qquad 3.1$$

Where DP_n is the degree of polymerisation and M_o and I_o are the moles of initial monomer and initiator (BuLi) present. Multiplying the DP_n with the molecular mass of one repeat unit gives the expected molecular weight of the polymer. Thus the amount of initiator added is determined by the desired molecular weight. After addition of the initiator the reaction mixture turns orange, characteristic of the living styrillithium anion. The reaction was left to run for 35 minutes at room temperature (RT) while stirring continuously. Termination of the reaction was achieved by adding CDMS or ACDMS for silane or vinyl functionality respectively. The reaction mixture immediately become colourless as the styrillithium anion terminated. The reaction scheme can be seen in scheme 3.1.
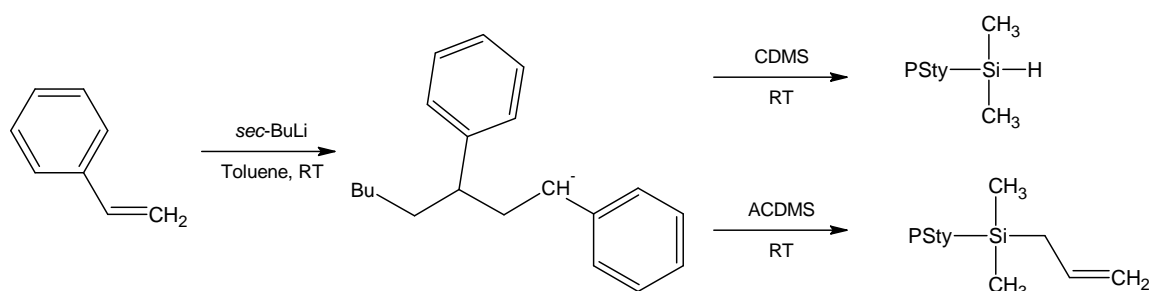
Scheme 3.1   Anionic polymerisation and termination of functionalised PS.

After 1 hour the contents of the flask was added slowly to rapidly stirring MeOH, causing the PS to precipitate out of solution. The precipitate was then filtered and dried under vacuum at 50°C, until constant weight, to remove any unreacted monomer and terminating agents.

3.1.5 Anionic polymerisation of polydimethylsiloxane

Anionic ring opening polymerisation of D_3 was employed to synthesise polydimethylsiloxane (PDMS) molecules. This procedure requires extremely stringent conditions, including: thoroughly cleaned and dried equipment (dried at 120°C overnight), no moisture or oxygen (Ar atmosphere). Schlenk tubes were utilised as the reaction vessels and were sealed with rubber septums and purged with Ar before

_____

use. All transfer of reagents into the reaction vessel were performed using glass syringes with stainless steel needles. The procedure used was as follows. The reaction vessel was charged with D_3 under Ar and sealed. Dried toluene and THF in a (30:70) v/v ratio were then added to the reaction vessel. The ratio of solvent to monomer was typically kept at (1:1) v/w. The mixture was stirred allowing the D_3 to dissolve. Initiation was achieved by the addition of BuLi to the reaction mixture. The amount of BuLi added is determined by the molecular weight desired, as shown in equation 3.1. The reaction was left to run at room temperature for 4 hours while stirring continuously. Termination of the reaction was achieved by adding CDMS for silane functionality or ACDMS for vinyl functionality. The mixture was then left to stir overnight. Removal of lithium chloride (LiCl) salt was achieved by filtering the reaction mixture through a 0.45μm filter. Solvent was then removed using a rotary evaporator. In most cases it was then necessary to redissolve the PDMS in hexane and then filter again using a 0.45μm filter to remove residual LiCl salt. The mixture was then rotary evaporated again and placed in a vacuum oven at 50°C, until constant weight, to remove unreacted terminating agents. The reaction scheme can be seen in scheme 3.2.
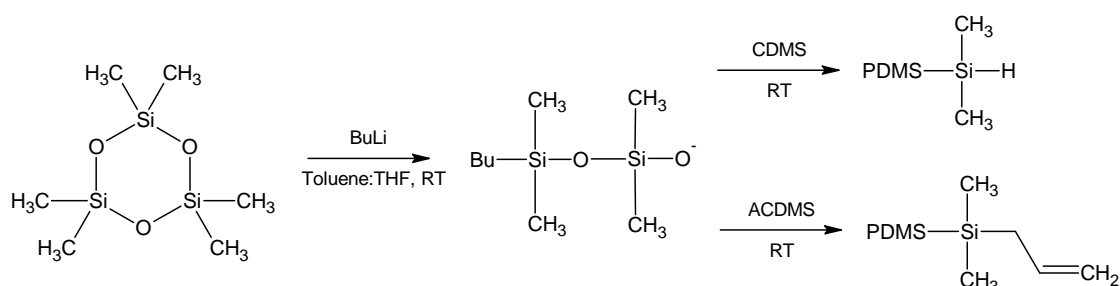
Scheme 3.2   Anionic polymerisation and termination of functionalised PDMS

3.1.6   Coupling reaction to synthesise block copolymers

The hydrosilylation reaction was used to couple the PS and PDMS prepolymers. This widely used reaction involves the coupling of a silane terminal species with a vinyl terminated species[4,5]. The synthesis of the PS and PDMS functionalised prepolymers has already been explained in section 3.1.4 and 3.1.5 of this chapter. A typical hydrosilylation coupling reaction was as follows. A Schlenk tube was charged with the functionalised PS and PDMS prepolymers in a 1:1 molar ratio as well as a magnetic stirrer bar. The reactor was then sealed and purged with N_2 gas for 10 minutes. Once purged, toluene was added to the reactor via syringe. The amount of

_____

solvent added typically gave a 50% solids content with regards to prepolymer added. The reactor was then submerged in an oil bath at 70°C while stirring. Once the prepolymer was fully dissolved the catalyst was added. The amount of Karstedt's catalyst used was typically kept at a 100:1 ratio with respect to the mol prepolymer present. The reaction was then allowed to proceed at 70°C for 24 hours. The final product was then added slowly to rapidly stirring methanol and the precipitate was filtered and dried in a vacuum oven at room temperature. See scheme 3.3.
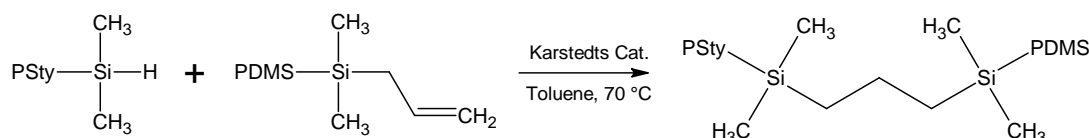
Scheme 3.3   Hydrosilylation coupling reaction to synthesise block copolymer

3.1.7   Sequential anionic block copolymerisation

It was found that it is best to initiate this polymerisation with the growth of PS followed by PDMS growth[6,7]. A typical procedure used was as follows. A Schlenk tube, clean, dried and flushed with Ar gas served as the reaction vessel. All transfer of monomer and solvent took place in a dry-box under Ar gas. The reactor was charged with styrene and toluene in a 1:1 volume ratio. Freeze-thaw cycles were repeated 3 times to ensure all oxygen removal. Depending on the molecular weight desired the required amount of BuLi solution, according to equation 3.1, was added to this mixture. The deep orange solution was allowed to react for 30 minutes at room temperature. After 30 minutes D_3 was added to the reaction vessel. This new mixture was then allowed to stir for 12 hours at room temperature or until the orange colour totally disappeared. Once colourless, THF was added to the reaction vessel, enough to ensure a 1:1 volume ratio with the toluene. This reaction mixture was then allowed to stir for 2 hours at room temperature. After 2 hours the temperature of the reaction vessel and contents were lowered to -20°C. The reaction was then continued at this lowered temperature for 7 days. The reaction mixture was finally placed on a rotary evaporator to remove solvent and further dried in a vacuum oven at 30°C until constant weight.

_____

3.1.8 ATRP macroinitiator method

This technique involved the synthesis of a PDMS macroinitiator that was used to initiate the ATRP polymerisation of St using CuCl as catalyst and dNbipy as ligand. First the PDMS was synthesised according to the procedure mentioned in section 3.2.3 yielding silane functionalised PDMS molecules. The silane group was then modified to produce the bromoisobutyrate-macroinitiator for the ATRP reaction as follows[8-10]. A hydrosilylation reaction was employed. A Schlenk tube flushed with Ar served as reaction vessel. The vessel was charged with silane terminal PDMS. To this was added dried toluene to give a 30% solids content. The ABMP compound was then added in 50% molar excess to the mol silane functional groups present. The reaction vessel was then purged with Ar gas for 15 minutes. Once purged, Karstedt's catalyst was added, 1% (mol) with regards to mol silane present. MENQ (stock solution) was then added to the reaction mixture in a 1:2 mol ratio (Karstedt's:MENQ). The reaction vessel was then submerged in an oil bath at 70°C and allowed to react overnight. Solvent was removed using a rotary evaporator and the product was dried in a vacuum oven at 50°C to remove excess solvent and unreacted ABMP. The reaction scheme is presented in scheme 3.4.
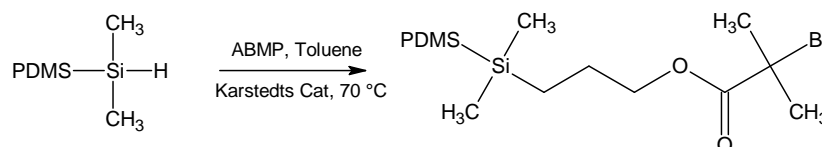
Scheme 3.4   Modification of silane terminal PDMS to ATRP macroinitiator

The ATRP procedure was as follows. A clean dry Ar flushed Schlenk tube served as reaction vessel and all transfer of reagents took place in a dry-box under Ar. The reaction vessel was charged with the bromoisobutyrate-functionalised PDMS macroinitiator. To this was added the styrene monomer and toluene. The toluene added typically gave a 40% solids content and the amount of styrene added was determined by the molecular weight desired according to the following relationship[11].

$$DP_n = [M]/[I_o] \qquad\qquad 3.2$$

Similarly to anionic polymerisation the ratio of consumed monomer to initiator determines the molecular weight. This, however, only holds true for low conversions

_____

of monomer[11]. Three freeze-thaw vacuum cycles were performed to remove any oxygen still present. The CuCl and dNbipy ligand were pre-weighed and mixed along with 1.5ml toluene in a 50 ml conical flask. The ratio of CuCl:dNbipy was kept at 1:2. After the freeze-thaw cycles the metal ligand mixture was added to the reaction mixture while stirring. The reaction vessels were then sealed and submerged in an oil bath at 100 $^{\circ}$C for approximately 24 hours. The reaction proceeded relatively slowly at this temperature, but it was necessary to prevent thermal initiation of Sty monomer.[12] The resultant product was rotary evaporated to remove solvent and dried at 50 $^{\circ}$C overnight in a vacuum oven till a constant weight. The dried product was then redissolved in THF and Cu^{+} ions were removed using a 1 inch alumina column flushed with THF. The collected fraction was then rotary evaporated and dried in a vacuum oven once again to remove solvent traces.
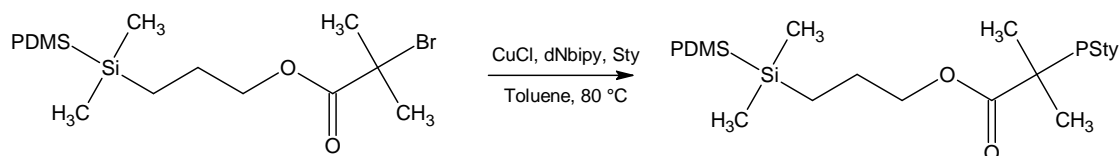
Scheme 3.5   ATRP with PDMS macroinitiator and polymerisation of PS block.

3.1.9 Extraction of homopolymers

Solvent extraction was used to extract unreacted PDMS and PS homopolymer from the block copolymer product material. The procedure for PS extraction found in literature[13] was as follows. The polymer was dissolved in dioxane containing 0.1% BHT to give a 1.3% solution. This solution was then titrated with a 50/50 mixture of MeOH and water until it became milky. This is where the difficulty of this extraction method came to light. The milky precipitate is the block copolymer that preferentially precipitates out of solution. However, if too much of the MeOH / water mixture is added, the homo-PS also precipitates out of solution. Therefore care must be taken not to add too much non-solvent mixture. Multiple extractions with the addition of small non-solvent amounts is the best route to follow.

PDMS proved to be much easier to extract. The procedure was found in literature[14]. In this case the polymer is dissolved in bromobenzene at a concentration of 0.05 g/ml. The solution is then cooled to 0 $^{\circ}$C and centrifuged at 2000 rpm for 30 minutes. PDMS homopolymer floats on the surface of the solution after centrifugation, while

_____

the block copolymer remains in solution. The best route to isolation of the PDMS layer, was by drawing out the block bromobenzene solution with a syringe, until only the PDMS layer was left in the centrifugation tube. Usually two extraction procedures were followed to maximise the removal of the unreacted PDMS homopolymer. The remainder is difficult to remove, as it is too little to form a definite layer on top of the bromobenzene solution in the centrifuge tube.

3.2 Characterisation

This section describes the equipment, conditions and sample preparation used during analysis or characterisation of the synthesised polymer materials.

3.2.1 Size exclusion chromatography (SEC)

This chromatographic technique separates polymer molecules according to size, or more correctly hydrodynamic volume. Depending on whether the chromatographic medium is a gel or not, the technique is also referred to as gel permeation chromatography (GPC). The SEC instrument used in this project comprised of the following units: Waters 1515 isocratic HPLC pump; Waters 717 plus Autosampler; Waters 2487 Dual λ Absorbance detector; Waters 2414 Refractive index (RI) detector at 30°C and data processing was performed using Breeze Version 3.30 SPA (Waters) software. Separation was achieved using two PLgel (Polymer Laboratories) 5μm Mixed-C (300×7.5mm) columns connected in series along with a PLgel 5μm guard column (50×7.5mm). The columns were kept at a constant temperature of 30°C. THF Chromasolve HPLC grade solvent (0.125% BHT stabilised) was used as mobile phase at a flow rate of 1ml/min. Samples were dissolved in the stabilised THF at a concentration of 5mg/ml and 100μl injection volumes were used. The system was calibrated using Polymer Laboratories PS Standards. It must be highlighted that due to PDMS and THF having almost identical refractive indexes (respectively) the RI detector was not suitable for obtaining chromatograms of the PDMS material. In this case analysis was achieved using a PL-ELS 1000 Evaporative light scattering detector (ELSD).

_____

3.2.2 Liquid chromatography at critical conditions (LC-CC)

One of the objectives of this project was to develop a chromatographic method that allowed LC-CC separation at the critical point of PS for PS-block-PDMS copolymers. The PDMS containing block copolymers had to elute in SEC mode. In this analytical technique, elution of the PS chains takes place independently of their molecular mass or hydrodynamic volume[15]. Therefore they elute at a constant elution volume and remain unseparated regardless of their molecular mass. Elution and separation of the PDMS-block-PS chains rely solely on the molecular weight of the PDMS segments. This technique was performed using a dual pump HPLC comprising the following units: Waters 2690 Separations module (Alliance); Agilent 1100 series variable wavelength detector; PL-ELS 1000 detector and data was recorded and processed using PSS WinGPC unity (Build 2019) software. The conditions used for the LC-CC separation were as follows. The mobile phase solvent composition used was hexane(adsorli):THF(desorli) (55:45) at a flow rate of 1ml/min. A bare silica column was used (Nucleosil 300Si 5μm 250×0.46mm Technokroma) at 30°C. Samples were prepared in the same solvent composition as the mobile phase, at concentrations of 5mg/ml. In this instance the solvent composition was varied and PS standards were run until the various molecular weight PS chains eluted at the same retention volume.

3.2.3 LC-CC coupled to FT-IR using the LC-Transform

This is an extremely powerful technique, in that it provides a connection between a chromatographic and spectroscopic technique. It allows one to view infra-red (IR) spectra of individual components of a chromatographically separated material. This is an offline coupled technique where the LC-transform instrument acts as the interface between the HPLC and the FT-IR instruments. Figure 3.1 below illustrates exactly how this technique works. The first step shows the chromatographic separation of the polymer material as explained in the previous section 3.2.2. The eluent with fractionated sample exits the HPLC instrument and enters the LC-Transform unit. It then flows into a sealed chamber under vacuum and exits via a nebulising nozzle. The nozzle is heated which aids in the evaporation of the mobile phase solvent. The germanium disk onto which the eluted fractions are deposited is on a heated rotating stage.

HPLC

LCCC

Fractionation of sample according to LC-CC mode.

Deposition of eluting sample onto germanium disk.

FT-IR spectra of each eluted fraction recorded.

Processing of data to yield 2D graphic representations, Gram-Schmidt plots and chemigrams.
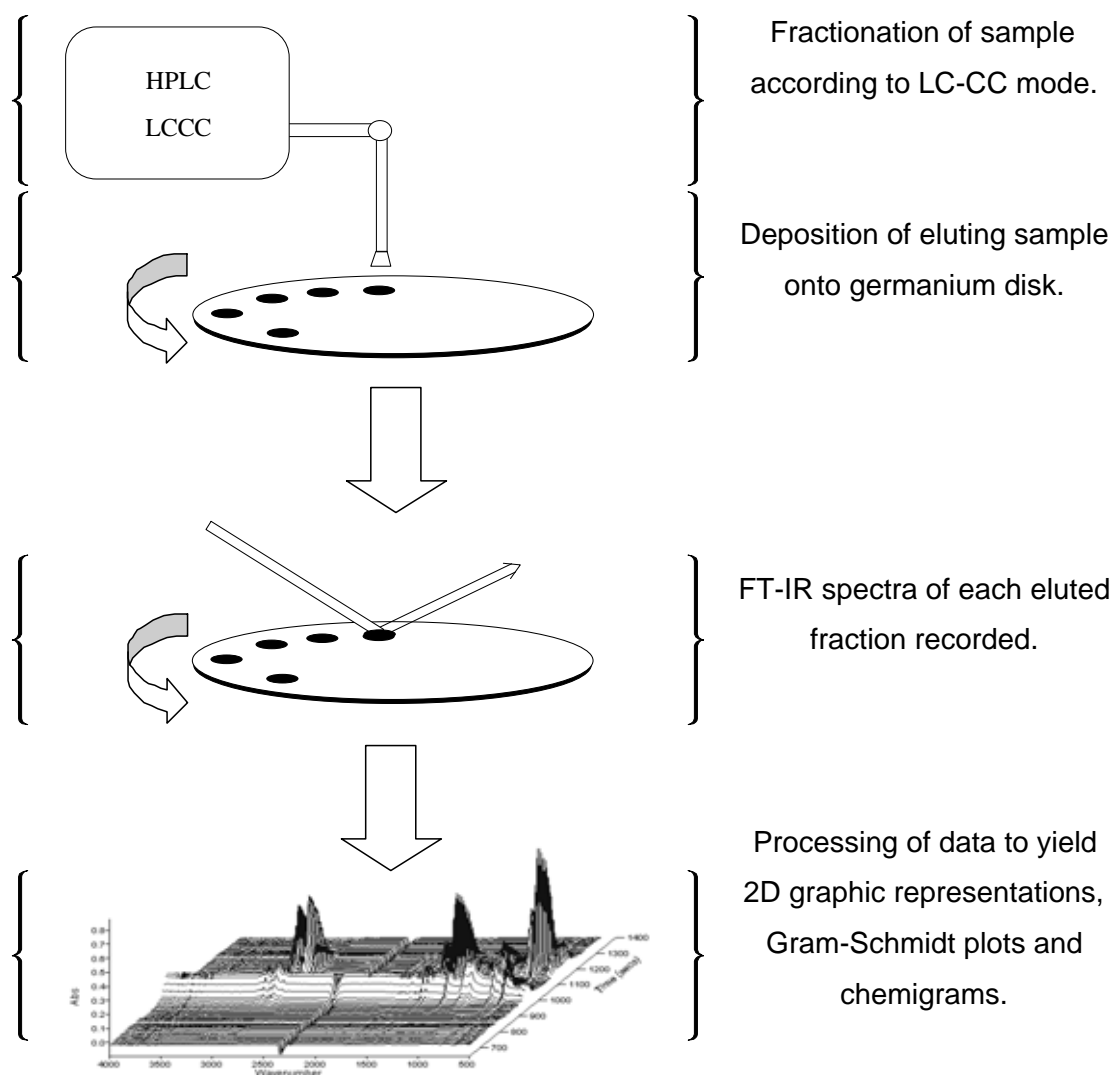
Figure 3.1   Stepwise illustration of the LC-Transform technique.

The heated stage evaporates any residual solvent which is pulled off by the vacuum pump leaving only the deposited polymeric material. The stage can be rotated at set speeds, those typically used in this project was $10^{o}.min^{-1}$ and $20^{o}.min^{-1}$. As the eluting material is deposited on the rotating disk one can see in the figure that the material spreads out in a thin strip along the outer rim of the disk. Once all eluted material is deposited the disk is removed from the LC-transform chamber and placed into a LC-Transform FT-IR unit, inside the FT-IR instrument sample chamber. The unit also rotates the disk at the same speed at which the sample was collected. This then enables the FT-IR to scan each eluted fraction as it would have exited the HPLC instrument as shown in figure 3.1. One can then obtain two-dimensional information where we have the elution time versus IR spectra as shown in figure 3.1. Processing

_____

of the data allows development of Gram-Schmidt plots and chemigrams which provide a wealth of information with regards to chemical composition of the analysed materials. The FT-IR instrument used for analysis was a Perkin Elmer, FT-IR spectrometer (Paragon 1000) with Spectrum TimeBase Version 2.0 software (Perkin Elmer) for processing of data. Typical LC-transform conditions during deposition were; nozzle (28°C), rotating stage (80°C) and a vacuum of 9 torr.

3.2.4 Gradient elution chromatography (GEC)

This technique is widely employed in the separation of polymers according to chemical composition[16]. This technique allows separation of block copolymer molecules from their respective homopolymers. This is achieved by varying the mobile phase solvent composition. This technique was performed using a dual pump HPLC comprising of the following units: Waters 2690 Separations module (Alliance); Agilent 1100 series variable wavelength detector; PL-ELS 1000 detector and data was recorded and processed using PSS WinGPC unity (Build 2019) software. The mobile phase flow rate was maintained at 1ml/min and the composition varied as described in section 4.2.2.3. A bare silica column was used (Nucleosil 300Si 5μm 250×0.46mm Technokroma) at 30°C. Samples were prepared in a solution of THF:hexane (20:80), and at a concentration of 5mg/ml.

3.2.5 Nuclear magnetic resonance (NMR)

^{1}H-NMR and ^{13}C-NMR were performed as routine analysis for the determination of molecular structure, and termination (with functionality) efficiencies. Routine identification was achieved using a Varian VXR, 300MHz, Spectrometer. When precise integration data was needed the Varian ^{Unity} Inova, 400MHz or 600MHz was used. Samples were prepared in NMR borosilicate tubes. Typically, 60mg of sample was added to the sample tube, topped up with *d*-chloroform to the 5mm height mark.

3.2.6 Film sample preparation

Samples were dissolved in dried THF and then added drop-wise to a Petri-dish containing distilled water. The THF, being miscible with water, diffused into the solution, while the hydrophobic polymer sample remained floating on the surface. The rapid diffusion of THF causes the dissolved polymer to spread over the water

_____

surface rapidly, as it precipitates onto the water surface. This allows development of thin films for various analytical needs. By varying the concentration of the polymer in THF one can vary the film thickness. Films are then scooped up off the surface onto supportive backing, such as glass slides or various grids depending on the analyses required.

3.2.7   Corona surface modification

A corona is a process by which a current develops from an electrode in a neutral fluid such as air. This is achieved by ionisation of the air to create a plasma around the electrode[17]. Depending on the shape of the electrode tip, and the charge gradient built up, a fully conductive path can be created resulting in a continuous arc. The free radicals and ions lead to the production of ozone. When this conductive path impinges on a polymeric surface, like that of PDMS, the ion bombardment and ozone causes a degradation of the surface layer. This surface modification leads to the switching between hydrophobic and hydrophilic surface properties of PDMS, as mentioned earlier in section 2.4.2. Figure 3.2 is a schematic diagram of the desktop corona discharger used in this study. A model BD-20 AC high frequency corona treater, supplied by Electro-Technic product (USA) was used. Sample preparation involved dripping a solution of the block copolymer, in distilled THF, into a Petri-dish containing distilled water. This formed a film in the same way as described in the section 3.2.6.
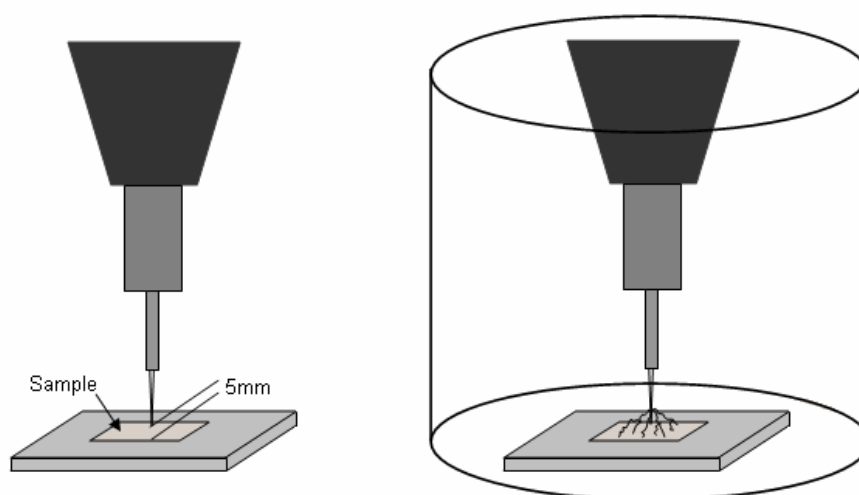
Figure 3.2   A schematic diagram of the desktop corona discharger showing tip to sample distance and operation in a glass beaker.

_____

For corona surface modification, typical concentrations were 40-50mg/ml. Normally, 2-3 drops of the solution gave sufficient film formation. The film was then "scooped" onto a glass slide as support backing. The sample was then placed in an oven to anneal for 48h at 120°C, promoting PDMS surface segregation. As can be seen in figure 3.2, the sample was kept at a distance of 5mm from the electrode tip. The sample is placed inside a glass beaker, to prevent dissipation of ozone into the atmosphere. Once powered, a visible purple arc impinged onto the polymer surface. The duration of the discharge varied between 1 to 30 minutes. After corona, samples were covered to prevent contamination and used for subsequent analysis.

3.2.8 Optical microscopy

This microscopic technique uses visible light, along with a series of lenses to obtain magnified images of a specific sample. A Carl Zeiss optical microscope unit (Axiolab) was used in this project. Images were captured using a Sony Hi Resolution CCD-IRIS colour video camera (model number SSC-C370P). The imaging software used was Honestech's V-stream, PVR-Plus program. Sample preparation was once again achieved using the film formation on water method, described in section 3.2.6. Sample films were then slid onto glass microscope slides for analysis.

3.2.9 Static contact angle measurements

This technique was used to monitor the changes in hydrophobicity of the polymer samples upon corona degradation. Analysis was performed at room temperature. The same film samples, used for the optical microscopy analysis, were also used for contact angle measurements. Magnification was once again achieved using the Zeiss microscope unit mentioned in the previous section 3.2.8. A 1μl drop of distilled water was placed onto the sample film and the magnified image was captured using a Nikon SMZ-2T (Japan), model VCC 250C digital video camera. Figure 3.3 shows an example of a captured image. Included on the image are the parameters used to determine the static contact angle according to the relationship in equation 3.3. PVR-plus software was used for imaging along with Able Image Analyser (μ-labs) version V3.6, which enabled determination of the lengths associated with contact angle calculation.

_____
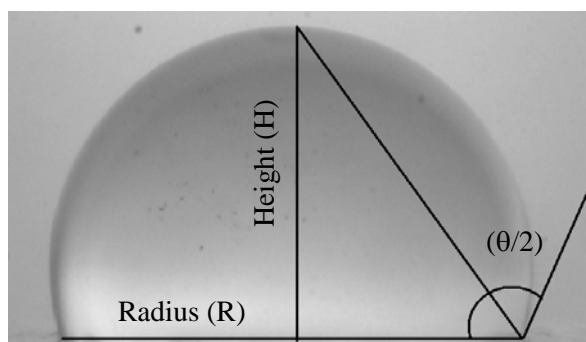
Figure 3.3   Image of water drop showing the height and radius used in determination of the contact angle Θ.

$$\theta = 2 \times tan^{-1}(H/R) \qquad\qquad 3.3$$

To minimise human error, a minimum of ten droplets were measured and average values were calculated.

3.2.10 Scanning electron microscopy (SEM)

Unlike the TEM microscope, this instrument uses electron back scattering to produce high resolution images of a sample surface. The resultant image is useful in evaluating surface structure and topography of a sample. Samples were prepared by film deposition on water as described previously in section 3.2.6. The films were then slid onto SEM pegs and subsequently coated in gold sputter. Analysis was performed using a Leo 1430VP Scanning Electron Microscope fitted with Backscatter, Cathodoluminescence, Variable pressure and Energy Dispersive detectors, as well as a Link EDS system and software for microanalysis.

3.2.11 Transmission electron microscopy (TEM)

This is an imaging technique whereby a beam of electrons is focused on a sample specimen. Differences in the electron densities of the sample are detected, developing an enlarged image of the focused area. This technique allows high resolution and magnification of sample morphology. Staining is usually required for imaging, but in this case the large difference between the electron densities of the PDMS and PS segments allowed imaging without staining. TEM images were obtained from a JEOL 1200 EXII instrument at the University of Cape Town's electron microscopy unit. Samples were prepared by casting a thin film onto the

_____

surface of distilled water as mentioned in section 3.2.6. This method allowed the preparation of films thin enough for TEM analysis. The samples are then "scooped" onto copper TEM grids and placed in a vacuum oven at 120°C for 48h to anneal. By varying the concentration of the polymer in THF, the thickness of the resultant film can be changed. Typical concentrations of the polymer samples in THF were approximately 5mg/ml.

3.2.12 Slow positron beam studies

Positrons (e^+) are anti-electrons. A positron has the same mass as an electron, a spin of ½ but a charge of (+1). When a positron collides with an electron, the two particles completely annihilate and their masses are converted to energy in the form of photons. These photons carry information on the electronic environment in which the annihilation occurred. Positrons and electrons can also combine and form a bonded state known as positronium. This technique is well recognised as a powerful tool in performing micro structural analysis of polymeric materials[18]. Direct determination of the free volume properties of polymeric materials is possible using this technique. It also has the ability to track structural changes at the very surface of polymer specimens, which is what makes it attractive to analyse the materials in this project. A basic overview of how this technique works is presented next.

In this study, radioactive ^{22}Na was used as the positron source. The positrons are accelerated from a vacuum into the sample, at which point they either penetrate the sample, or are reflected back to the surface. Once inside the sample, they localise themselves inside the free volume holes of the polymer, as positronium. Depending on the size of the hole, the positronium particles have different momentum as the move inside the space. Upon collision with electrons on the free volume hole walls, annihilation occurs. The energy given off is dependant on the various momentums of the positron particles and once detected, provides information on the free volume hole size.

In this study the positron beam results are reported as the S parameter, or defect parameter, and it is calculated from the Doppler broadening energy spectra. The S parameter is defined as the ratio of the central area to the total area of the annihilation peak after background subtraction. This is presented in figure 3.4. The S parameter is thus related to the free volume holes sizes.

_____

By varying the incident energy of the incoming positrons, the depth of penetration can be varied according to the relationship in equation 3.4[19], where Z is the depth pentrated (nm), ρ is the density of the sample (kg/m^3) and E_+ is the incident energy (keV).

$$S = \frac{\sum_{E_1}^{E_2} N(E_i)}{\sum_{0}^{\infty} N(E_i)}$$
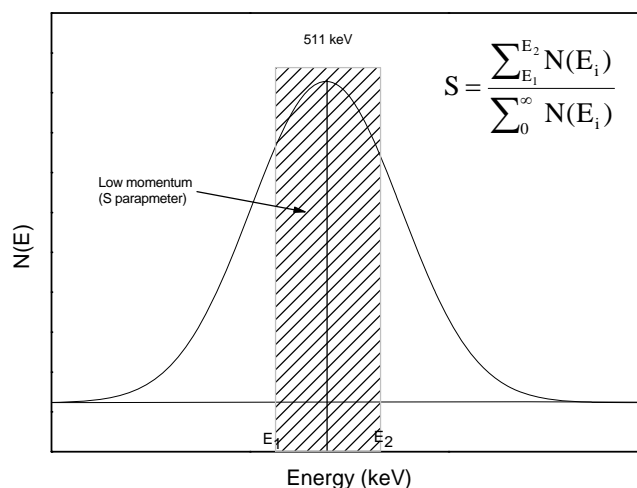
Figure 3.4   The Doppler broadening energy distribution of annihilation radiation and definition of the S parameter.

$$Z(E_+) = (400/\rho)E_+^{1.6} \qquad\qquad 3.4$$

The ability to vary depth of penetration, allows depth profiling. This can provide information on free volume structure from the very surface of the sample ($<1\mu m$), into the bulk material ($\pm 9\mu m$). The variable mono-energetic positron beam at the University of Missouri, Kansas City, USA was used for sample analysis. A detailed description can be found in work by Zhang *et al.*[20] Sample preparation was achieved as described in section 3.2.6.

3.2.13 Attenuated total reflectance (ATR)

This technique allows FT-IR analysis of samples, without the need for strict sample preparation. Sample films were prepared as mentioned in section 3.2.6. Material for analysis was scraped off the glass using a sharp blade. FT-IR analysis was achieved

_____

using a Thermo Nicolet (Nexus model) instrument. The ATR attachment was a Smart Golden Gate accessory (ZnSe lenses) with diamond window.

3.2.14 Confocal raman spectroscopy

This technique relies on inelastic scattering, or Raman scattering of monochromatic light, usually from a laser in the visible, near infrared, or near ultraviolet range. Confocal Raman spectroscopy allows depth profiling of a sample, by focusing the laser at various points along the sample depth.[21] The focusing of the laser is crucial in obtaining good Raman spectra. The difficulty with the samples under study in this project is that they are clear. This makes focusing extremely difficult as there is no fixed point to focus on. Films were once again prepared as per the method described in section 3.2.6 of this work. Analysis was achieved using a Hobin Yvon Horiba HR 800UV confocal Raman instrument using the 714nm Green laser at the Swedish Royal Institute of Technology in Sweden.

This concludes the experimental chapter. The following chapter discusses the results of the synthetic and analytical procedures performed.

_____

3.3 References

(1)   Furness, B. S., Hannaford, A.J., Smith P.W.G., Tatchell, A.R. *Vogel's Textbook of practical organic chemistry*, 5th ed.; Pearson Prentice Hall, 2000.

(2)   Schwartz, A. M. *Chem. Eng. News* **1978**, *56*, 88.

(3)   Morton, M. *Anionic polymerization principles and practice*; London: Academic Press Inc., 1983.

(4)   Faglioni, F., Blanco, M., Goddard, W.A., Saunders, D. *J. Phys. Chem. B* **2002**, *106*, 1714-1721.

(5)   Stein, J., Lewis, L.N., Gao, Y., Scott, R.A. *J. Am. Chem. Soc.* **1999**, *121*, 3693-3703.

(6)   Tezuka, Y., Nobe, S., Shiomi, T. *Macromolecules* **1995**, *28*, 8251-8258.

(7)   Bellas, V., Iatrou, H., Hadjichristidis, N. *Macromolecules* **2000**, *33*, 6993-6997.

(8)   Miller, P. J.; Matyjaszewski, K. *Macromolecules* **1999**, *32*, 8760-8767.

(9)   Shinoda, H., Miller, P.J., Matyjaszewski K. *Macromolecules* **2001**, *34*, 3186-3194.

(10)   Shinoda, H., Matyjaszewski, K. *Macromolecules* **2003**, *36*, 4772-4778.

(11)   Matyjaszewski, K., Xia, J. *Chem. Rev.* **2001**, *101*, 2921-2990.

(12)   Parker, J., Jones, R.G., Holder, S.J. *Macromolecules* **2000**, *33*, 9166-9168.

(13)   Zilliox, J. G., Roovers, J.E.L., Bywater, S. *Macromolecules* **1975**, *8*, 573-578.

(14)   Saam, J. C., Gordon, D.J., Lindsey, S. *Macromolecules* **1970**, *3*, 1-4.

(15)   Macko, T., Hunkeler, D. *Adv. Polym. Sci.* **2003**, *163*, 61-136.

(16)   Park, I., Park, S., Cho, D., Chang, T., Kim, E., Lee, K., Kim, Y.J. *Macromolecules* **2003**, *36*, 8539-8543.

(17)   Zhu, Y., Otsubo, M., Honda, C. *Polym. Test.* **2006**, *25*, 313-317.

(18)   Jean, Y. C., Mallon P.E., Zhang R., Chen, H., Wu, Y., Li, Y., Zhang, J. *Chapter 11: Applications of slow positrons to polymeric surfaces and coatings.* In: Jean, Y. C., Mallon, P.E., Schrader, D.M. editors, *Principles and applications of postronium and positronium chemistry*; Singapore: World Scientific Publishing, **2003**.

(19)   Cao, H., Zhang, R., Sundar, C.S., Yuan, J.P., He, Y., Sandreczki, T.C., Jean, Y.C. *Macromolecules* **1998**, *31*, 6627-6635.

(20)   Zhang, R., Cao, H., Huang, C.M., Mallon, P.E., Sandreczki, T.C., Richardson, J.R., Jean, Y.C., Nielson, B., Suzuki, R., Ohdaira, T. *J. Radiat. Phys. Chem.* **2000**, *58*, 639-644.

_____

(21)   Bae, S. C., Lee, H., Lin, Z., Granick, S. *Langmuir* **2005**, *21*, 5685-5688.

-65-

-66-

Chapter 4

Results and discussion

This chapter combines the results obtained from the synthetic and experimental procedures, as well as a discussion of these results.

4.1   Coupling of prepolymers to synthesise blocks

The synthesis and characterisation of PS and PDMS prepolymers terminated with silane or allyl functionality, as well as their coupling via a hydrosilylation reaction, is discussed in this section of work.

4.1.1 Synthesis of PS and PDMS prepolymers

PS chains of varying molecular weight were prepared by living anionic polymerisation and characterised using SEC and NMR to determine efficiency of termination with functionality. In order to determine the optimal time for termination, it was necessary to determine the conversion of PS with time. This is shown in figure 4.1.
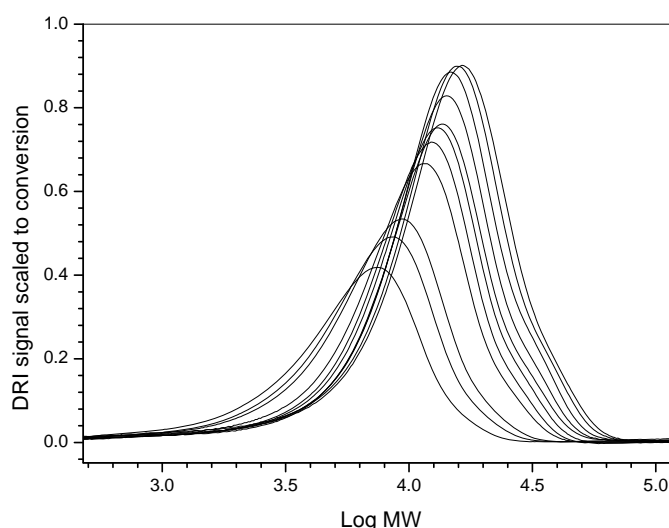
Figure 4.1   SEC overlays of PS % conversion with Log(MW).

It is clear from the above result that PS conversion reaches a maximum at approximately 30 minutes. It was thus decided that termination of all subsequent PS reactions would be done after 30 minutes reaction time. It is important to note that at 30 minutes we have approximately 90% conversion of PS. Termination at this point yields higher termination efficiency, as the longer the reaction is left to run until completion, the higher the chances of possible termination due to contamination. We thus terminate slightly before 100% conversion. Figure 4.2 shows a typical SEC chromatogram of anionically prepared PS. PS has a strong UV absorbance at 254nm due to the aromatic ring, thus resulting in a perfect overlay with the RI signal. This

property will be exploited in further analysis of the block copolymers, as PDMS has no UV absorption at 254nm.
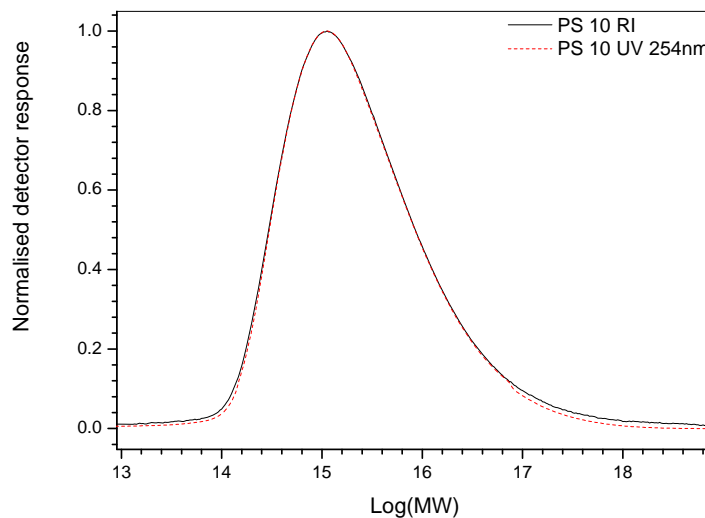
Figure 4.2   Typical SEC trace of PS (PS10) with RI signal and UV254nm overlay.

It must be noted that chlorosilane (Si-Cl) terminating agents were used. Allyl chlorodimethylsilane, for allyl functionality and chlorodimethylsilane, for silane functionality. This is because the (Si-Cl) bond is highly reactive towards nucleophiles. The reactivity of the chain ends increases with a decrease in the steric hindrance and an increase in charge delocalisation. The chlorosilanes generally give a more efficient and quantitative termination of the living anionic system, than the (C-Cl) equivalent. A number of PS prepolymers were synthesised with varying molecular weight and are summarised in table 4.1 to avoid repetition of SEC data plots. The yields were calculated gravimetrically by comparing the mass of resultant polymer to that of the initial mass monomer added. It must be noted that the yields do appear lower than the expected values (termination occurred around 95% conversion of monomer) but several factors could lead to this decreased value. Firstly the argon purging step of the monomer before addition of initiator leads to some loss of the volatile monomer out of the reaction vessel. Secondly, the precipitation and filtration steps could also lead to loss of polymer as possible remnants could remain behind on the filter paper after removal. The data in table 4.1 includes the expected molecular weight (MW) and the experimentally determined values, number average molecular weight ($\overline{M}n$) and weighted average molecular weight ($\overline{M}w$). The polydispersity index (PDI) is also given as an indication of the molecular uniformity.

Table 4.1: Summary of anionic PS reactions including theoretical and experimentally obtained molecular weights and yields (mass %).

Sample code	PS added (mmol)	BuLi (mmol)	Expected MW	$\overline{Mn}$ [a]	$\overline{Mw}$ [a]	PDI	% Yield
PS4	8.70	0.018	50000	55000	66100	1.20	88
PS5	17.5	0.364	5000	4200	5260	1.24	90
PS6	87.4	0.910	10000	8600	10100	1.17	86
PS7	87.4	3.040	3000	2800	3400	1.22	92
PS8	87.4	0.910	10000	8700	11000	1.25	91
PS9	87.4	0.455	20000	17800	22700	1.27	88
PS10	87.4	0.455	20000	17100	21300	1.24	90

[a]*Values reported relative to PS standards used in the calibration*

Table 4.1 shows a good correlation between the expected and obtained molecular weights. The PDI values also range between 1.17 and 1.27 which is a good indication of uniform chain growth. Proton nuclear magnetic resonance (^{1}H-NMR) was used to characterise the end group termination efficiency. Below in figures 4.3 and 4.4 one can view typical ^{1}H-NMR spectra obtained for silane terminal and allyl terminal PS respectively. Integration of the chemical shift at δ 0.9ppm (d in figure 4.3 and b in figure 4.4) for the methyl group protons of the initiator fragment was compared to the proton integrations of the terminal groups. Namely, the allyl proton (c in figure 4.3) at δ 5.8ppm and the silane proton (a in figure 4.4) at δ 3.9ppm.
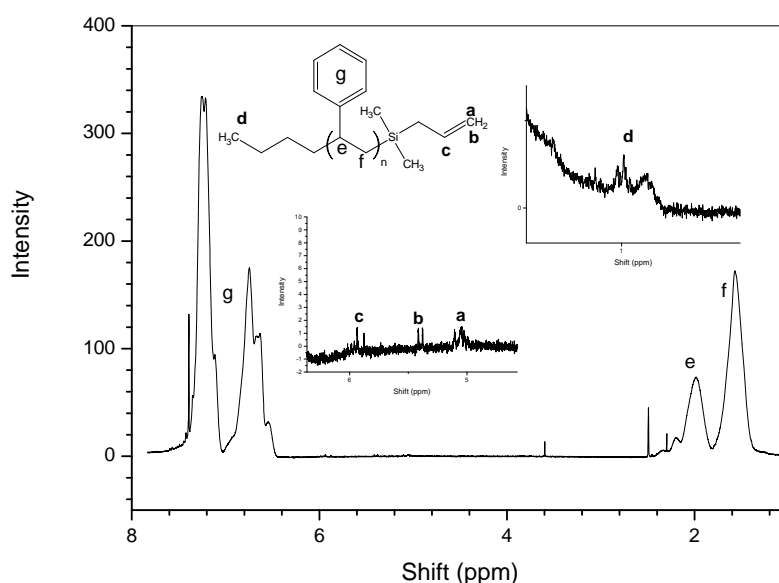
Figure 4.3   A typical ^{1}H-NMR spectrum of an allyl terminal PS prepolymer.
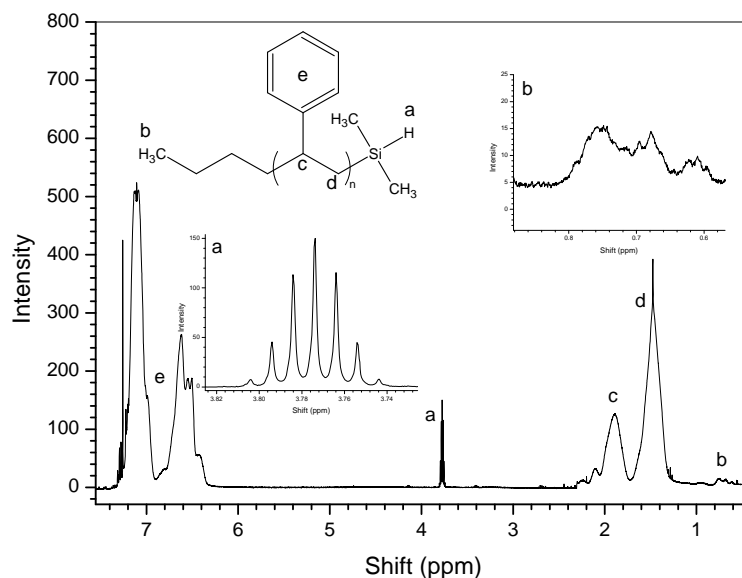
Figure 4.4   A typical ^{1}H-NMR spectrum of silane terminal PS prepolymer.

A summary of the PS prepolymer termination efficiencies are presented in table 4.2, as determined previously using ^{1}H-NMR. Termination efficiency is excellent, ranging from 78% to 85%.

Table 4.2: A summary of the termination efficiency for each of the PS reactions calculated using ^{1}H-NMR.

Sample code	$\overline{M}n$	Functionality	Termination efficiency[a]
PS 4	55000	$-C=CH_2$	79%
PS 5	4200	$-C=CH_2$	85%
PS 6	8600	$-C=CH_2$	82%
PS 7	2800	$-Si-H$	84%
PS 8	8700	$-Si-H$	78%
PS 9	17800	$-Si-H$	79%
PS 10	17100	$-C=CH_2$	80%

[a]*Determined from H^1-NMR spectra by integrating chemical shifts as mentioned above*

PDMS chains of varying molecular weight were prepared and once again characterised using SEC and ^{1}H-NMR to determine efficiency of termination with functionality. In this case it was very difficult to determine a conversion versus time plot due to the sensitivity of the reaction. Ring opening anionic polymerisation of D_3 to synthesise the PDMS is extremely sensitive to external contaminants such as water

and oxygen. Reactions were performed to calculate the conversion with time, but the intermittent sampling caused the reactions to terminate prematurely. It was, however, determined by running several reactions at varying duration that the optimal time for termination with functionality was after 4 hours. It must be noted that this was for polymerisations run in a solvent mixture of THF: Toluene (70:30) by volume. Increasing the content of polar THF causes an increase in the reaction rate, by delocalising the counter-ion from the anionic centre[1,2]. Decreasing the amount of THF has the opposite effect.

Figure 4.5 shows a typical SEC chromatogram of anionically prepared PDMS. It must be noted that there is no UV overlay, as PDMS does not have UV absorbing groups in this range of analysis. It must be further noted that the refractive index of PDMS (1.430) is almost identical to that of THF (1.407)[3]. Being the mobile phase in our SEC experiments, the differential refractive index (DRI) detector did not allow detection of polymer. However the use of an ELSD detector allowed detection of the polymer as the solvent is vaporised before detection.
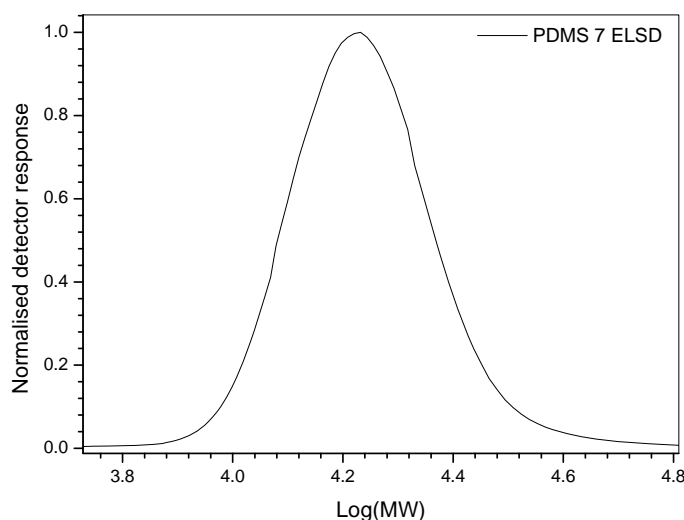
Figure 4.5   Typical SEC trace of PDMS (PDMS 7) with ELSD signal.

Another issue that needed to be addressed was the fact that PS standards were used to calibrate the system, so any values for the PDMS are relative. Table 4.3 lists the functionalised PDMS prepolymers, comparing predicted MW to the chromatographically obtained values. These values will differ due to the calibration being relative to PS standards and not PDMS standards. The percentage yield was determined gravimetrically compared to the initial mass D_3 monomer used. Once again, living anionic polymerisation gave excellent correlation between the expected

and obtained molecular weights. The PDI values range from 1.07 to 1.12. This indicates the synthesis of exceptionally narrowly dispersed polymer chains.

Table 4.3   Summary of anionic PDMS reactions run including theoretical and experimentally obtained molecular weights and yields (mass %).

Sample Code	D_3 added (mmol)	BuLi (mmol)	Expected MW	Mn^a	Mw^a	PDI	% Yield
PDMS 4	8.99	0.666	3000	3280	3630	1.11	81
PDMS 5	8.99	0.200	10000	10650	11900	1.12	79
PDMS 6	8.99	0.133	15000	15620	17500	1.12	78
PDMS 7	8.99	0.400	5000	5370	5860	1.09	80
PDMS 8	8.99	0.133	15000	15880	17400	1.10	75
PDMS 9	8.99	2.00	1000	1530	1650	1.07	70

^{a}Values reported relative to PS standards used in the calibration

^{1}H-NMR was again used to characterise the end group functionality efficiency. Below in figures 4.6 and 4.7 one can view typical ^{1}H-NMR spectra obtained for silane terminal and allyl terminal PDMS respectively. Once again integration of the chemical shift at δ 0.9ppm (d in figure 4.6 and c in figure 4.7) for the methyl group protons of the initiator fragment was compared to the proton integrations of the terminal groups. Namely, the allyl proton (a in figure 4.6) at δ 5.8ppm and the silane proton (a in figure 4.7) at δ 4.7ppm.
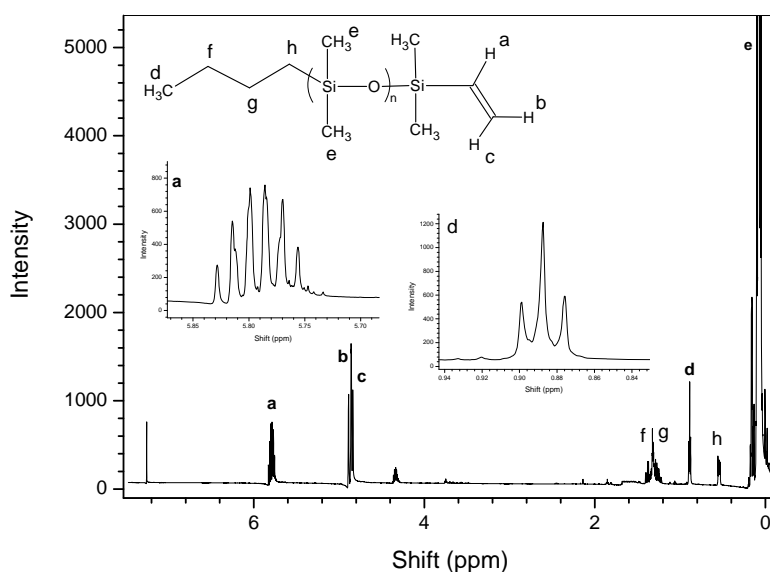
Figure 4.6   Typical ^{1}H-NMR spectra of allyl terminal PDMS prepolymer.
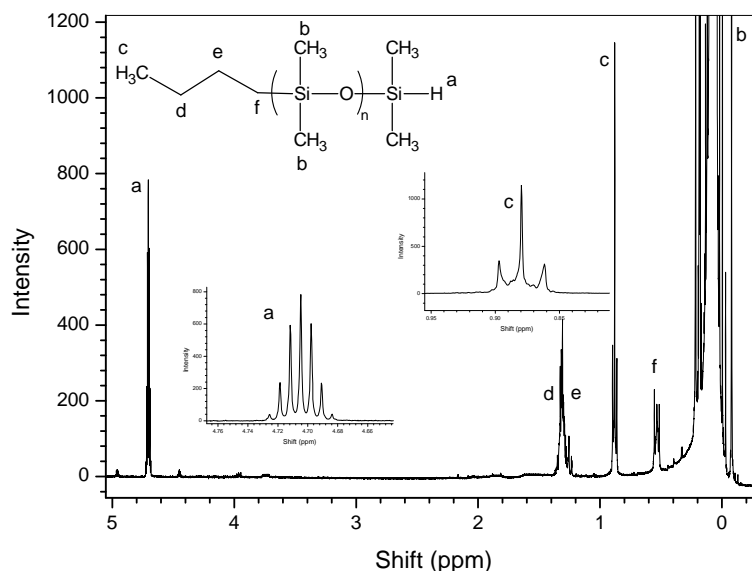
Figure 4.7   Typical ^{1}H-NMR spectra of silane terminal PDMS prepolymer.

A summary of the PDMS prepolymer termination efficiencies are given in table 4.4 as determined previously using ^{1}H-NMR. Excellent termination efficiencies were obtained and ranged from 78% to 81%. The functional prepolymers of PDMS and PS discussed in this section were used in further reactions to synthesise blocks, as will be discussed in the subsequent sections of this work.

Table 4.4   A summary of the termination efficiencies for each of the PDMS reactions   calculated using ^{1}H-NMR.

Sample code	$\overline{M}_n$	Functionality	Termination efficiency[a]
PDMS 4	3280	-C=CH$_2$	78%
PDMS 5	10650	-C=CH$_2$	80%
PDMS 6	15620	-C=CH$_2$	81%
PDMS 7	5370	-Si-H	79%
PDMS 8	15880	-Si-H	78%
PDMS 9	1530	-Si-H	80%

[a]*Determined from* [1]*H-NMR spectra by integrating chemical shifts as mentioned above*

4.1.2 Coupling of the PDMS and PS prepolymers

Prepolymers of varying molecular weight and functionality were used to synthesise block copolymers via a hydrosilylation reaction. As mentioned earlier in section 2.3.3, this technique involves coupling of a silane functional species with an allyl functional species using a platinum catalyst. In this project a divinyl-platinum complex, Karstedts catalyst, was chosen to catalyse the reaction. This reaction occurs fast at room temperature requiring very small amounts of catalyst. The ratio of catalyst to functional molecules was typically 1:100. Table 4.5 gives a summary of the coupling reactions performed.

Table 4.5   A summary of the various hydrosilylation coupling reactions performed to synthesise the block copolymers.

Sample code	PDMS prepolymer		PS prepolymer	
	Mn	Functionality	Mn	Functionality
HS 1	15620	$-C=CH_2$	17800	-Si-H
HS 2	15880	-Si-H	17100	$-C=CH_2$
HS 3	1530	-Si-H	4230	$-C=CH_2$
HS 4	3280	$-C=CH_2$	2790	-Si-H
HS 5	3280	$-C=CH_2$	8770	-Si-H
HS 6	5370	-Si-H	4230	$-C=CH_2$
HS 8	5370	-Si-H	8650	$-C=CH_2$
HS 9	5370	-Si-H	17100	$-C=CH_2$

It can be seen that a pattern was followed in the coupling reactions. HS 1 and 2 as well as HS 3 and 4 and to an extent HS 5 and 6, look at varying the functionality type of similar prepolymers. It was, however, noted that the functionality "order" did not have a noticeable effect on the coupling efficiency. Whether PS was silane functional and PDMS was allyl functional or vice versa, no differences were evident. This can be seen in the SEC chromatograms in figures 4.8 and 4.9. In both cases, the amount of block copolymer formed is exceedingly small. Extraction of the block material by subsequent removal of the homopolymers proved problematic, due to the small amount of block species present. It was thus impossible to determine gravimetric yields for comparison. The chromatograms below were determined using a DRI detector, explaining the absence of the PDMS homopolymer peak.
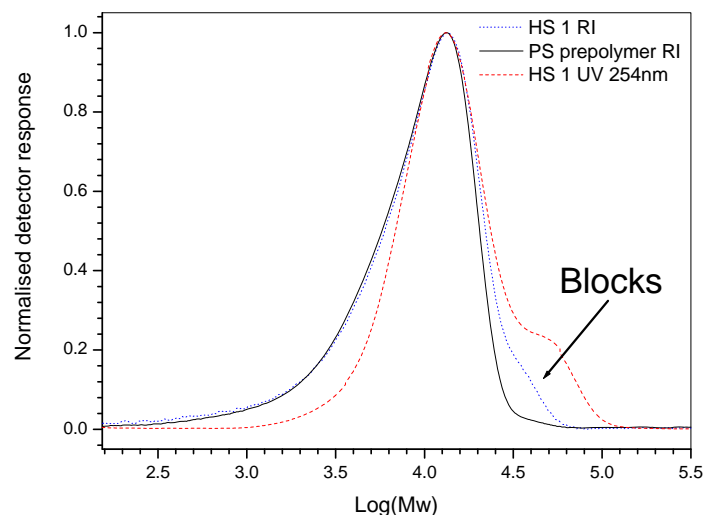
Figure 4.8   SEC chromatogram of HS 1, showing the RI trace of the PS prepolymer overlaid with the coupled product's RI and UV traces.
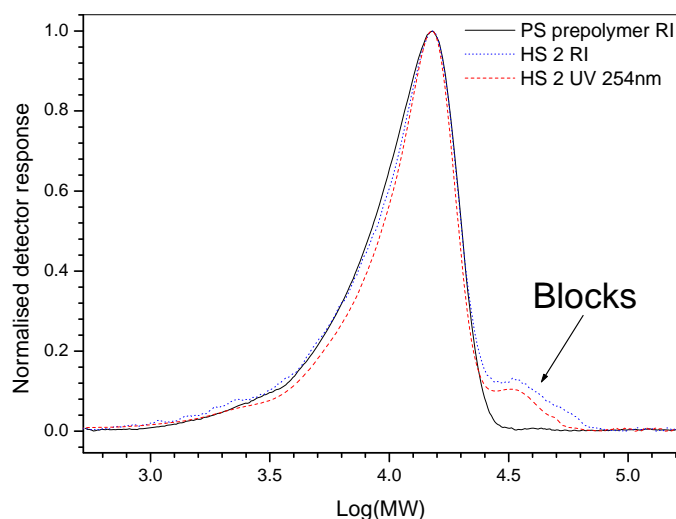
Figure 4.9   SEC chromatogram of HS 2, showing the RI trace of the PS prepolymer overlaid with the coupled product's RI and UV traces.

Another pattern used was the variation of molecular weight as can be seen in HS 2, HS 3 and HS 6 where the functionality order is kept constant, but the molecular weight of both prepolymers are reduced each time. Also in HS 6-9, the functionality order and PDMS prepolymer is kept constant while the PS prepolymer molecular weight is decreased. In all cases, GPC results indicated that this was an extremely inefficient method of synthesising block copolymers of this type. The same problem of determining gravimetric comparisons of the various reactions was found in the second pattern, of varying molecular weight. As can be seen from the SEC

chromatograms in figures 4.10 and 4.11, there is a slight trend, as we move from high molecular weight to lower values. Reactions HS 8 and HS 9 were chosen as a typical example of this trend. It must also be noted, that an ELSD detector was used in this SEC analysis, allowing detection of the PDMS homopolymer.
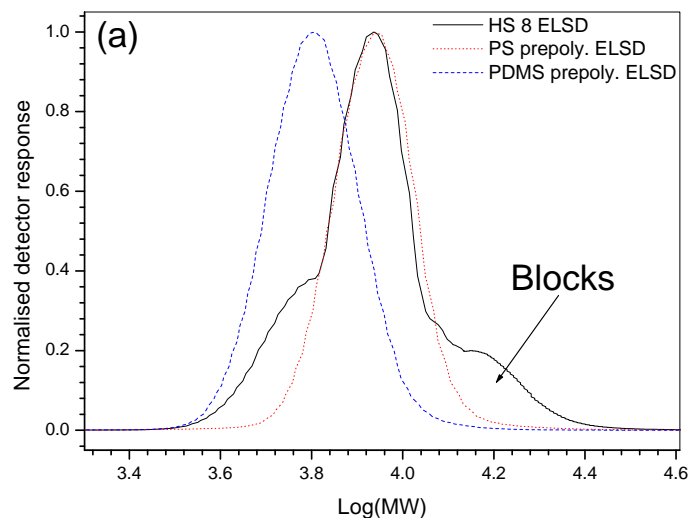
Figure 4.10   SEC chromatogram of HS 8, showing the ELSD trace of the PS and PDMS prepolymers overlaid with the coupled products' ELSD trace.
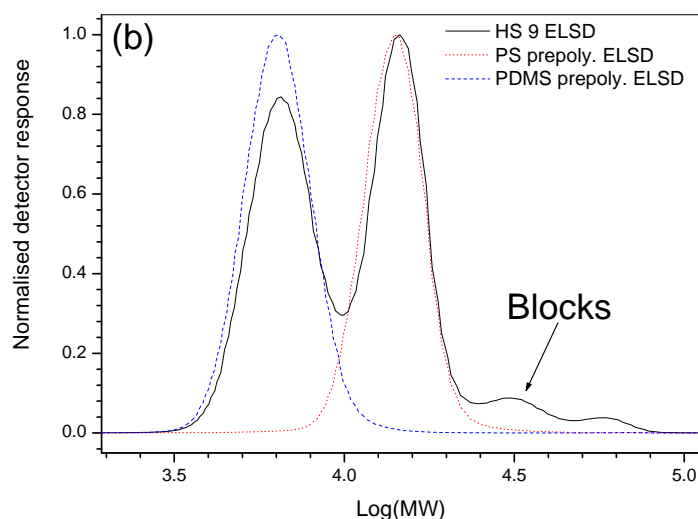
Figure 4.11   SEC chromatogram of HS 9, showing the ELSD trace of the PS and PDMS prepolymers overlaid with the coupled products' ELSD trace.

HS 8 used a lower molecular weight PS prepolymer than HS 9. There appears to be an increase in the amount of block material for HS 8, if one visually observes the block area below the chromatogram. This is purely speculative due to the heterogeneous nature of the reaction product. The immiscibility of the various

components causes segregation upon reaction completion. It is difficult to retrieve a sample for analysis that represents the entire product composition. Using this coupling reaction to join our functionalised PS and PDMS polymers poses a problem, due to the severe incompatibility of the PS and PDMS components. The problem is that the reaction medium tends to start off heterogeneously. This is further compounded by the fact that a relatively concentrated reaction is needed (little solvent). Work done by Chaumont *et al.*[4] showed that the coupling of PS and PDMS occurred less readily than other immiscible blends of PDMS with Substituted PS. This reaction took the longest to react and gave the poorest yields. It did also appear that the higher the molecular weights of the prepolymers the more difficult the coupling reaction, probably due to difficulty in getting the reactive end-groups of the incompatible materials close enough to react. This possible molecular weight effect was studied as can be seen in reactions HS 6-9, where the functionality groups were kept constant and the length of the PS segment was varied. The incompatibility and phase segregation of these two very different polymeric materials as discussed earlier in this work all allude to the fact that this technique may prove to be the least successful in synthesising the block copolymers.

No further time was spent analysing the material synthesised using this coupling method. The amount of block material produced and the difficulty in extracting this minute amount made further characterisation unfeasible. It was clearly seen that this technique yielded poor block copolymer product, and a different technique would have to be approached.

4.2   Sequential anionic block copolymerisation

The sequential anionic polymerisation of PS followed by PDMS resulting in block copolymer synthesis is discussed in this section. The living nature of anionic polymerisations is exploited to create block copolymers directly, without an intermediate functionalisation step.

4.2.1 Synthesis of block copolymers

As stated in the experimental chapter, the PS block was grown first, followed by the PDMS block. Literature on this technique[5] lead to the preference of this specific order. PS is synthesised in a non-polar medium, whereas PDMS requires a polar

medium. Growth of the PS block followed by addition of PDMS with polar solvent gives the optimum results. Table 4.6 lists the block copolymers prepared using this sequential anionic method. Once again there is a strong correlation between the expected and obtained molecular weights. Various segmental molecular weights and ratios of PS to PDMS were synthesised for analysis. Approximately 35 minutes was allowed for the synthesis of the PS segment, before addition of the subsequent monomer. The polystyrillithium anion of the living PS chain imparts a deep orange colour to the reaction.

Table 4.6   Summary of all the sequential anionic reactions performed, comparing theoretical and actual molecular weights and yields.

Sample code	PS aimed[a]	PDMS aimed[a]	PS block ($\overline{M}_n$)[b]	Block copolymer[c]
LS 5	7500	15000	7330	22130
LS 7	10000	5000	8800	13780
LS 8	30000	20000	27600	46590
LS 9	10000	5000	9440	14440
LS 10	10000	10000	9360	18320
LS 11	20000	20000	19030	37800
LS 12	20000	30000	18950	48540
LS 13	5000	10000	4850	14380
LS 14	5000	20000	4910	23670
LS 15	20000	5000	18960	23910

[a]Determined using molar ratio of monomer to initiator.
[b]Values reported relative to PS standards.
[c]After homo-PS extraction.

This was exploited in the sequential addition of the D_3 monomer. Upon addition, time is needed to anionically ring open the first D_3 monomer units to add to the living PS chains. This was observed as a gradual decrease in the intensity of the deep orange colour to a pale yellow, and finally colourless solution. This took approximately 18hrs at room temperature. The solvent used for the PS growth step was 100% toluene. This solution is not polar enough to promote propagation of D_3 monomer to form PDMS. THF was added to make up a (50:50) ratio of toluene to THF. This was only done, after the initial D_3 units were allowed enough time to add to the ends of all the living PS chains. In doing this, all the PDMS segments could start propagating at the same time, ensuring a narrower molecular weight distribution. Before addition of the D_3 monomer, a sample of the reaction mixture was taken for SEC analysis. This

allowed the length of the PS segment to be recorded as shown in table 4.6. Typical SEC chromatograms of the block copolymers produced this way are given in figures 4.12 and 4.13, overlaid with the PS segment traces. One can see a clear chain extension shift to a higher MW upon growth of the PDMS segment. It is clear from the SEC chromatograms that this technique provides a feasible route to synthesise PS-block-PDMS copolymers, due to the large block copolymer peak. It was also found that little to no PDMS homopolymer was produced, as initiation of this segment occurs primarily due to anionic ring opening via the living polystyrillithium anions.
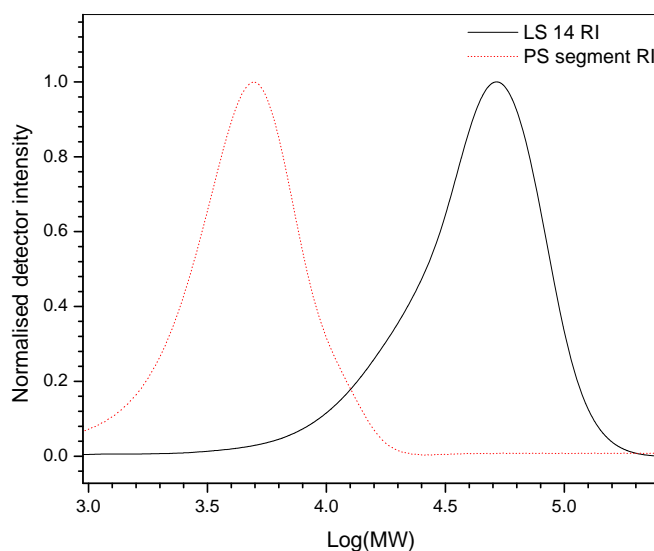

Figure 4.12   SEC chromatogram of LS 14, showing the DRI traces of the block copolymer and the PS segment before addition of D_3.
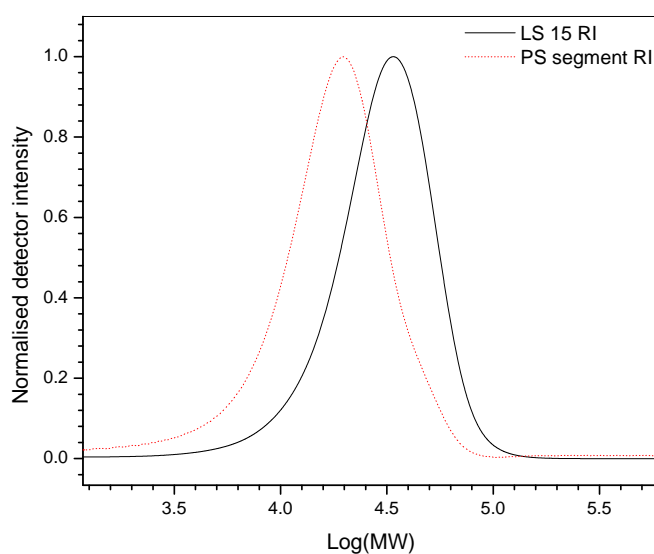

Figure 4.13   SEC chromatogram of LS 15, showing the DRI traces of the block copolymer and the PS segment before addition of D_3.

There is, however, a small amount of PS homopolymer (homo-PS) present, due to chains that terminated before reacting with the added PDMS monomer. This homo-PS is viewed as a slight shoulder in the lower molecular weight side of the SEC chromatogram. This slight shoulder is more evident in figure 4.12 of sample LS 14. This is not to say that there is less homo-PS in LS 15, as it could be hidden by the block copolymer peak. Homo-PS has to be extracted before doing bulk sample analysis, such as FT-IR, as it will not give a true reflection of the pure block material. It was difficult to obtain molecular weight values for the block copolymer due to the presence of homo-PS chains, even after extraction, so care must be taken when interpreting these results.

Extraction was performed as explained in section 3.1.9. It must be said that the extraction of homo-PS is extremely difficult, due to the similarity in the polarities of the PS and PDMS-b-PS block material. It was not possible to remove all of the homo-PS using this method, which is why a (% yield) column was not included in table 4.6. Gravimetric determination of the yield would be inaccurate due to the presence of the unreacted homo-PS material. This also poses a problem for analysis of the block material produced by this method, so an alternative approach to analysis had to be followed and is discussed further in this chapter. Further analysis was also required to better understand the chemical composition distribution (CCD) of these block copolymers. This lead to the necessary development of liquid chromatographic techniques that could supply such information, namely, liquid chromatography at critical conditions (LC-CC) and gradient elution chromatography (GEC).

4.2.2 HPLC analysis

This section discusses the development of LC-CC and GEC techniques, suited to studying the block copolymers synthesised in this project. LC-CC at the critical point of PS was chosen to allow CCD analysis of the block copolymer in combination with FT-IR using the LC-transform device. GEC was used to detect the presence of PDMS homopolymer.

4.2.2.1 Development of LC-CC system and characterisation

There are various conditions presented in literature that allow LC-CC of various polymers, well documented in a review by Macko and Hunkeler[6]. The main objective

of this chromatographic system is making the PS segments in our block copolymer "invisible" to the chromatographic system. This would allow characterisation of the blocks irrespective of the PS segment, thus solely reliant on the distribution of the PDMS segment. That would say, whilst the PS homopolymer elutes irrespective of molecular weight, the PDMS containing blocks elute in SEC mode. Careful choice of column packing material and solvent combinations were needed. It was decided to use a polar bare silica column to avoid interaction of the non-polar polymer segments and possible adsorption to the column. A solvent combination of THF and hexane was deemed appropriate to allow preferential solubilisation of the PDMS containing blocks, as PS is insoluble in hexane. This would allow the PDMS containing blocks to elute before PS homopolymer in SEC mode. Various solvent combinations were used while running PS standards on the column. This was continued until the standards eluted at the same retention volume irrespective of molecular weight as shown in figure 4.14.
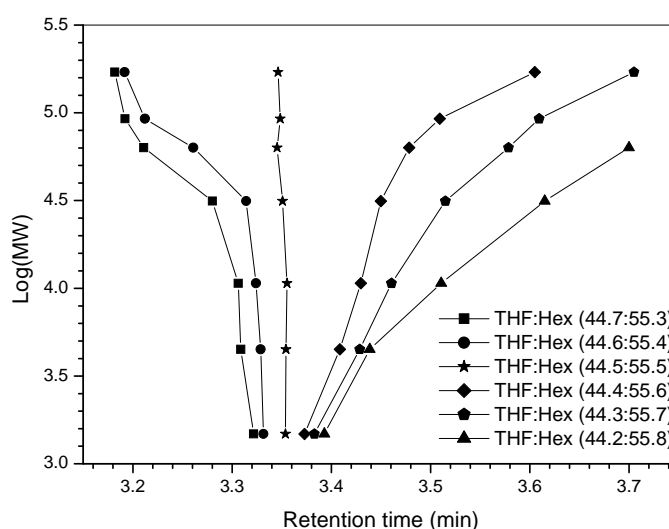
Figure 4.14   Determination of critical conditions by varying the ratio of THF to hexane and plotting log(MW) against retention time, using a Nucleosil 300 Si 5μm 25×0.46mm column at 30°C.

It can be seen from figure 4.14 that the optimum solvent composition of PS desorli (THF) : adsorli (hexane) is (44.5 : 55.5). This allowed elution of PS irrespective of molecular weight. The temperature was kept constant at 30°C throughout elution. The sample injection solvent was kept at the same composition as the mobile phase. The sensitivity of this technique is evident, as we can move from LC-CC mode to SEC mode or LAC mode, simply by changing the mobile phase composition by 0.1%. Typical LC-CC results are presented in figures 4.15 and 4.16. We see the PS

homopolymer eluting at approximately 3.35 minutes, with a strong UV absorption at 254nm due to the high concentration of aromatic rings. The power of this technique is evident in the results presented. It can clearly distinguish between the efficiency of the two reactions.
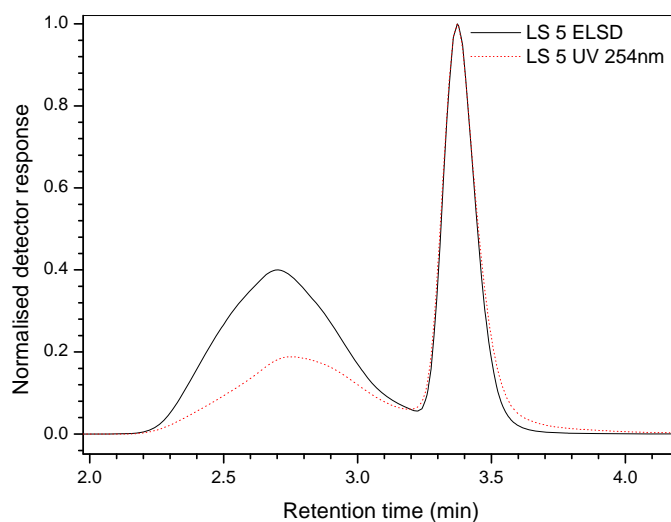
Figure 4.15   Normalised LC-CC chromatogram of LS 5 showing UV overlay.
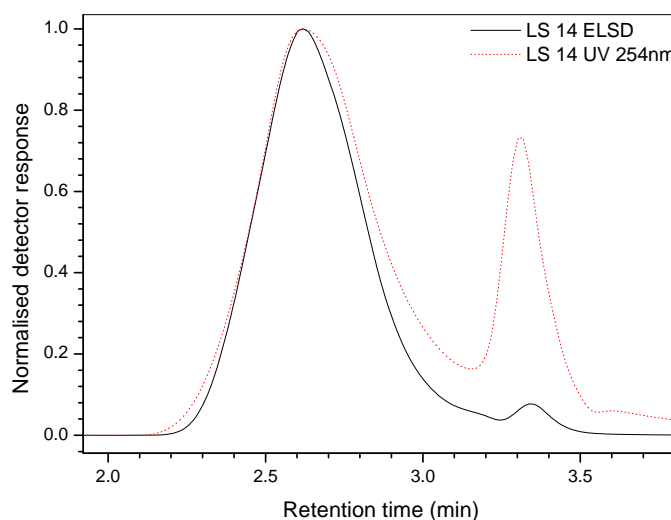
Figure 4.16   Normalised LC-CC chromatogram of LS14 showing UV overlay.

LS 5 was one of the first sequential reactions performed and was included in this section to illustrate a point. When synthesised, conditions were not yet optimised, resulting in a lower blocking efficiency. This is observed by the distinct difference in sizes of the relative homopolymer peaks to block copolymer peaks. The UV trace at

254nm is included to show the presence of UV absorbing groups in the block copolymer elution range. PDMS does not absorb UV in this range proving the presence of PS segments. These segments must in turn be joined to the PDMS segments, or else they would have eluted along with the PS homopolymer at 3.35 minutes. This proves that block copolymer formation did in fact take place. This technique allows excellent separation of the homo-PS from the bulk block material. It will be seen later in this chapter that this chromatographic technique can be coupled to other characterisation techniques, in a novel way, allowing analysis of the pure block material avoiding bulk extraction of the homo-PS.

When LC-CC is used to prove successful block formation, critical conditions of both constituents are usually needed (ie: PDMS and PS). In this case it is not necessary as LC-CC at the critical point of PS, combined with the fact that PDMS does not absorb UV at 254nm while PS does, is enough proof. It would, however, be useful in determining the distribution of PS in the block copolymer, at the moment only the PDMS distribution is determinable. A search of literature did not yield any work where the critical point of PDMS has been determined and it proves to be a difficult task to accomplish. Even after determining the critical point of PDMS the conditions must be so, that PS elutes in SEC mode. If not there is the risk of irreversible adsorption to the column in LAC mode. Time constraints did not allow development of this critical point in this project. We do, however, need a method to determine whether or not any PDMS homopolymer is present. This would elute along with the block material and would need to be extracted to get a clear indication of the block copolymer distribution. In the case of sequential anionic polymerisation the presence of PDMS homopolymer is little to non-existent due to mechanistic reasons, however, in the next technique this may pose a problem. That is why a gradient chromatographic technique was also developed to indicate the presence of any PDMS homopolymer, and monitor the successful removal thereof after extraction.

4.2.2.2 Coupling of LC-CC to FT-IR

This technique allows FT-IR characterisation of chromatographically fractionated samples. As explained in section 3.2.3, FT-IR spectra are taken at regular intervals along the polymer elution range to monitor chemical composition. This powerful technique shows the composition of the block material across the distribution range as determined by the LC-CC chromatographic system. The data obtained is illustrated by a waterfall plot in figure 4.17.
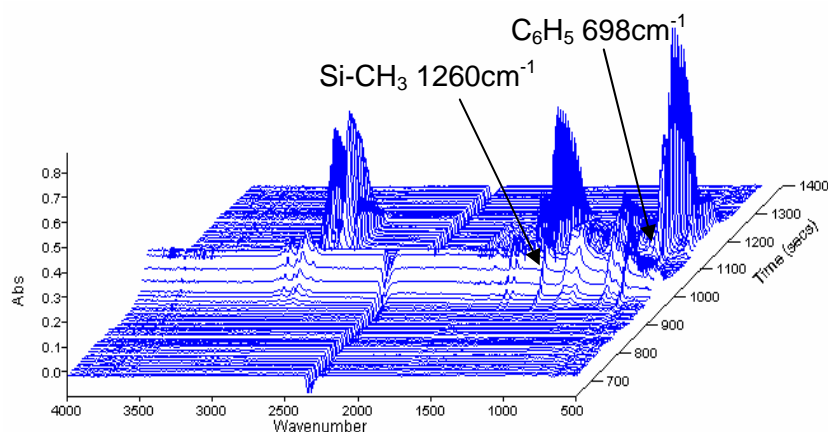
Figure 4.17   A stacked waterfall plot indicating the absorption bands used for the determination of the PS-b-PDMS chain compositions.

In figure 4.17 one can clearly see how this technique works. Note how full FT-IR spectra are taken at regular intervals along the time axis. Also note the outline of the peak heights along the time axis. This outline corresponds to the LC-CC elution profile of the analysed polymer. This information allows one to construct Gram-Schmidt plots. Two examples are given in figures 4.18 and 4.19.

Moving along the elution range (retention time) infra-red spectra are obtained at each point. The solid smooth lines in these figures consist of points that are calculated by integrating the entire infra-red spectrum at that specific scanned time. Note that these plots closely resemble the chromatograms obtained from the conventionally detected LC-CC system. This is obvious, as the higher the peak intensity in both cases, the more molecules there are present. The great benefit of this technique comes to light when overlaying the chemigrams (line with circular symbol). A chemigram is constructed by choosing a functional group IR band (e.g. carbonyl absorbance) and plotting this peak height against an in situ standard peak height. In this case a ratio was taken between IR bands arising from solely PDMS functional groups and PS functional groups. The Si-CH$_3$ absorbance at 1260cm^{-1} was taken as representative of PDMS and the C$_6$H$_5$ ring absorbance at 698cm^{-1} was taken as the representative of PS. The peak heights of these respective IR bands, was determined and the ratio of Si-CH$_3$/C$_6$H$_5$ was calculated. These ratios were then plotted against time and overlaid with the Gram-Schmidt plots. In figure 4.18 there is a clear separation between the block material and the homo-PS. The ratio drops close to zero across the homo-PS peak which is expected due to the absence of PDMS moieties.
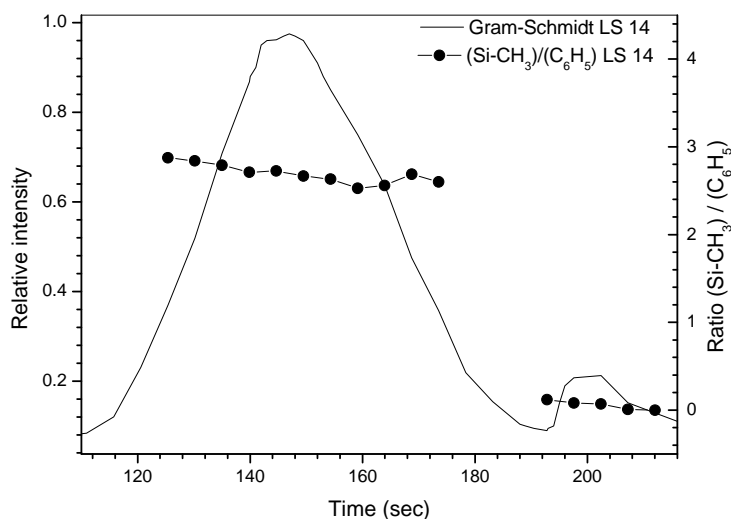
Figure 4.18 Gram-Schmidt plot of LS 14 along with the ratio between $Si-CH_3/C_6H_5$
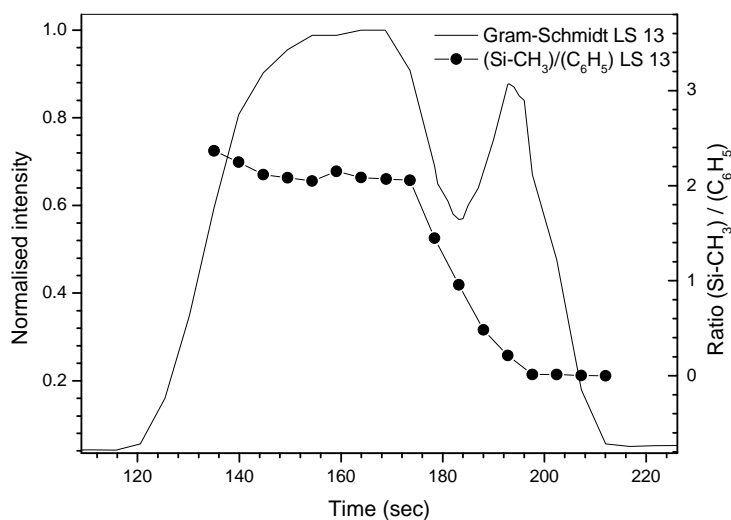
Figure 4.19 Gram-Schmidt plot of LS 13 along with the ratio between $Si-CH_3/C_6H_5$

The relatively uniform line across the block region indicates that the distribution of PDMS and PS in the blocks is fairly constant, proving the success of this technique for controlled block synthesis. There is a slight decrease in the ratio moving to the lower molecular weight PDMS side, which indicates a slight decrease in the PDMS composition. This is not surprising, as the PDMS decreases in molecular weight from left to right while PS, being "invisible", is distributed randomly. This would say that the lower molecular weight PDMS chains are not arranged in order of PS segmental length. The plot in figure 4.19 is not as clearly separated as with the previous plot. This is because the PDMS segments in LS13 are not as large as in the case of LS14,

meaning that it elutes closer to the homo-PS region. When spraying onto the germanium disc during sample collection (refer back to section 3.2.3) there tends to be slight overlap due to the nature of this spraying method. Clear separation occurs more readily for samples with larger molecular weight PDMS segments. Still, the same can be seen as with figure 4.18. A relatively constant ratio across the block region and a drastic decrease towards zero as the homo-PS range is reached. We see a drop in PDMS composition at the point where the overlap in peaks occurs, as the homo-PS peak contains no PDMS components.

The advantage of this coupled technique, allows IR analysis of the pure block material without any contribution from the homo-PS molecules which are difficult to extract. A similar approach to this was used in a novel way for morphological characterisation, as will be seen later in this work.

4.2.2.3 Development of GEC system and characterisation

As stated in the theoretical chapter, this technique separates polymer species by manipulating there relative solubilities or polarities[7,8]. In this case the solubility differences were used. Use of a polar bare silica column minimised column interaction. The solvent combination used was THF and hexane. The gradient profile used is illustrated in figure 4.20.
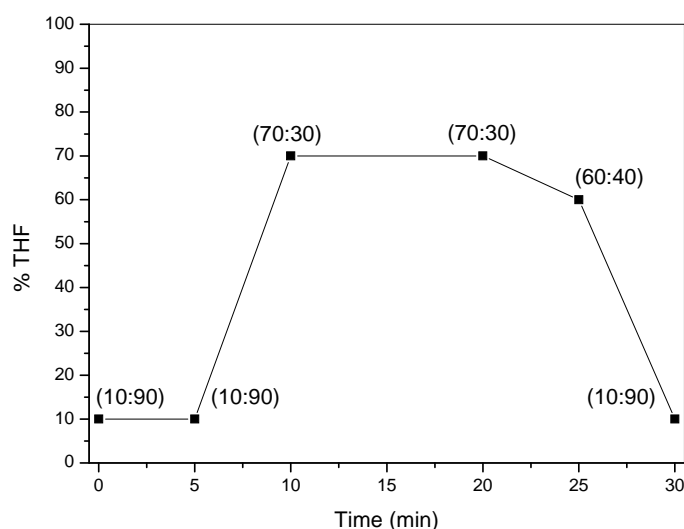

Figure 4.20   Gradient profile for GEC system with % THF plotted against time.

It was found during optimisation of this technique that PDMS being easily soluble in both solvents remained in solution and eluted easily through the column. PS homopolymer and PS containing block copolymer tended to precipitate out of the solutions with high hexane content. PDMS homopolymer samples were run on this gradient and it was found that they eluted in the region of 0-6 minutes in SEC mode. Even low molecular weight PDMS (± 1000) eluted before 6 minutes as shown in figure 4.21. These narrowly distributed PDMS samples were run to make sure that no PDMS material eluted later along the retention range, after 6 minutes, possibly being mistaken for block material. As can be seen this is not the case.
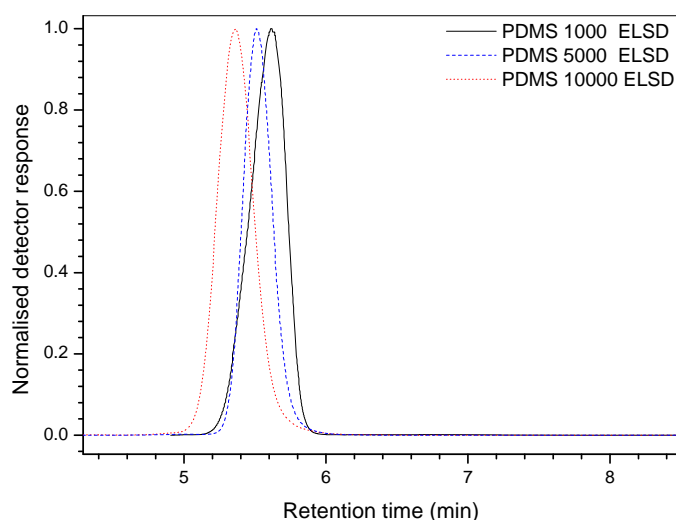
Figure 4.21   Overlaid GEC chromatograms of three PDMS samples with molecular weights of 10000, 5000 and 1000.

Figure 4.22 shows a typical GEC chromatogram obtained for one of the sequentially synthesised block copolymers. Note the size of the PDMS elution peak. As expected there is a negligibly small amount of PDMS homopolymer present. This was also the case for the other sequentially synthesised block copolymers under study. Another important fact to note is that in this case the block copolymer is not distinguishable from the PS homopolymer. Usually the block copolymer elutes in a "window" between that of the respective homopolymer species. Due the similar hydrophobic nature of these PDMS-b-PS blocks and PS homopolymers, separation was not readily achieved. Once again it was not necessary to separate the two as this technique is used solely to identify PDMS homopolymer. The UV trace is not a perfect overlay, due to the change in mobile phase composition along the gradient. The UV baseline drifts as the solvent composition changes, but a strong peak

overlaying with the peak of the ELSD trace indicates the presence of strong UV absorbing groups in this region.
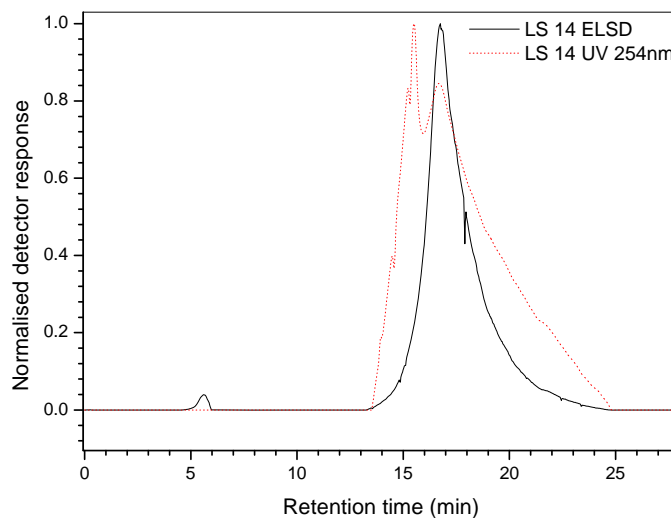
Figure 4.22   GEC chromatogram of LS 14 showing UV overlay.

The sequential anionic technique allowed synthesis of block material with well controlled structure. The presence of homo-PDMS was negligible in this case, however, the homo-PS material was present in significant amounts. This is due to the nature of the reaction, as any PS chains that terminate before the addition of D_3 monomer would be present as homopolymer in the final reaction product. Being difficult to remove, alternate methods were used to analyse the block material as shown. The next synthetic technique was decided on as a route to synthesise block material with minimal homo-PS formation, due to the difficulty in removing it.

4.3   ATRP macroinitiator technique

This synthetic technique uses a functionalised PDMS macroinitiator to initiate the controlled radical polymerisation of PS using ATRP. This method yields block copolymers of PDMS and PS with controlled structure. It will also be shown that the presence of homo-PS species are kept to a minimum using this technique.

4.3.1 Synthesis of block copolymers

As previously stated, this approach utilises PDMS macroinitiators. PDMS macroinitiators were synthesised by converting silane functionalised PDMS

molecules to bromoisobutyrate functionalised molecules, via a hydrosilylation reaction. These bromo functional molecules are well known initiators for the ATRP of styrene[9,10]. They were used along with a copper catalyst and bidentate ligand (4,4'-dinonyl-2,2'-bipyridyl (dNbipy)) to mediate the polymerisation of the PS segment, creating blocks. Scheme 4.1 illustrates the reaction mechanism.
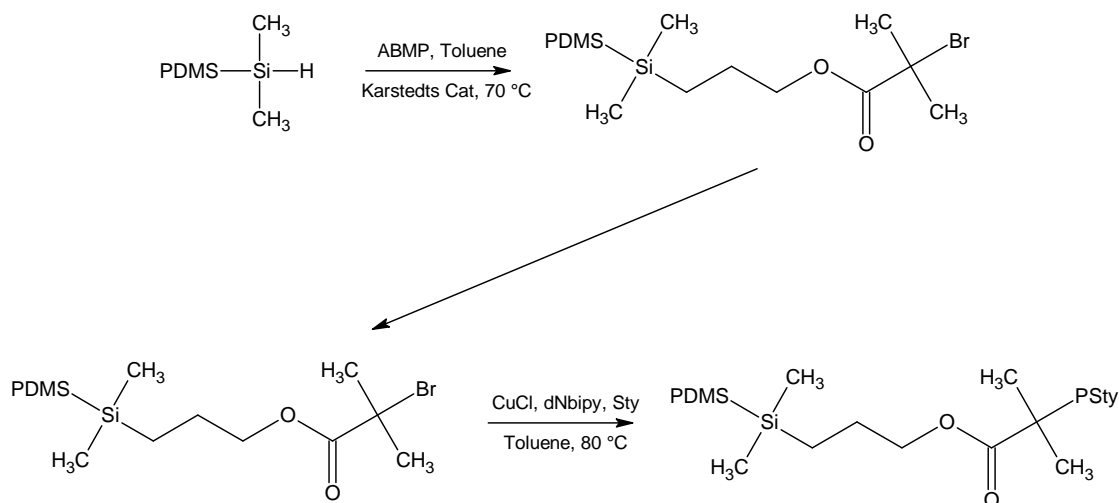
Scheme 4.1   A reaction scheme showing the PDMS macroinitiator terminal group modification, followed by the ATRP of styrene to form the block copolymer.

Silane functionalised PDMS was procured from earlier experiments used for the coupling technique (see table 4.4). Successful reaction of the allyl-2-bromo-2-methyl-propionate (ABMP) molecules with the silane terminal moieties was monitored by ^{1}H-NMR. The NMR spectra for silane terminal PDMS was presented earlier in figure 4.7. The NMR spectra of the bromoisobutyrate functionalised PDMS is presented in figure 4.23.

Note the singlet at δ 1.93ppm representative of the methyl group protons (h in figure 4.23). Integration of this shift compared to that of the methyl protons of the initiator fragment at δ 0.93ppm (a in figure 4.23), yielded the functionalisation efficiency. Figure 4.24 has been included to highlight the disappearance of the silane proton septuplet at δ 4.7ppm. The ^{1}H-NMR spectra of silane functional PDMS (A) is overlaid with that of the bromoisobutyrate functionalised PDMS (B). The peak at δ 4.1ppm (i in figure 4.24) is due to the proton shift of the -CH$_2$- marked as (i) in figure 4.23.
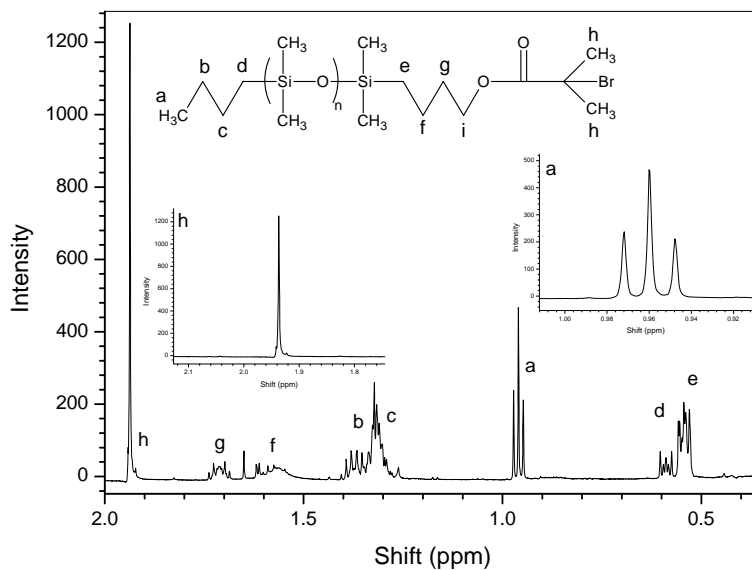
Figure 4.23   A typical ^{1}H-NMR spectrum of bromoisobutyrate terminal PDMS macroinitiator for the ATRP of styrene.

One clearly sees the disappearance of the silane proton shift. Further proof is the appearance of proton shifts at δ 1.93ppm and δ 1.5ppm-1.75ppm, indicative of the new bromoisobutyrate functional group. This proves successful modification of the silane moiety to a bromoisobutyrate moiety.
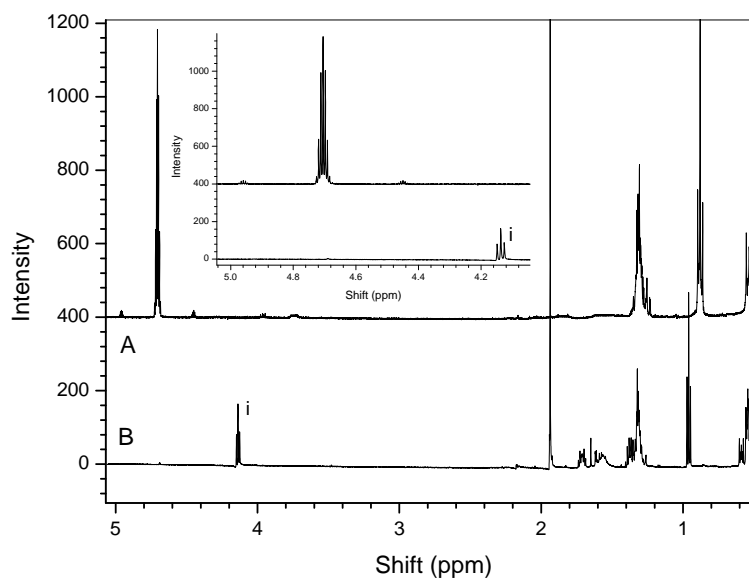
Figure 4.24   ^{1}H-NMR spectra of (A) silane functionalised PDMS and (B) it's respective bromoisobutyrate functionalised counterpart, after hydrosilylation.

Table 4.7 summarises all the PDMS macroinitiators synthesised, along with functionalisation efficiency determined as mentioned previously. Note that this functionalisation efficiency only takes the silane terminal molecules into consideration, so as to monitor the hydrosilylation reaction efficiency. The termination efficiency column gives the percentage bromoisobutyrate functionalised molecules in the sample. Table 4.8 summarises the block copolymers synthesised using these PDMS macroinitiators.

Table 4.7   A summary of the PDMS macroinitiators synthesised for the ATRP of styrene.

| Sample code	$\overline{M}_n$ [a]	Functionality after hydrosilylation	Functionalisation efficiency	Termination efficiency
PDMS 7	5370	$-CH_2COOC(CH_3)_2Br$	97%	77%
PDMS 8	15880	$-CH_2COOC(CH_3)_2Br$	95%	74%
PDMS 9	1530	$-CH_2COOC(CH_3)_2Br$	95%	76%
PDMS 10	20160	$-CH_2COOC(CH_3)_2Br$	96%	78%

[a]*Values reported relative to PS standards used in the calibration.*

Note the excellent functionalisation efficiencies ranging from 95 to 97%. The hydrosilylation reaction gave excellent conversion. A new PDMS macroinitiator, of approximately 20 000 molecular weight, was synthesised for this reaction only. The other silane functional macroinitiators were obtained from earlier experiments.

Table 4.8   A summary of all the macroinitiated ATRP reactions performed.

Sample code	PDMS $\overline{M}_n$ [a]	PS aimed	PS $\overline{M}_n$ [b]	Block $\overline{M}_n$ [a]	PDI[a]	% yield[c]
ATRP 3	5366	5000	2628	7994	1.147	61
ATRP 5	1531	50000	44812	46343	1.20	73
ATRP 6	20162	20000	18825	38987	1.23	72
ATRP 7	15888	1500	984	16872	1.17	69
ATRP 8	20162	5000	3535	23697	1.13	68
ATRP 9	20162	20000	19462	39624	1.21	72
ATRP 10	15888	65000	63358	79246	1.31	79
ATRP 11	20162	30000	27176	47338	1.25	81

[a]*Values reported relative to PS standards used in the calibration.*
[b]*Approximate values obtained by subtracting the PDMS (Mn) from the block (Mn).*
[c]*Determined gravimetrically after extraction of homo-PDMS.*

The PDMS Mn values were obtained by SEC prior to reaction. The block copolymer Mn was obtained by SEC using a conventional DRI detector. PDMS having the same refractive index as the mobile phase was not detected, therefore any homo-PDMS material did not influence the determination of the block copolymer molecular weight. The homo-PDMS would have appeared as a shoulder on the SEC profile, making molecular weight determinations of the block copolymer difficult. Figures 4.25 and 4.26 are typical examples of the SEC data obtained for this polymerisation technique. The PDMS macroinitiator overlay shows successful chain extension with PS.
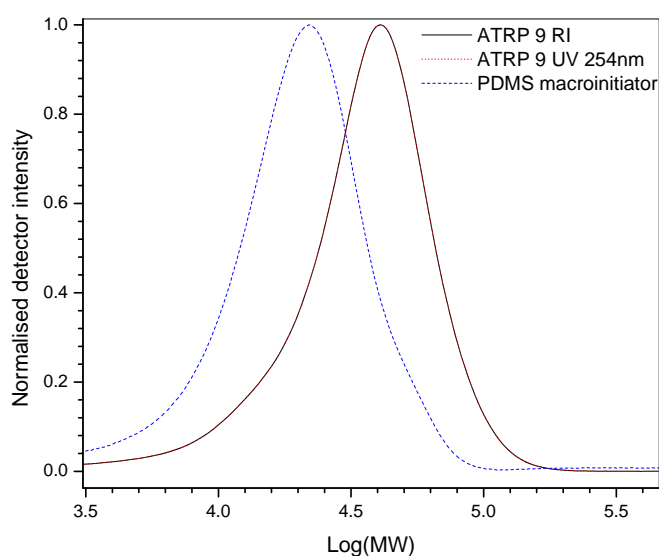

Figure 4.25   A typical SEC chromatogram obtained using a DRI detector with UV overlay at 254nm.
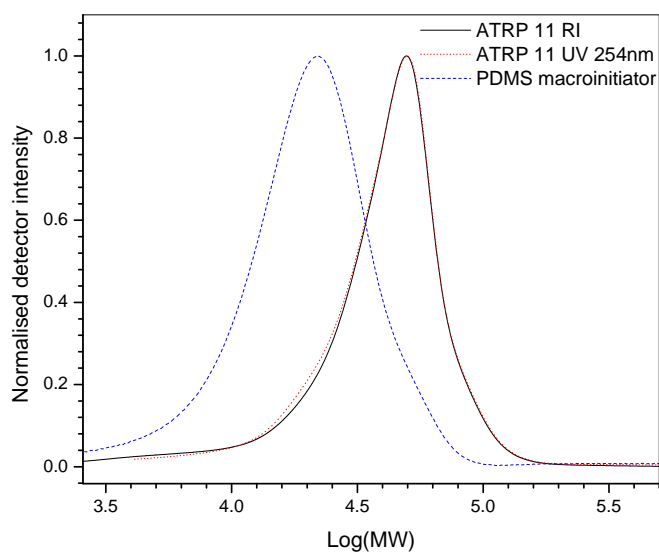

Figure 4.26   A typical SEC chromatogram obtained using a DRI detector with UV overlay at 254nm.

The Mn value of the PS segments in the block copolymers was estimated by subtracting the initial PDMS Mn value from the resultant block copolymer Mn. This is not strictly true, as SEC determines the hydrodynamic volume of the polymer in solution. Differences in the constituent segments mean that they assume different volumes in solution as a function of molecular weight. A PDMS molecule the same molecular weight as a PS molecule will not necessarily occupy the same volume in solution. It is, however, a fair estimate of the PS segmental block length.

As can be seen in the table of polymerisations, reactions ATRP 10 and ATRP 11 have PS segments with higher molecular weights than any of the other reactions. It was decided at this stage to synthesise blocks with much higher PS segmental length and composition to study the effects on morphology and PDMS surface segregation. The amount of PS-homopolymer synthesised using this technique is very little. The small amount of PS-homopolymer molecules are due to thermal autopolymerisation of styrene. It is known from literature that at temperatures > 80°C styrene tends to undergo thermal initiation[11]. A compromise had to be established between reaction temperature and reaction duration. In ATRP a lower reaction temperature leads to longer reaction durations[1], and to keep the time reasonable a temperature of 100°C was chosen for these reactions. In most cases a very small amount of homo-PS was present, too small to extract and was thus considered negligible.

Homo-PDMS was, however, detected in reasonable amounts. This is to be expected when studying the termination efficiencies in table 4.7. There appeared to be between 20-25% non-bromoisobutyrate terminated chains. These chains would therefore not undergo ATRP growth with PS and remain as unreacted homo-PDMS in the final product. This can pose a problem, as the chromatographic approach of separating the homo-PS from the block material does not work in this case. The critical point of PDMS would be needed to separate the PDMS from the block material. PDMS homopolymer is, however, easily extracted as explained in section 3.1.9. Simple extraction with bromobenzene removed the vast majority of homo-PDMS before analysis. This will be shown later in the following GEC analysis section.

The macroinitiator technique seems to have been successful judging by the good PDI values and close correspondence between aimed and actual molecular weights. The PDI values tend to be higher for the higher molecular weight PS samples, but in this case the reactions were run longer, closer to 100% conversion. In ATRP it is

known that side reactions tend to occur more readily at higher conversions[1,10] which explains this broadening in the molecular weight distributions. Further characterisation using critical point and gradient chromatography follows.

4.3.2 HPLC analysis

GEC will be under discussion first, as this technique was used to monitor the removal of homo-PDMS by solvent extraction, before subsequent analysis.

4.3.2.1 Characterisation using GEC

For the development and solvent profile of this technique, I refer back to section 4.2.2.3 of this work. Figures 4.27 and 4.28 show the GEC profiles of two of the products synthesised using the macroinitiator method. Note the PDMS peak at approximately 5.8 minutes in both cases. The sizes of these PDMS peaks are clearly larger than those obtained after analysing the sequentially synthesised blocks. This homo-PDMS cannot be seen as negligible and must be removed by some form of solvent extraction procedure. This procedure is explained in section 3.1.9. The UV overlays at 254nm have been included in the plots. This gives an indication of the PS material present in the eluting block material after 15 minutes.
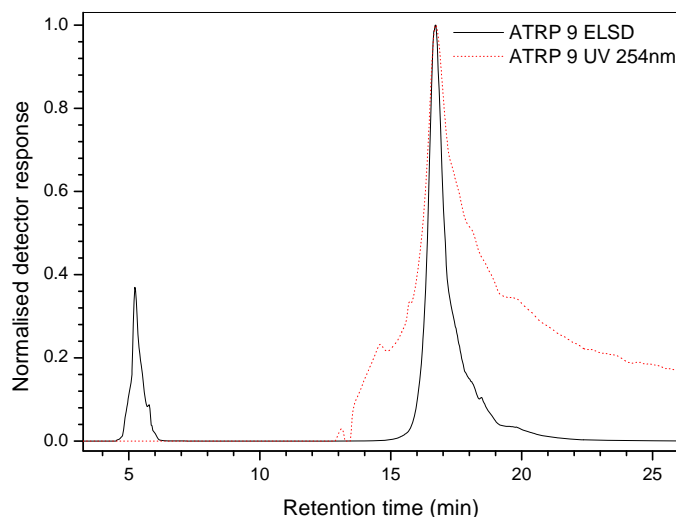
Figure 4.27   A typical GEC chromatogram (ATRP 9) including UV overlay.
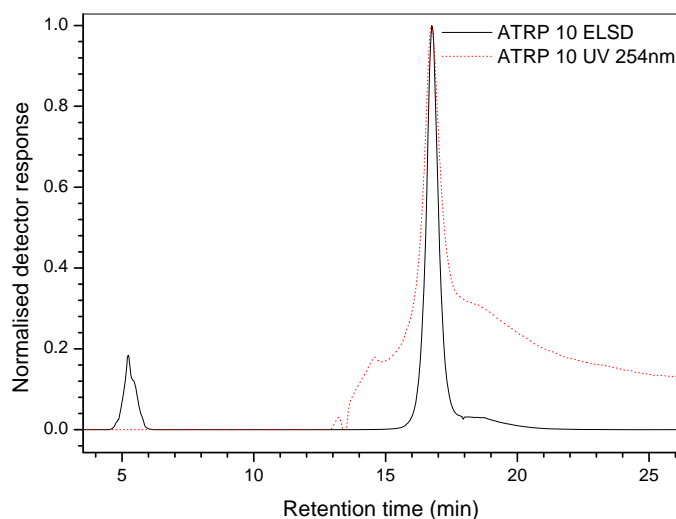
Figure 2.28   A typical GEC chromatogram (ATRP10) including UV overlay.

Note the lack of UV absorbance across the homo-PDMS peak around 5 minutes. The UV trace is not a perfect overlay, due to the constant change in mobile phase composition along the gradient. The UV baseline drifts as the solvent composition changes, but a strong peak overlaying with the peak of the ELSD trace indicates the presence of strong UV absorbing groups in this region. As mentioned earlier, extraction of homo-PDMS is much easier than extraction of homo-PS. Figures 4.29 and 4.30 show the same respective polymers after two extraction procedures.

Figure 4.29   A typical GEC chromatogram (ATRP 9) after two bromobenzene extraction steps.

Figure 4.30   A typical GEC chromatogram (ATRP 9) after two bromobenzene
extraction steps.

There is a clear decrease in the homo-PDMS peaks, while the block material peaks
remain unchanged. This proves the successful removal of the PDMS molecules via
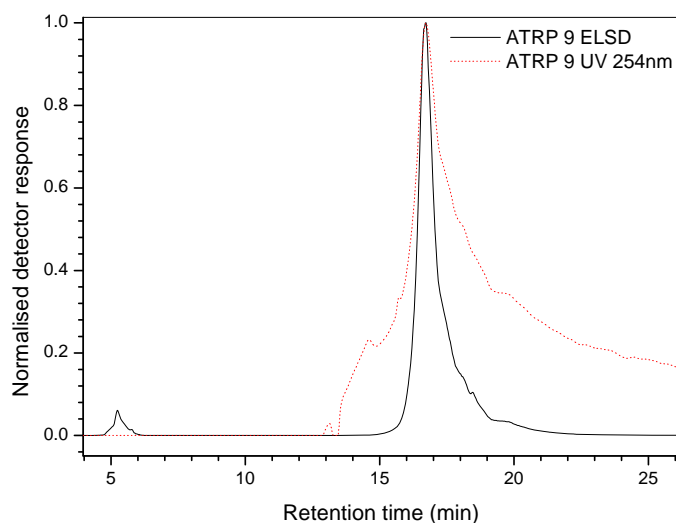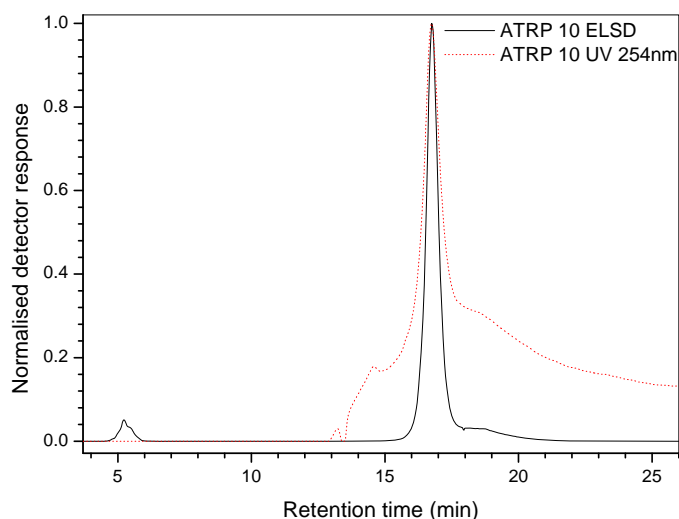extraction. There is still a small amount of homo-PDMS present, but subsequent
extractions were not able to get rid of this small amount of material.

Due to the nature of the extraction technique as explained in section 3.1.9, it was just
not possible to visibly see any homo-PDMS floating on the surface of the centrifuge
tube. The residual homo-PDMS was considered negligible in comparison to the block
copolymer present.

4.3.2.2 Characterisation using LC-CC

LC-CC at the critical point of PS was once again used to characterise the distribution
of the PDMS segments across the block copolymer region, as well as highlight the
presence of any homo-PS material and separate it from the blocks. As can be seen
in figures 4.31 and 4.32, the amount of homo-PS present in the sample is negligibly
small. Analyses of these samples were, however, performed in the same way as with
the sequentially synthesised products. Where possible, analysis was performed after
chromatographic separation, including morphological characterisation, which will be
discussed later. This allowed investigation of pure block copolymer effects, without
interference from homopolymer contaminants. The UV 254nm overlay indicates
successful block formation. The large UV absorbance over the homo-PS critical point

is due to the high concentration of aromatic rings, even though the amount of material is very little here.
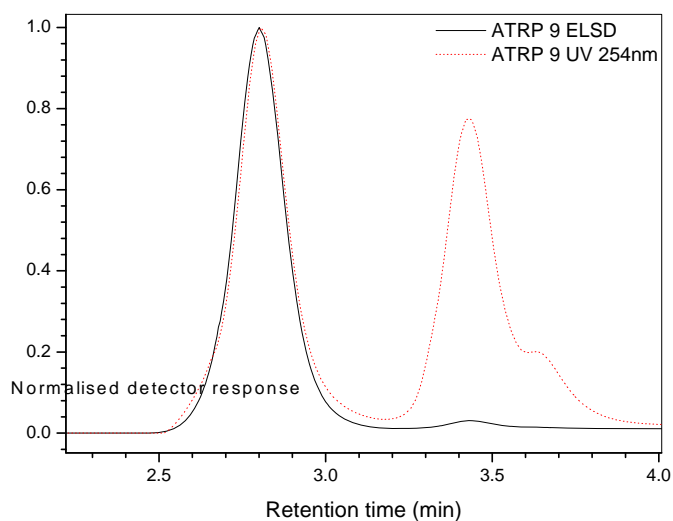
Figure 4.31   Normalised LC-CC chromatogram of ATRP 9 showing UV overlay.
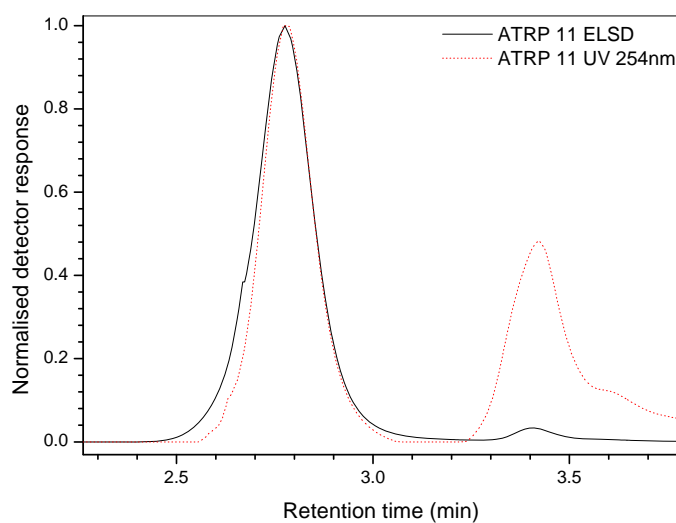
Figure 4.32   Normalised LC-CC chromatogram of ATRP 11 showing UV overlay.

4.3.2.3 Coupling of LC-CC to FT-IR

This technique was once again employed to analyse the chemical compositional distribution of the PDMS and PS segments in the block material. Figures 4.33 and 4.34 show typical Gram-Schmidt plots obtained from the macroinitiated ATRP polymerisation of styrene. Once again there seems to be a relatively constant PDMS to PS block composition in the block elution peak. This is indicated by the horizontal

plot of the ratio between Si-CH$_3$ and C$_6$H$_5$ absorption bands. There does seem to be a slight increase in the PDMS composition at the higher molecular weight side of the block copolymer peak. This could be due to the presence of unextracted homo-PDMS. Remember, it was not possible to extract all of the homo-PDMS material as mentioned earlier and shown in the GEC analysis. It could be that the remaining homo-PDMS consists of the longer homopolymer chains. This would explain the slight increase in PDMS composition in these regions. Once again, the ratio strives towards zero across the homo-PS critical point.

Figure 4.33   Gram-Schmidt plot of (ATRP 9) along with the ratio between Si-CH$_3$/C$_6$H$_5$

Figure 4.34   Gram-Schmidt plot of (ATRP 11) along with the ratio between Si-CH$_3$/C$_6$H$_5$.

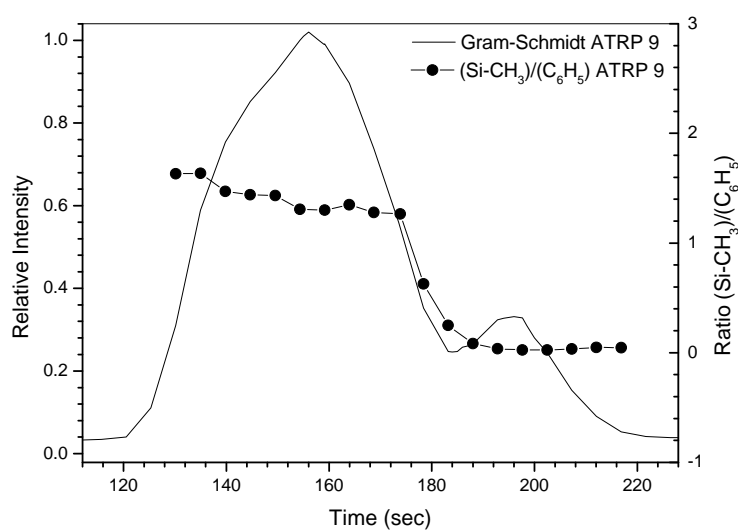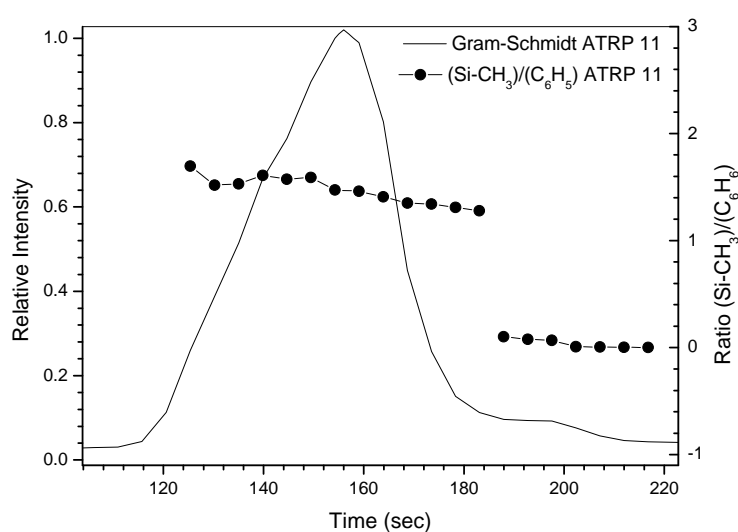This is expected as there is no PDMS material present here. It is also seen that due to a slight overlap of the sprayed polymer, this ratio does not start at zero at the beginning of the PS homopolymer peak, but slightly higher. It must also be noted that the amount of material eluted at this point is minute, which leads to diluted IR spectra intensities. Great care must be taken when interpreting these regions of low polymer concentration.

4.4 Surface segregation, modification and morphological studies

This part of the project deals with the phenomenon of phase segregation between the incompatible PDMS and PS segments. PDMS surface segregation and degradation using corona is discussed, as well as, morphological characterisation using a novel coupled approach.

4.4.1 Surface analysis

It is known from literature that PDMS has very interesting surface properties after corona treatment. These properties were aimed to be studied in the case of PDMS block copolymers as synthesised in this project. Thus, for this analysis, PDMS surface segregation would have to be ensured. This section of the study focuses on PDMS surface segregation in the block copolymer samples, as well as the properties after corona treatment.

4.4.1.1 Contact angle measurement

PDMS displays characteristically high contact angles with water drops, due to its hydrophobic nature. PS gives a lower contact angle, typically 95°. Contact angle measurement is therefore the first and simplest way to detect successful segregation of PDMS to the surface of a polymer sample. In this study, films of the block copolymers were prepared by casting from THF onto water. The films were then placed onto glass slides for support and annealed for 48hrs at $120^{o}C$ to promote PDMS surface segregation. Table 4.9 gives a summary of the studied block copolymer samples, along with contact angle (θ) measurements. There is not much difference between the samples, as the incorporation of PDMS in the block copolymer changes. There appears to be a slight increase in the contact angle

values for the higher PDMS content polymers (see LS 14), although very slight. The opposite extreme (see ATRP 5) shows a noticeably smaller contact angle value. This would imply that surface segregation takes place to such an extent, that the composition of the block copolymers does not affect the contact angles much, unless the ratios between the PDMS and PS segments are extreme. The exceptional hydrophobicity character is a result of two phenomena[12]. Firstly the methyl groups on the backbone provide hydrophobic characteristics and secondly, the flexibility of the silicone polymer chain allows rearrangement of the backbone to allow for methyl group orientation at the surface.

Table 4.9   A summary of the contact angle data of several corona treated sample films.

Sample Code	Ratio PDMS/PS	θ before corona	θ 24hrs after corona[a]
LS 5	2:1	110.9	95.7
LS7	1:2	110.7	94.8
LS 8	1:1	110.3	95.8
LS 9	1:2	110.8	95.1
LS 10	1:1	110.0	95.2
LS 14	4:1	113.7	96.5
LS 15	1:4	110.0	95.4
ATRP 5	1:8	109.1	94.4
ATRP 10	2:5	112.1	95.4
ATRP 11	4:5	111.6	95.1

[a]*Samples were exposed to 30min corona discharge.*

A very interesting phenomenon occurs after corona treating the surface of a PDMS-b-PS sample. The normally hydrophobic nature of the PDMS surface switches to hydrophilic. This indicates that corona treatment leads to drastic changes in the surface structure of the PDMS layer. The change is so drastic, that directly after corona treatment, contact angles cannot be measured as the water drop just spreads on the surface wetting it. Interestingly this hydrophilic character is lost with time. After 24hrs the PDMS sample gradually regains its hydrophobic nature, although not to its original state. A plot showing the hydrophobic recovery with time for a PDMS-b-PS copolymer is presented in figure 4.35. A column has also been included in table 4.9 displaying the contact angles after 24hrs after corona treatment. It appears that the samples do not regain their full hydrophobicity. The hydrophobicity recovery

phenomenon is well documented for pure PDMS samples after corona treatment and explained as being due to one of the following mechanisms[13]:

a)   Diffusion of pre-existing low molecular weight silicone fluid from the bulk to the surface.

b)   Re-orientation of polar groups from the surface to the bulk phase or reorientation of the non-polar group from the bulk to the surface.

c)   Condensation of the surface hydroxyl groups.

d)   Migration of *in situ* created low molecular weight species during discharge, to the surface.

Several researchers have suggested that the diffusion of low molecular weight species (mostly cyclics) tends to be the dominant factor in hydrophobic recovery[14,15]. After formation of the silica like layer, the low molecular weight molecules diffuse through the cracks and back to the surface.

This study shows the first evidence that a similar hydrophobicity recovery phenomenon occurs in PDMS based hybrid materials after corona treatment. This is clearly presented in figure 4.35.
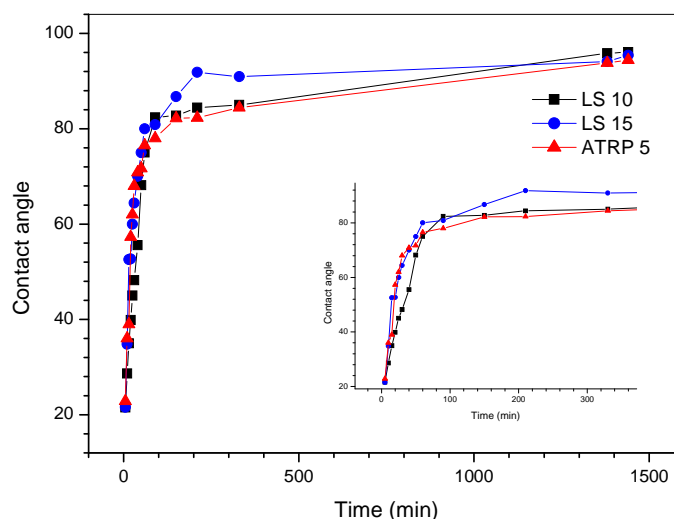

Figure 4.35   Typical hydrophobic recovery plotted against time for block copolymer samples.

Contact angle data indicates drastic changes in the surface structure of these samples after corona treatment. This study has shown that a PDMS containing

hybrid material exhibits hydrophobic loss and recovery after corona treatment, similarly to pure PDMS polymer. Further analysis was performed to confirm these drastic changes and to try and characterise them.

4.4.1.2 Optical microscopy and SEM analysis

Sample films were cast from a THF solution onto the surface of water and slid onto glass slides, as described in section 3.2.6. The samples were then transferred to an oven to anneal for 48hrs at 120°C. This allowed for equilibration of these phase segregated materials. PDMS is known, from literature[16,17], to preferentially surface segregate, due to its lower surface energy. The aim of this study was to analyse this surface segregation and to modify the surface using corona treatment. After annealing, samples underwent corona discharge treatment for 30 minutes. Figures 4.36(a) and 4.37(a) show the surface of the annealed films before corona, while figures 4.36(b) and 4.37(b) show the surfaces of the corona treated analogues. These images were obtained using an optical microscope. Note the fine cracks on the surface of the corona treated samples, and the "rainbow" effect. This is all due to the formation of a Si-Ox (this is a network of silicon bonded to more than to oxygen atoms) degradation layer on the surface due to corona treatment. This thin brittle layer acts like a fine glass layer and cracks very easily, due to the soft nature of the substrate polymer. Formation of this glassy layer in pure PDMS is well documented in literature[18,19]. This is the first evidence that a similar glassy layer is formed in PDMS hybrid copolymers. As mentioned in section 4.4.1.1 the hydrophobic recovery after corona is thought to be due to the diffusion of low molecular weight species to the surface. Diffusion to the surface is speculated to occur through the cracks visible in figures 4.36(b) and 4.37(b).

Scanning electron microscopy was also used to gain a closer look at the surface after corona treatment. These images are presented in figures 4.38(a) and (b). The crack in figure 4.38(a) is clearly evident and measures approximately 3μm across the width. A very interesting surface anomaly was also located on many of the samples. This crater is shown in figure 4.38(b). It is presumed that this was caused by strong bombardment from the corona arc. One can also see cracks spreading from the centre of this crater. The optical microscopy, SEM and contact angle experiments all allude to the fact that PDMS surface segregation did indeed take place. These results correspond well to those of cross-linked PDMS found in literature[18,19], strengthening the point that PDMS surface segregation occurred.
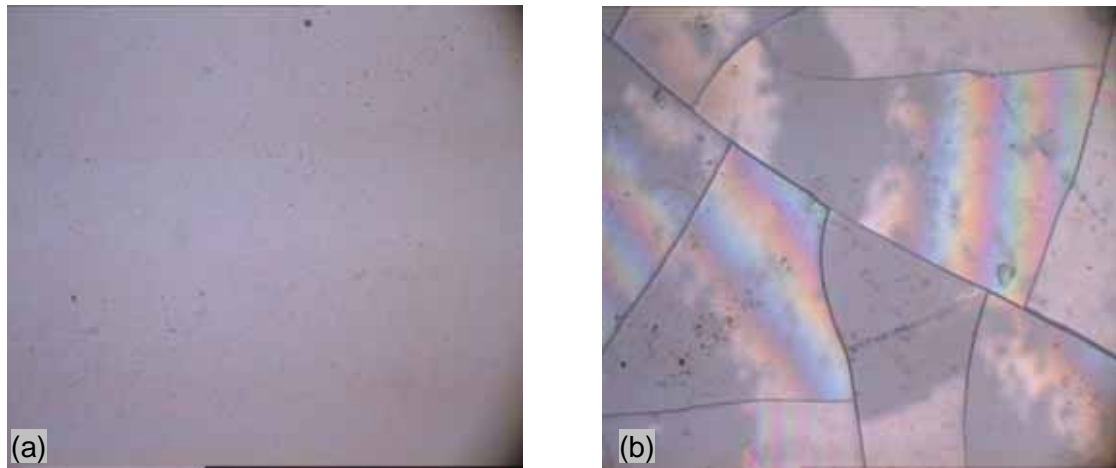
Figure 4.36   Optical microscopy image of LS 14 (a) before and (b) after corona.
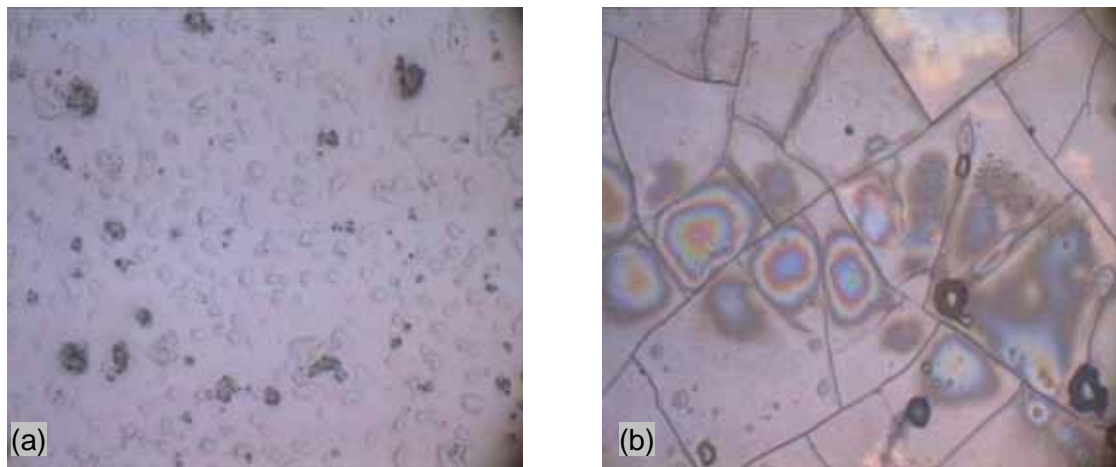

Figure 4.37   Optical microscopy images of ATRP 9 (a) before and (b) after corona.
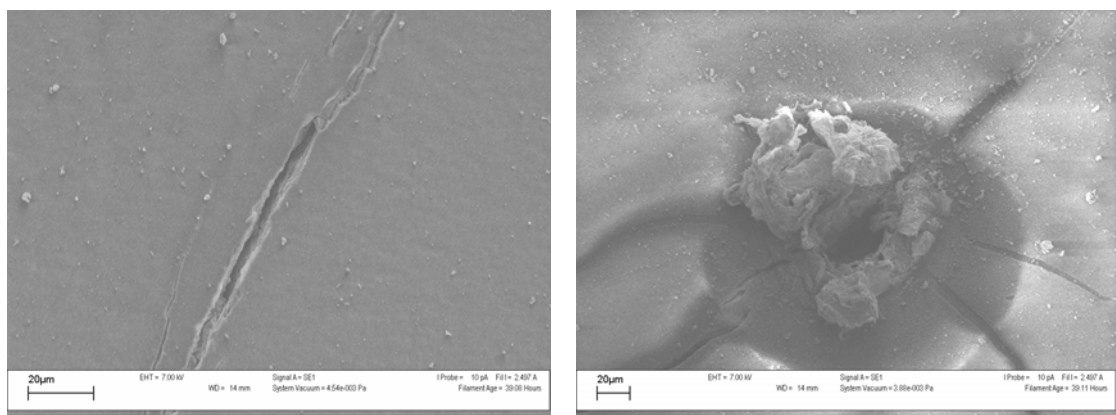

Figure 4.38   SEM images of LS 14 showing (a) surface crack and (b) corona damage.

It also confirms large changes in surface structure due to the change in hydrophobicity and the development of a glassy layer, showing as surface cracks on the polymer films. The following analysis looked at quantifying the thickness of this glassy layer, by studying free volume effects. It also looked at studying the free volume changes when moving from a glassy polymer (PS) to a highly viscous liquid polymer (PDMS) as well as an intermediate (PDMS-b-PS) polymer.

4.4.1.3   Slow positron beam analysis

This relatively new technique was used to study the phenomenon of Si-Ox formation on the surface of the PDMS-b-PS block copolymer films. Work by Mallon *et al.*[18] has shown that the slow positron beam technique can provide unique information on the SiOx layer formation and allows for an estimation of the SiOx film thickness in pure PDMS compounds. This study aimed to apply this technique to studying, not pure PDMS, but PDMS hybrid material. Films were prepared by spin coating samples from a solution of THF onto glass slides, as described in chapter 3. Films were then placed into an oven and annealed for 48hrs at 120°C. This allowed for surface segregation of the PDMS segments. Successful migration to the surface was proved by the preceding contact angle, optical microscopy and SEM analysis. After annealing, films were exposed to corona discharge for 30 minutes as mentioned previously. Optical microscopy analysis showed the development of surface cracks, due to the formation of a very thin Si-Ox layer.

Figure 4.39 shows the S parameter profile of a pure crosslinked PDMS compound, a pure polystyrene sample and one of the PDMS-b-PS block copolymers. In all cases the S parameter is low at the surface and increases to a maximum at higher position implantation energies, or at higher depths. This is typical for the S parameter profile in amorphous polymers[20]. It is clear from the figure that the maximum S parameter is largest for the pure crosslinked PDMS compound, and smallest for the PS sample. This is due to the three main factors that contribute to the S parameters in polymers: 1) the free volume content, 2) the free volume hole size, 3) the chemical composition (to a lesser extent)[20]. The S parameter is, therefore a direct qualitative measure of the free volume properties in the polymer. The larger S parameter measurement in the PDMS can be attributed to its considerably larger free volume properties compared to polystyrene at room temperature. (PDMS has a Tg of -127°C while PS has a Tg of 100°C). The block copolymer has a value that is intermediate between PDMS and PS.
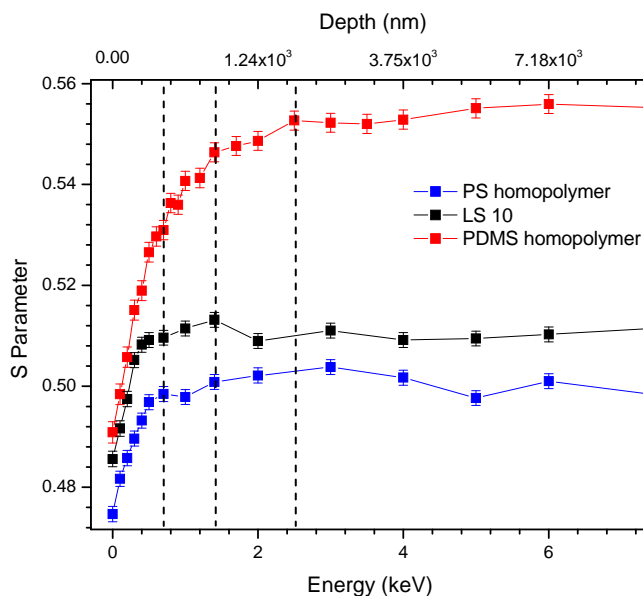
Figure 4.39   Slow positron beam overlays of a PS homopolymer, a PDMS homopolymer and a PDMS-b-PS block copolymer.

In figure 4.39, the point at which the S parameter reaches a maximum value, corresponds to the diffusion length of the positrons in the polymer. At low implantation energies the positrons and positronium formed in the polymer may diffuse back to the vacuum before annihilation in the polymer[21]. It is clear from the figure that once again the PDMS compound has the highest diffusion length as the S parameter only reaches its maximum value at implantation depths of 1.24μm. This once again can be attributed to the higher free volume in the polymer and the correspondingly larger (longer) diffusion length. The block copolymer profile lies between that of the two homopolymers. At low implantation energies, however, the measured S-parameter profile more closely matches that of the PDMS polymer. This can be attributes to the preferential surface segregation of the PDMS component and a correspondingly higher free volume at the surface in these materials.

Note how the incident energy on the lower x-axis is related to depth on the upper x-axis.   As mentioned in the discussion of the positron beam technique in section 3.2.12, this relationship is expressed in equation 4.1.[22]

$$Z(E_+) = (400/\rho)E_+^{1.6}$$ 4.1

It must also be noted that the depth (Z) is an average value for the positron implantation depth. In reality there is a distribution in the positron implantation depth

due to the positron stopping profile. This distribution becomes broader at higher implantation depths. The S-parameter profile at higher implantation energies will be the average S-parameter of the annihilation in each of the two phases in the polymer. It is not possible to distinguish the different phases at higher implantation depths due to the distribution of the position stopping profiles at higher implantation energies[23] leading to a measured S parameter that is an average of each of the different phases. This is why the bulk S-parameter of the block copolymer appears between the constituent homopolymers.

Figures 4.40 and 4.41 show typical slow positron beam results, before and after corona, for samples LS 4 and LS 10 respectively. These figures show the dramatic effect that the corona treatment has on the measured S parameter particularly at the surface of the polymer (note that the corona treated samples have been arbitrarily shifted on the y-axis for clarity in the figures). A similar effect was observed by Mallon *et.al.*[18] in pure PDMS compounds. The measured S parameter at the very near surface region (magnified inserts on the figures 4.40 and 4.41) shows a flattening. This behaviour is never observed for the surface of a polymer and provides further strong evidence for the formation of a SiOx type degradation layer on the surface of the polymer, similar to that observed in pure PDMS compounds. The flattening of the S parameter at the surface can be used to estimate the thickness of the SiOx layer which in these cases are approximately 55-60nm.
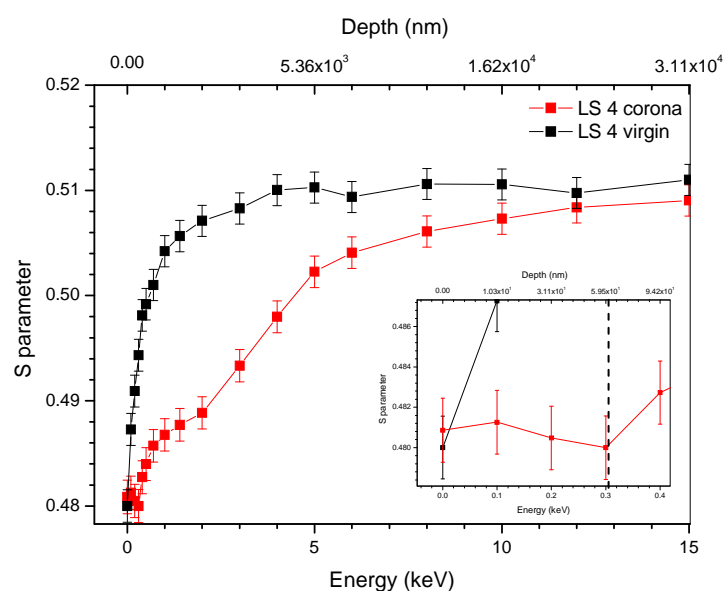

Figure 4.40   A typical S-parameter overlay of virgin and corona treated (LS4) block copolymer film, with magnified inset.
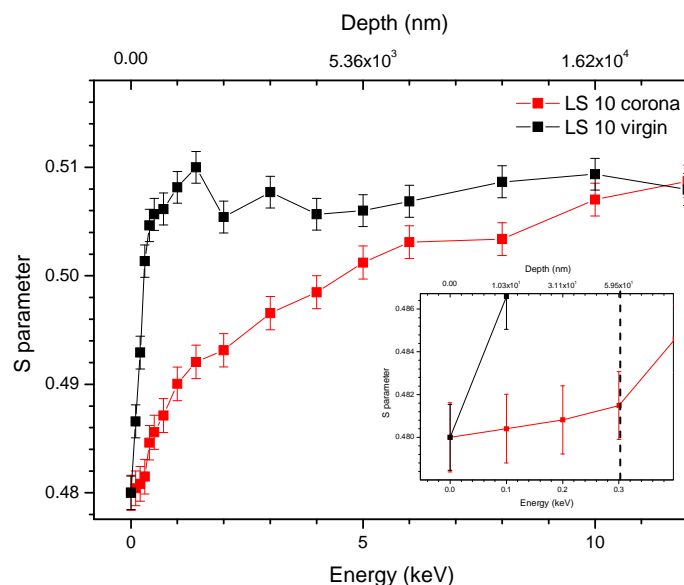
Figure 4.41   A typical S-parameter overlay of virgin and corona treated (LS10) block copolymer film, with magnified inset.

Figure 4.42 shows a plot of the ΔS parameter calculated according to equation 4.2. This illustrates clearly the difference in S parameter at the very surface of the material after corona indicating high surface specificity. This difference tends to zero towards the bulk material where no structural changes occurred.

$$\Delta S = S_0 - S_t \qquad\qquad 4.2$$

Figure 4.42   A typical plot of the difference in S parameter for corona treated and untreated samples.

It must be noted that all samples showed this flattening after corona indicating the depth of the silica like layer. Further analysis can be seen in appendix A titled slow positron beam analysis. These examples emphasise the powerful morphological depth profiling capabi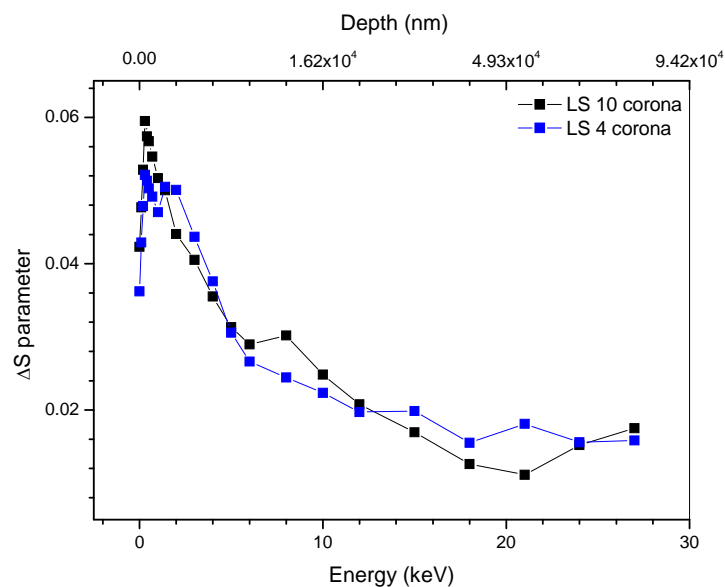lities of this technique, allowing distinction of nanometer thick layers. This allows very early detection of degradation by minute changes in material structure, such as free volume changes. This is the first evidence that the same degradation layer found after corona of pure PDMS, is formed on hybrid block copolymers of PDMS. It also showed differences in the diffusion length and bulk s-parameter values between the block copolymers and its constituent homopolymers. This technique has once again proved its value as one of the few available techniques that allows for the estimation of the SiOx degradation layer thickness. It also showed permanent surface changes even after hydrophobic recovery.

4.4.1.4 Degradation study using chromatographic and FT-IR techniques

Studying the results obtained after corona treatment, it is clear that there are drastic structural changes occurring on the surface of these films. This section focused on trying to describe the degradation behaviour induced by corona treatment. It was decided to use LC-CC and conventional SEC coupled to FT-IR to study this degradation process. By using this method, not only can molecular 'breakdown' be studied (shifting of the SEC distributions to lower molecular weights), but the FT-IR data can indicate the presence of new or altered chemical groups. These could be carbonyl peaks or hydroxyl groups after chain scission. The change in the Si-O absorption bands could also be tracked, as this is bound to change as the $(Si-O)_x$ layer forms. The only way to obtain this glassy layer is by modification of the PDMS backbone. This would imply that the CH_3 groups along the backbone undergo drastic changes or even removal. Combination of the molecular weight changes (chromatography) with chemical group information (FT-IR) appears to be the answer to unravelling the corona degradation process. Unfortunately the main characteristic of this surface degradation lead to analytical sensitivity problems. The fact that this degradation layer is so surface specific, when compared to the bulk material, no structural or chemical changes could be detected. Below in figure 4.43 is an LC-CC overlay of LS 14 showing the traces before and after corona. The traces are a perfect fit, showing no shifts or shoulders in molecular weight which could indicate possible molecular degradation. Also when coupled to the FT-IR no difference in any of the IR spectra taken along the elution volume was found.

These results were typical for all the polymers studied using this technique. The sensitivity of this method is not astute enough to allow characterisation of such small changes. It is clear that there needs to be a drastic increase in the surface areas of the sample specimen before corona treatment. This would allow a greater concentration of degradation species to be present, allowing easier detection. A possibility would be increasing the surface area by spinning nano-fibres of the polymer. This is discussed in the section 5.2 recommendations, and was beyond the scope of this project.
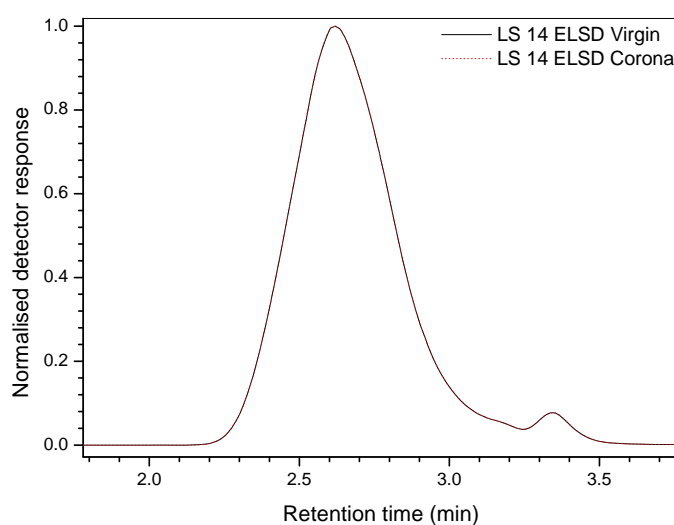

Figure 4.43   LC-CC overlay of LS 14 before and after 30min corona treatment, showing no changes in distributions of peaks.

The formation of thin films was also looked at as a possible solution. Corona on these thin films could possibly give a high enough ratio of degradation layer to bulk material to allow detection of changes. Once treated these films were analysed using attenuated total reflectance (ATR) FT-IR studies, a result of which is shown in figure 4.44. Small changes in the overlay of these untreated and corona treated films were noticed. The changes are minute, so only the ratio of Si-O ($1100cm^{-1}$) to Si-CH$_3$ ($1260cm^{-1}$) was studied. This should be the most visible chemical change, judging by the positron and surface microscopy analysis. The development of the SiOx layer should lead to noticeable changes in these ratios. Only a few of the samples studied this way gave differences in these absorption values. They are listed in table 4.10 along with the peak height intensity changes.
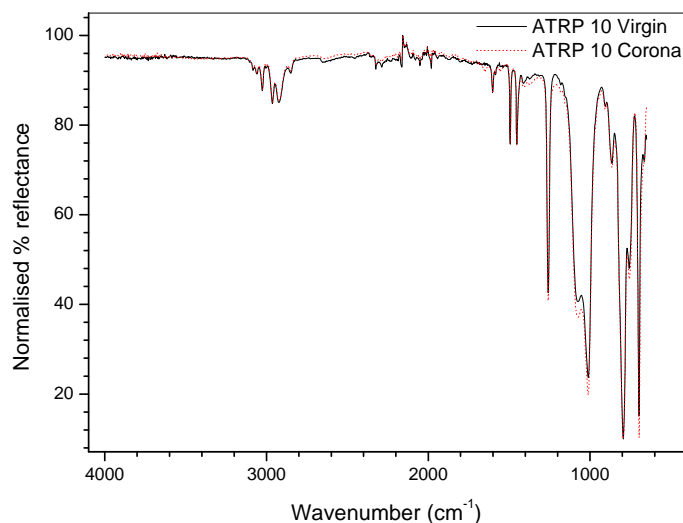
Figure 4.44   ATR overlays of ATRP 10 before and after 30min corona treatment.

Table 4.10   A summary of the peak area intensities of block copolymer samples, before and after corona discharge.

Sample	Virgin		Corona		Ratio	Ratio
code	Si-O-Si[a]	Si-CH$_3$[b]	Si-O-Si[a]	Si-CH$_3$[b]	virgin	corona
LS 14	5553	2039	5234	1502	2.7	3.4
LS 15	6811	888	6701	824	7.6	8.1
ATRP 5	5935	780	6170	943	7.6	7.7
ATRP 10	5726	767	6981	869	7.4	8.0
ATRP 11	2443	1254	7473	2227	1.9	2.3

[a]*Peak area intensity at 1100cm^{-1}*
[b]*Peak area intensity at 1260cm^{-1}*

These values do indicate a slight increase in the ratio between the Si-O-Si and the Si-CH$_3$ absorption bands, after corona treatment. This result is expected due to the development of the (Si-O)$_x$ glassy layer after corona. Unfortunately other possible degradation peaks such as carbonyls (around 1650-1700cm^{-1}) or hydroxyl groups (around 3300cm^{-1}) could not be established due to concentration issues. Work by Hillborg and Gedde[24] studied pure crosslinked PDMS after extended times of corona. Similar results were found, were the degradation is too surface specific to detect using this technique. Equation 4.3[24] calculates the depth of surface layer assessed by ATR. Here, λ is the wavelength in air, θ is the angle of incidence, n$_1$ is the refractive index of the ATR crystal and n$_{21}$ is the ratio of the refractive index of the sample to that of the ATR crystal.

$$d_p = \lambda \, / \, [\, 2\pi n_1 (sin^2\theta - n_{21}^{\,2})^{1/2} \,] \qquad\qquad 4.3$$

This was shown by Hillborg and Gedde to be approximately 0.45-4.5μm. This is too deep to be strictly surface related.

A new technique that shows a lot of promise is that of confocal raman spectroscopy. This advantage of this technique is its ability to depth profile from the very surface of a sample specimen. This is perfect in our case, as the degradation layer is so surface specific. We were fortunate enough to have access to such an instrument. Unfortunately due to time and travel constraints towards the end of this project, only a few samples could be analysed. The transparency of these samples posed a problem when it came to focusing the IR beam onto the surface. Figure 4.45, however, shows an overlay of confocal raman spectroscopic analysis of an untreated and treated LS 14 film sample. These spectra were normalised to the CH in plane bending of the PS segments at 1126 cm^{-1}. Although small, changes are evident in the pre and post corona treated samples. The range shown below includes the Si-O-Si symmetric stretching at 492 cm^{-1} and the Si-CH$_3$ symmetric rocking at 623 cm^{-1}, which were used to monitor changes after corona treatment. As mentioned previously changes in this region should be the most obvious, as seen by the dramatic change in surface character with the formation of a nano (Si-O)$_x$ layer. The peak height ratio of Si-O-Si to Si-CH$_3$ was found to be 4.59 in the virgin sample and 7.62 in the corona treated sample. These values show a definite decrease in the relative amount of Si-CH$_3$ groups relative to the Si-O-Si groups after corona. For a more conclusive result more samples would have to be analysed and compared, but unfortunately due to time and travel constraints this was not possible in this research project. Confocal Raman spectroscopy, however, shows great potential as a technique for studying this surface specific corona induced degradation behaviour.

In summary, it has been shown from the dramatic contact angle changes after corona discharge and the development of a glassy surface layer studied by positron beam and optical analysis, that drastic structural changes occur after corona treatment. Trying to pin down the exact degradation process proved most difficult due to the surface specificity of the degradation layer. Conventional FT-IR and chromatographically coupled FT-IR showed no real differences between treated and untreated samples. ATR of thin films showed slight changes in the ratio between the Si-O-Si and the Si-CH$_3$ absorption bands.
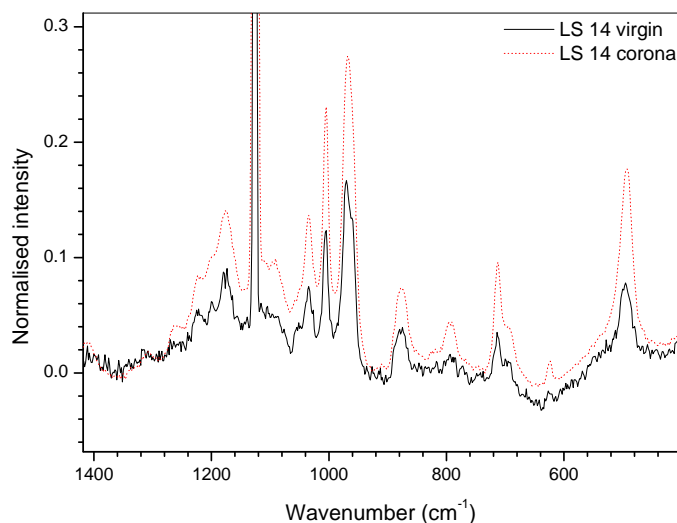
Figure 4.45   Overlay of confocal raman spectra of virgin and corona treated LS 14.

Other degradation peaks were, however, not detected. A similar difference in the ratio was also evident in the confocal Raman spectra. This surface specific technique appears to have much potential in studying this degradation process, but further analysis time is required to obtain a more conclusive result.

4.4.2 Morphological analysis

As mentioned in chapter 2, section 2.4, PDMS-b-PS block copolymers exhibit distinct morphological configurations, due to the incompatibility of the constituent segments. These morphological characteristics were studying using a novel approach. Conventional TEM was used for morphological characterisation, coupled to the LC-CC chromatographic technique developed in this project. This novel approach to analysis has powerful potential as a method to study molecular weight or chemical composition dependant morphological features. A brief explanation of the development of this technique follows. Initially this technique was developed to avoid laborious removal of homopolymer contaminants from the pure block copolymer material. With conventional solvent extraction, it is extremely difficult to remove 100% of the homopolymer material. Chromatography, however, allows excellent separation of the block material from homopolymer contaminants, depending on the operating mode.

4.4.2.1 LC-CC coupled to TEM via direct deposition.

In this technique the LC-transform device is used to directly deposit the eluent onto TEM grids. This is shown in figure 4.46. After separation according to the LC-CC (critical conditions of PS) mode, the polymer exits the HPLC machine, and is deposited directly onto the TEM grids, which are used as sample supports in the TEM module. These TEM grids are fixed to the germanium disk in line with the eluting material. After deposition the TEM grids are transferred to an oven for annealing at 120°C for 48 hrs. These samples are then placed directly into the TEM module for image analysis. Unfortunately, this method of preparing samples, was not as efficient, due to the thickness of the deposits. By decreasing the concentrations of the samples injected into the HPLC, it was thought that the thickness of the deposit could be varied. This was not entirely true due to the spraying action of the nebulising nozzle. The exiting material coalesced before deposition onto the grids and formed "clumps" of material all across the TEM grids.
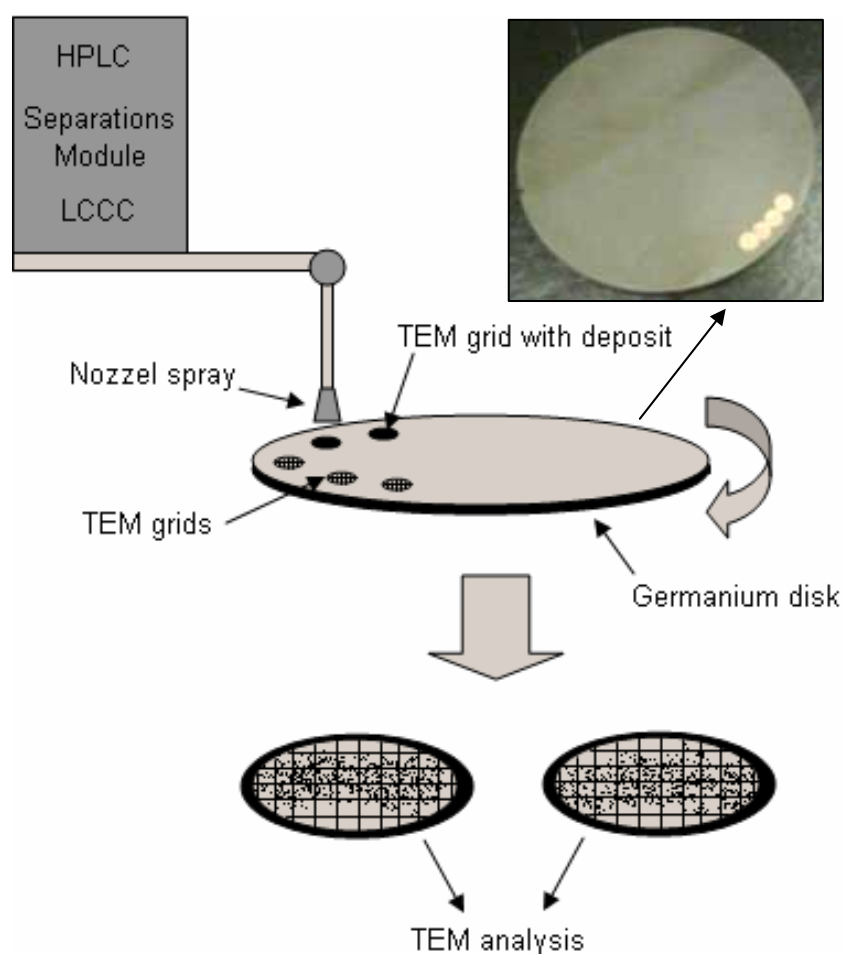

Figure 4.46   A simple diagram showing the direct deposit method of coupling TEM and LC-CC.

It was, however, possible to obtain a few good TEM images using this technique and these are shown in figures 4.47 (a) and (b). Note how they represent ranges A and B of the eluting molecules, indicated by the chromatogram in figure 4.47 (c). These are good images, but much time was spent on finding a region thin enough to analyse using TEM. As can be seen, LS 14 exhibits typical cylindrical morphology in figure 4.47 (a). The light areas are PS and the dark areas are PDMS, due to the differences in electron densities. We therefore see PS cylinders present in a continuous phase of PDMS. This morphology follows from literature, as the PDMS segments are much larger than the PS segments in LS 14 (5000 PS:20000 PDMS). In figure 4.47 (b) we have what appear to be block copolymer micelles present in a PS continuous phase. This is entirely plausible, as the retention range collected includes a large amount of homo-PS material due to overlapping spray of the deposited samples.
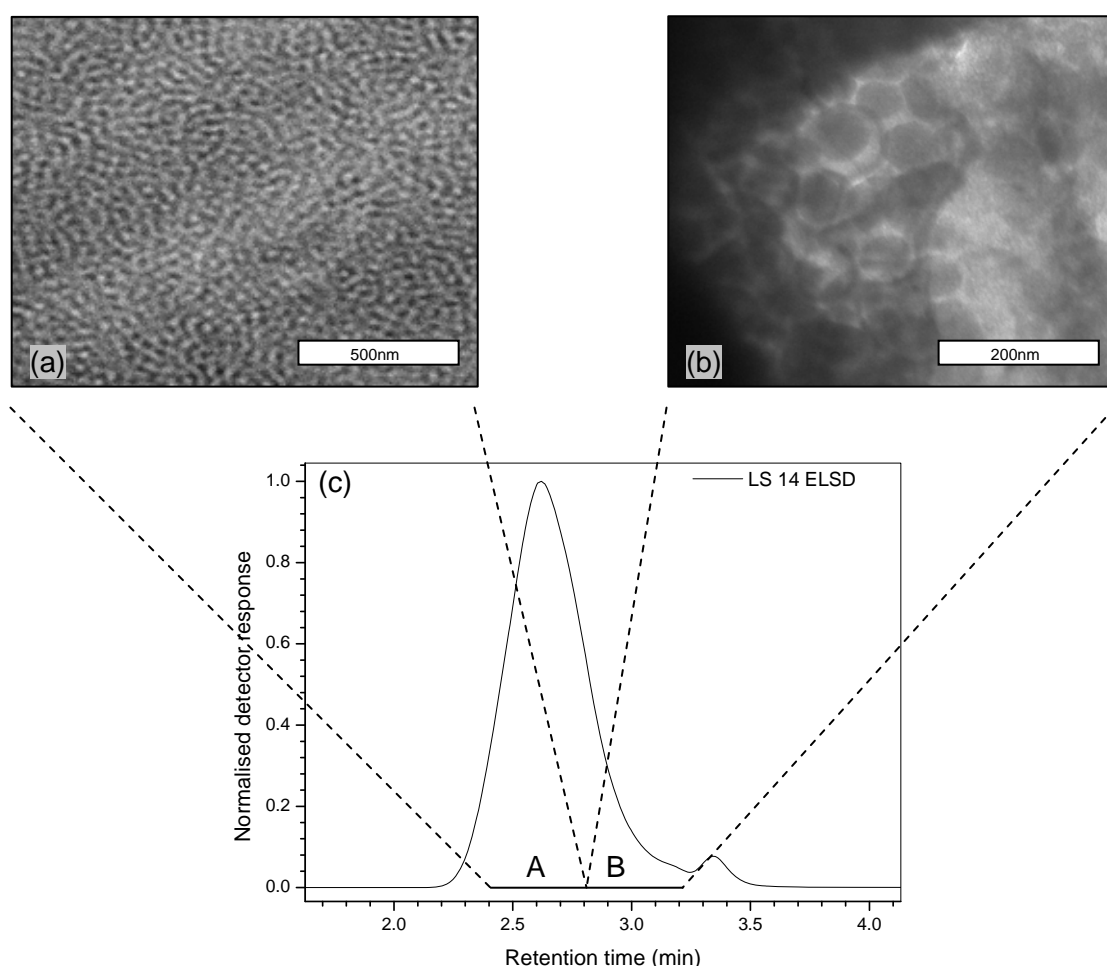
Figure 4.47   LC-CC chromatogram of LS 14 (c) with corresponding TEM images of the material in the highlighted retention ranges, (a) A and (b) B.

The small amount of block copolymer present forms micelles with inner PDMS cores, illustrated in the image. This morphology arises as a result of the minimisation of the interfacial surface tension between the opposing segments. This micelle formation of PDMS-b-PS copolymers blended with their respective homopolymers was studied in work by Mari'c and Macosko[25].

A second, more refined method, was developed to improve on these results. This is discussed in the following section of work.

4.4.2.1 LC-CC coupled to TEM via indirect deposition.

This technique proceeds similarly to the previously discussed method, except direct deposition onto the TEM grids does not take place. A diagram of this technique is presented in figure 4.48.

In this case the eluting material is deposited onto silica chips that have been fixed to the germanium disk. These silica chips are then transferred to 2ml vials where they are rinsed with a few drops of THF. This is shown in figure 4.48. After rinsing off the deposited polymer, the solution is then dropped onto a Petri-dish of water. The hydrophobic material forms a film on the surface, while the THF diffuse into the water. This film stretches as the THF rapidly diffuses, leaving a very thin film, ideal for TEM analysis. Using tweezers, TEM grids are used to "scoop" up the film off the water surface. These film supporting grids are then transferred to a vacuum oven where they are annealed at 120°C for 48hrs. This method allows the polymer to be deposited in the form of a thin film, rather than clumps, as was the case with the preceding method. This is a vast improvement on the previous technique, due to the ease of TEM analysis using these films. There is no more problem finding thin enough areas, conducive for TEM analysis. This novel coupling technique gave excellent results, a few of which are now discussed.

Firstly, the analysis of LS 15 is shown in figure 4.49. This block copolymer sample had a larger PS segment of 20000 compared to that of PDMS which was 5000. Interestingly this composition gave distinctive lamellae morphology. The PDMS appears as dark areas, while the PS appears lighter in colour. This morphology is expected for compositions in the region of 50:50, but work by Chu *et al.*[26] showed that this composition dependence is strongly skewed in PS-b-PDMS copolymers, especially towards lower PS content.
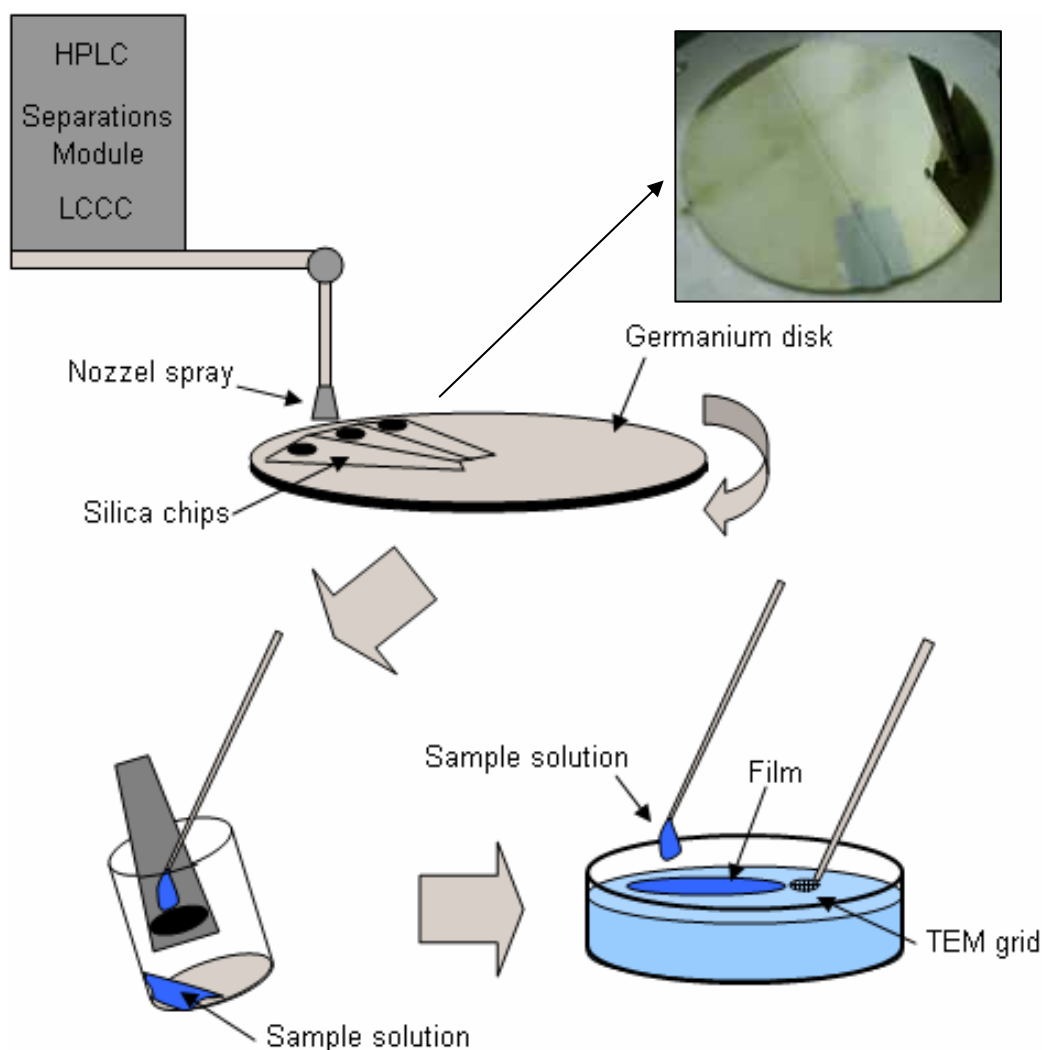
Figure 4.48   A basic diagram of the indirect deposition method of coupling TEM to LC-CC.

This morphology is therefore not surprising. Note the regions of the eluted material analysed. The block copolymer peak was divided in two halves. The first half (region A) contained the block copolymer with the longer PDMS segments. The second half (Region B) contained the block copolymer with the shorter PDMS segments.

The elution chromatogram shown in figure 4.49 (c) is the LC-CC chromatogram at the critical point of PS, so the block region is separated in SEC mode according to the PDMS segmental length only. Therefore the polymer molecules in the block elution region are arranged from long PDMS segments (left) to short PDMS segments (right). The differences in the TEM images for the respective regions, is clearly evident.

In 4.49 (a) the lamellae have repeat layers of PDMS and PS, where the PDMS averages 13nm cross width and the PS averages 14nm cross width. This changes drastically in figure 4.49 (b). Here the PS cross width remains relatively the same, whereas the PDMS cross width drops drastically to about 7nm. This is because the PDMS segments in this region are much shorter, giving narrower PDMS bands. The PS remains the same, as it has not undergone chromatographic SEC separation, so these segments remain mixed. This result emphasises the characterisational power of this technique. There is a clear distinction between the morphology as the PDMS block length changes.
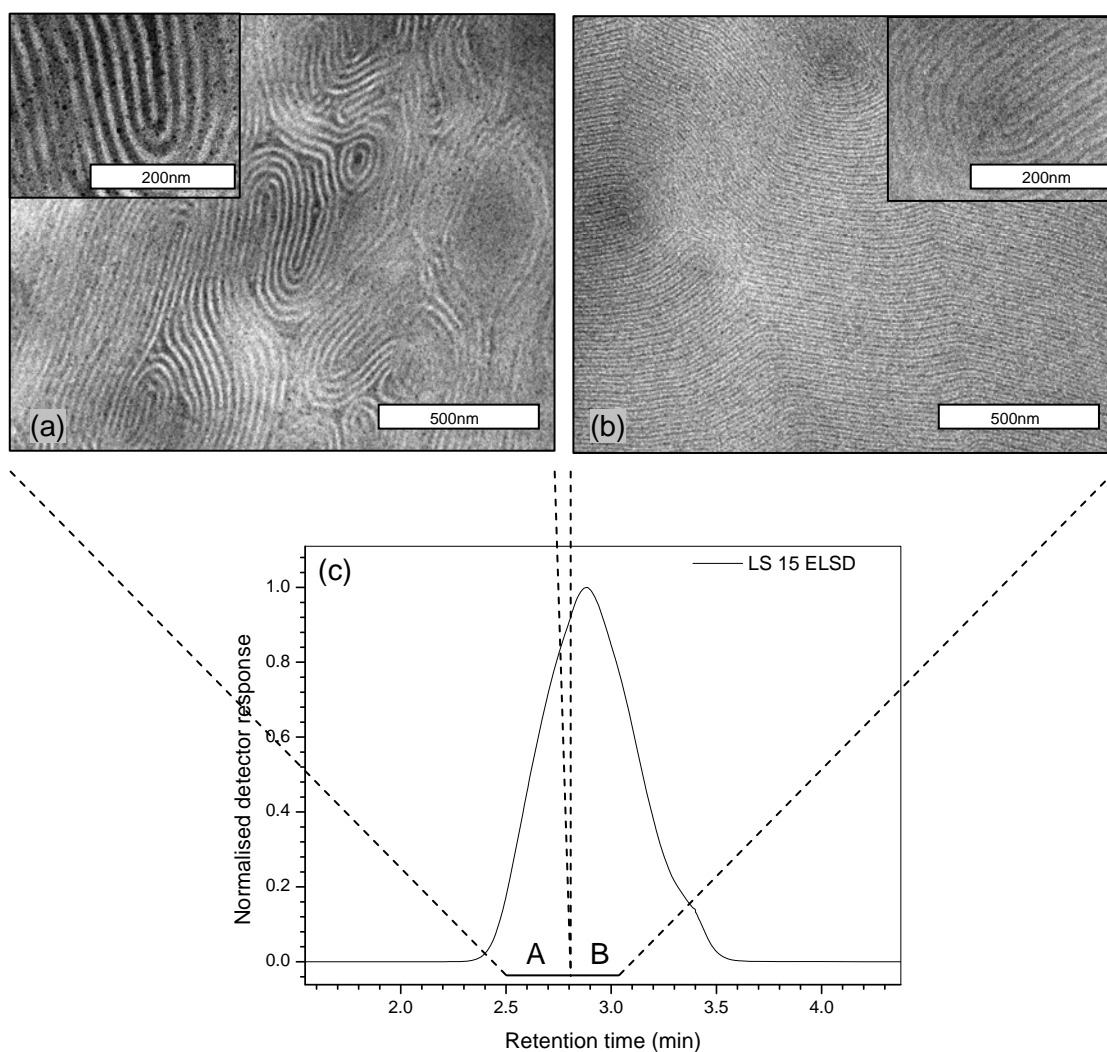

Figure 4.49   LC-CC chromatogram of LS 15 (c) with corresponding TEM images of the material with magnified insets in the highlighted retention ranges, (a) region A and (b) region B.

Another example is that of LS 14, pictured in figure 4.50. Here there is clear cylindrical morphology. There are PS cylinders in a PDMS continuous phase. This

corresponds to the chain composition, as the PDMS is much longer with a ratio of (2000 PDMS : 5000 PS). Here once again the material is separated according to PDMS segmental length as shown in the LC-CC chromatogram in figure 4.50 (c). There is again a clear decrease in the interstitial thickness, or area, of the PDMS regions between the PS cylinders. The PS cylinder structures remain relatively stable in dimension. Once again this example highlights the usefulness of this technique in studying molecular weight dependant morphology.
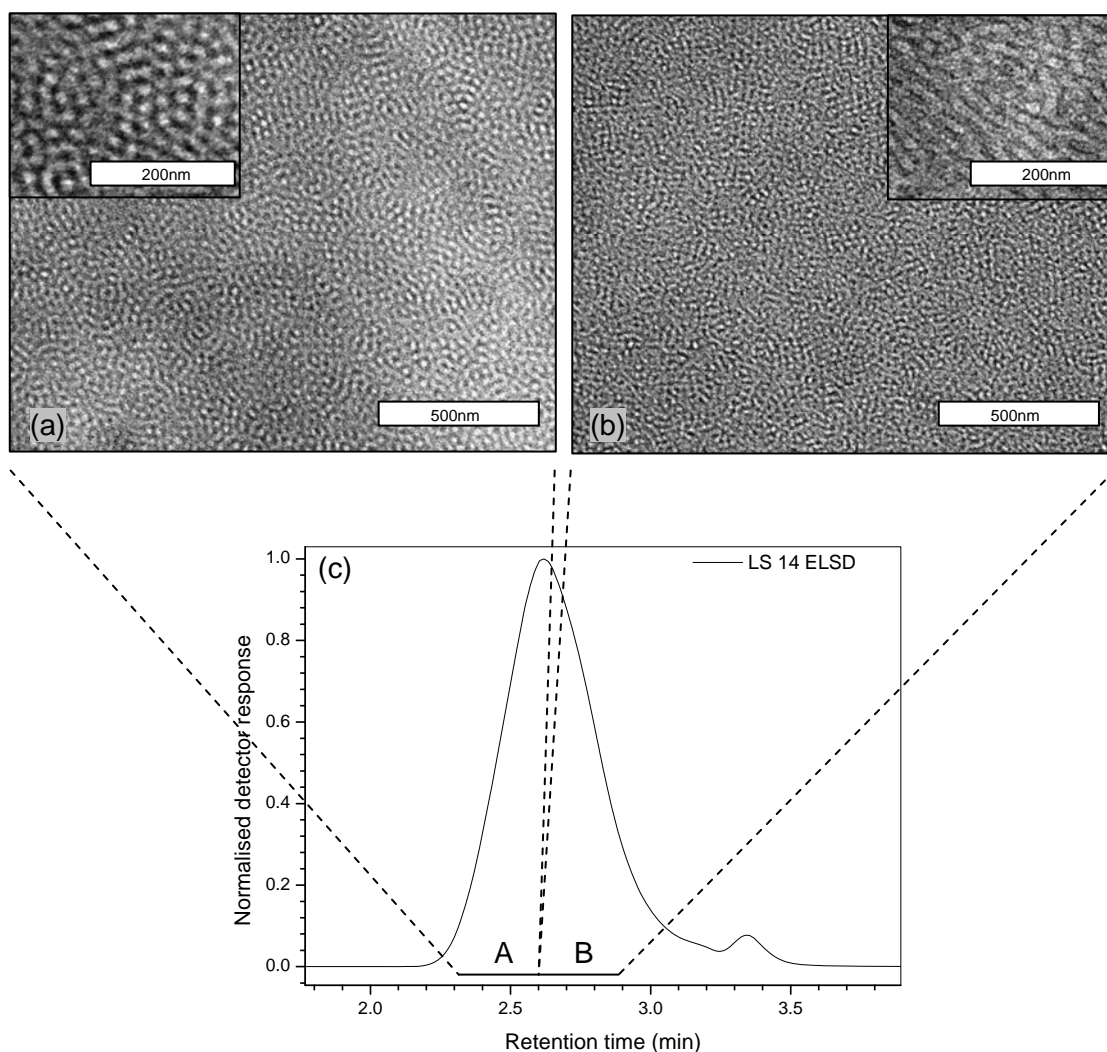

Figure 4.50   LC-CC chromatogram of LS 14 (c) with corresponding TEM images of the material with magnified insets in the highlighted retention ranges, (a) region A and (b) region B.

Another example has been included where overlapping of the block material peaks with the homopolymer peaks occurred. ATRP 10 showed this overlap behaviour. Also, this sample did not have homo-PDMS extracted prior to analysis. Referring

back to section 4.3, PS-homopolymer was synthesised via thermal initiation. The sample collection ranges shown on the chromatograms previously, stayed away from the PS homopolymer region. This was to avoid any overlapping spray, contaminating the pure block sample with homo-PS. The images in figure 4.51 shows the morphology when homo-PS is included due to overlapping spray. The background appears to be dark PDMS cylinders in a continuous PS phase.

This is expected as the PS segments in this copolymer are much larger than the PDMS counterparts, see table 4.8. The white spheres scattered throughout the image is the homo-PS material.
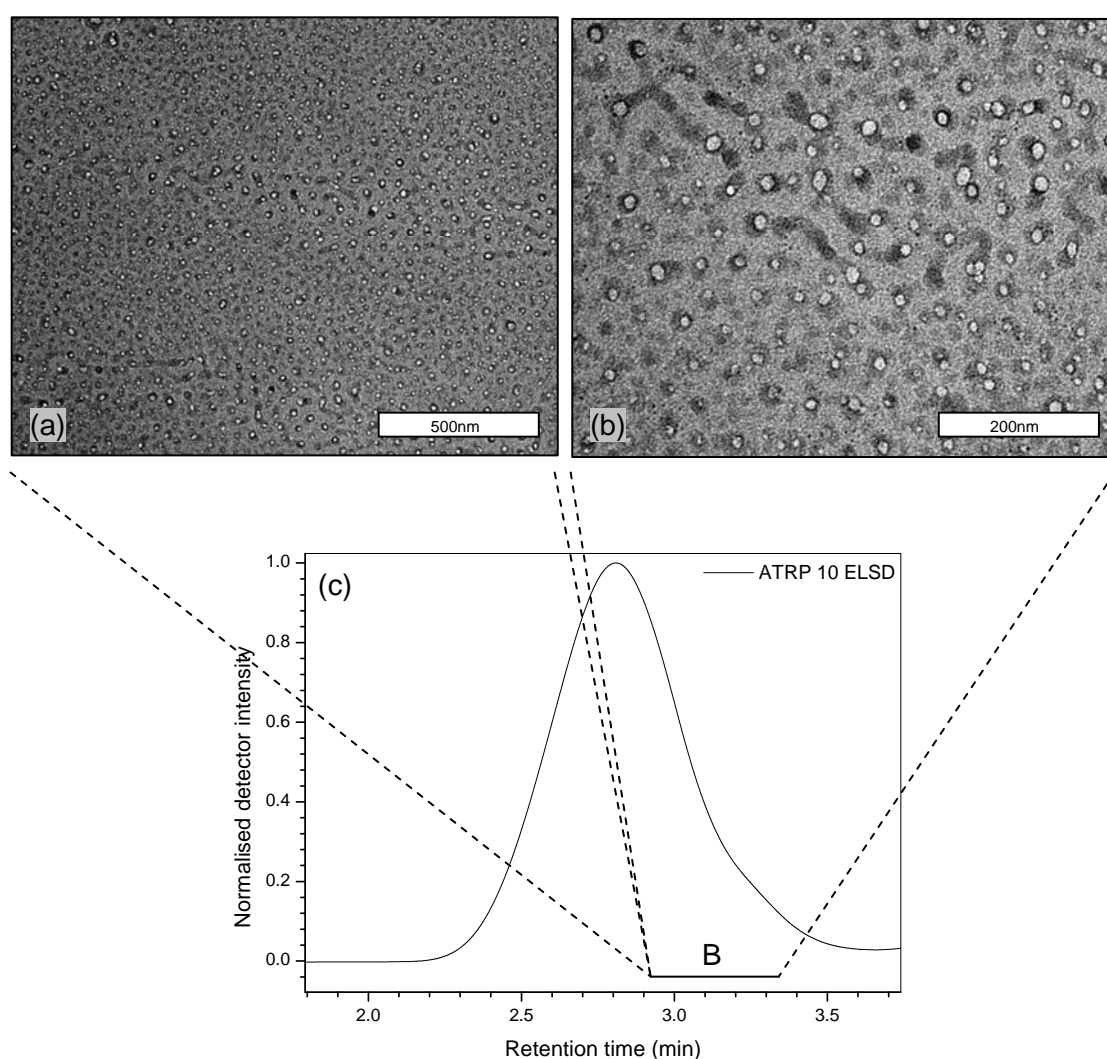

Figure 4.51   LC-CC chromatogram (c) with TEM images showing the presence of homo-PS contaminants, at (a) 10000 magnification and (b) 25000 magnification for region B.

Figures 4.52 (a) and (b) show TEM images of ATRP 10, but in region A. This sample did not undergo PDMS extraction, allowing image analysis of homo-PDMS contaminants in the block material. There appears to be disrupted lamellae morphology. The periodicities of the lamellae appear to be disrupted by the presence of PDMS homopolymer. This is due to the lack of homo-PDMS material extraction. This sample was the only ATRP synthesised sample that showed such phenomena, implying that the PDMS was not successfully extracted in this instance. The PDMS forms globules that are located along PDMS segmental lamellae.
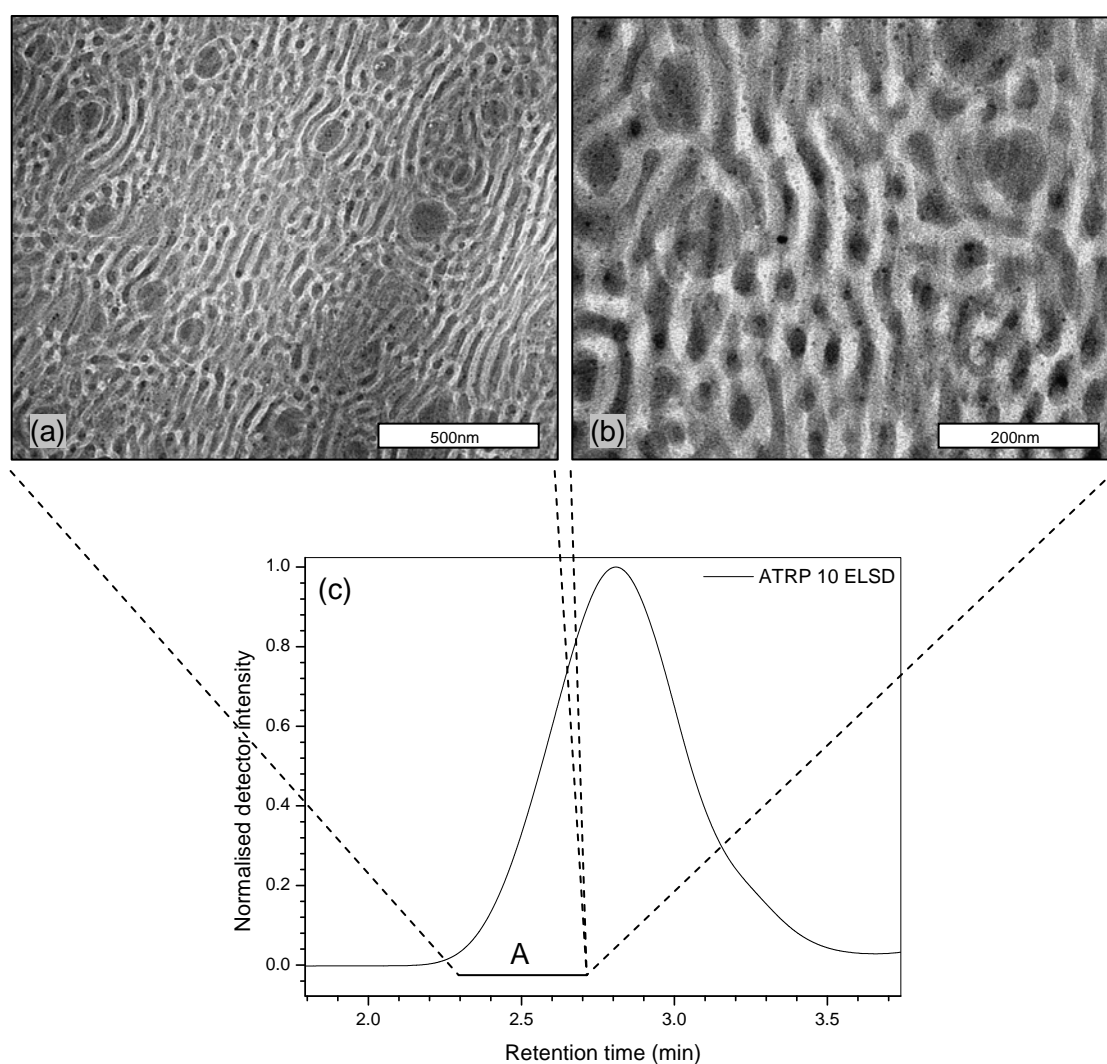

Figure 4.52   LC-CC chromatogram (c) with TEM images showing the presence of homo-PDMS contaminants, at (a) 10000 magnification and (b) 25000 magnification for region A.

Firstly, by separating the block material on the HPLC prior to analysis, one ensures complete removal of all homo-PS molecules, whether pre-extracted or not. If

overlapping does occur, then shifting of the regions analysed away from the homo-PS elution solves this problem. In products where extraction of a constituent homopolymer is difficult, as for the homo-PS in this case, this technique allows morphological characterisation without prior extraction. As was shown throughout this project, coupling analytical techniques with chromatographic separation allowed for analysis without interference from the homo-PS material. Although coupled to the HPLC using LC-CC mode, in this project, this novel technique can be applied to conventional GPC separation of polymers in SEC mode or any other liquid chromatographic separation.

In summary, this technique provides an easy route to sample preparation, avoiding conventional cryo-microtoming. The most powerful aspect of this coupled technique is the ability to study morphology as a function of molecular weight. The samples studied in this project showed distinct morphological changes even though they were prepared using controlled techniques which gave narrow structural distributions. Analysis of samples that were synthesised using uncontrolled methods, where a wide variety of chain lengths and segments is produced, could prove very interesting indeed. In these cases one may be able to see even more dramatic morphological changes for the different molecular weight regions. With conventional bulk TEM sample preparation we lose this interesting morphological information.

This concludes chapter 4. The following chapter is a summary of the conclusions of this research project, as well as a list of recommendations for future work.

4.5   References

(1)   Odian, G. *Principles of Polymerisation*, 4th ed.; New Jersey: John Wiley and Sons, **2004**.

(2)   Smid, J., Van Beylen, M., Hogen-Esch, T.E. *Prog. Polym. Sci.* **2006**, *31*, 1041-1067.

(3)   Elkins, C. L., Long, T.E. *Macromolecules* **2004**, *37*, 6657-6659.

(4)   Chaumont, P., Beinert, G., Herz, J., Rempp, P. *Polymer* **1981**, *22*, 663-666.

(5)   Bellas, V., Iatrou, H., Hadjichristidis, N. *Macromolecules* **2000**, *33*, 6993-6997.

(6)   Macko, T., Hunkeler, D. *Adv. Polym. Sci.* **2003**, *163*, 61-136.

(7)   Park, I., Park, S., Cho, D., Chang, T., Kim, E., Lee, K., Kim, Y.J. *Macromolecules* **2003**, *36*, 8539-8543.

(8)   Venkatesh, R., Klumperman, B. *Macromolecules* **2004**, *37*, 1226-1233.

(9)   Matyjaszewski, K., Patten, E., Xia, J. *J. Am. Chem. Soc.* **1997**, *119*, 674-680.

(10)   Matyjaszewski, K., Xia, J. *Chem. Rev.* **2001**, *101*, 2921-2990.

(11)   Parker, J., Jones, R.G., Holder, S.J. *Macromolecules* **2000**, *33*, 9166-9168.

(12)   Brook, M. A. *Silicon in organic, organomettalic and polymer chemistry.*; Canada: John Wiley and Sons, **2000**.

(13)   Kim, J., Chaudhury, M.K., Owen, M.J., Orbek, T. *J. Colloid Interface Sci.* **2001**, *244*, 200-207.

(14)   Hillborg, H., Karlsson, S., Gedde, U.W. *Polymer* **2001**, *42*, 8883-8889.

(15)   Toth, A., Bertoti, I., Blazso, M., Banhegyi, G., Bognar, A., Szaplonczay, P. *J. Appl. Polym. Sci.* **1994**, *52*, 1293-1307.

(16)   Chen, X., Gardella Jr, J.A., Kumler, P.L. *Macromolecules* **1992**, *25*, 6631-6637.

(17)   Chen, X., Gardella Jr, J.A., Kumler, P.L. *Macromolecules* **1993**, *26*, 3778-3783.

(18)   Mallon, P. E., Greyling, C.J., Vosloo, W., Jean, Y.C. *Radiat. Phys. Chem.* **2003**, *68*, 453-456.

(19)   Zhu, Y., Otsubo, M., Honda, C. *Polym. Test.* **2006**, *25*, 313-317.

(20)   Jean, Y. C., Mallon P.E., Zhang R., Chen, H., Wu, Y., Li, Y., Zhang, J. *Chapter 11: Applications of slow positrons to polymeric surfaces and coatings.* In: Jean, Y. C., Mallon, P.E., Schrader, D.M. editors, *Principles and applications of postronium and positronium chemistry*; Singapore: World Scientific Publishing, **2003**.

(21)   Cao, H., Zhang, R., Yuan, J.P., Huang, C.M., Jean, Y.C., Suzuki, R., Ohdaira, T., Nielsen, B. *J. Phys.: Condens. Matter* **1998**, *10*, 10429.

(22)   Cao, H., Zhang, R., Sundar, C.S., Yuan, J.P., He, Y., Sandreczki, T.C., Jean, Y.C. *Macromolecules* **1998**, *31*, 6627-6635.

(23)   Cao, H., Zhang, R., Sundar, S.C., Yuan, J.P., He, Y., Sandreczki, T.C., Jean, Y.C. *Macromolecules* **1998**, *31*, 6627.

(24)   Hillborg, H., Gedde, U.W. *Polymer* **1998**, *39*, 1991-1998.

(25)   Maric, M., Macosko, C.W.,. *J. Polym. Sci. Part B: Polym. Phys.* **2002**, *40*, 346-357.

(26)   Chu, J. H., Rangarajan, P., Adams, J.L., Register, R.A. *Polymer* **1995**, *36,* 1569-1575.

Chapter 5

Conclusions and recommendations

This chapter provides a brief summary of the conclusions of this research study. It also includes a brief section on recommendations for future work.

5.1   Conclusions

The summarised conclusions of this research endeavour are as follows:

❖ The synthesis of PDMS-b-PS block copolymers via three different techniques was successfully evaluated.

- The coupling of functionalised prepolymers technique, proved to yield poor block copolymer formation with the product consisting mainly of the constituent homopolymers.

- The sequential anionic polymerisation technique was successful in synthesising block copolymers of controlled structure, with a small amount of homo-PS due to chains that did not initiate ring opening of the D_3 monomer.

- The macroinitiated ATRP technique was successful in synthesising block copolymers of controlled structure, with a small amount of homo-PDMS due to PDMS that was not bromoisobutyrate functionalised.

❖ Successful development of a LC-CC chromatographic system at the critical point of PS was achieved, allowing CCD analysis of the block copolymer products

❖ Successful development of a GEC profile, allowed the monitoring of PDMS homopolymer, before and after extraction.

❖ Successful surface segregation and corona modification allowed characterisation of the ultra-thin $(Si-O)_x$ glassy layer using optical and scanning electron microscopy combined with the depth profiling capabilities of the slow positron beam technique.

❖ This study shows the first evidence for the formation of a silica like (SiOx) layer in PDMS containing hybrid materials, the thickness of which was determinable using the slow positron beam technique.

❖ This study also shows the first evidence for hydrophobic loss and recovery for PDMS based hybrid materials after corona treatment. The surface degradation was however shown by the positron studies to be permanent.

❖ Studying this surface degradation mechanism using the developed LC-CC technique coupled to FT-IR proved difficult due to the small concentration of degradation products. Further FT-IR analysis included ATR analysis of the treated thin films and confocal raman spectroscopy to study the outer surface layer. These results showed small but definite changes in the IR absorption bands.

❖ The development of a novel coupled technique, namely, LC-CC coupled to TEM allowed successful analysis of the morphological features of the block copolymers. This technique avoids difficult homo-polymer extraction and sample preparation (cryomicrotoming). Due to the chromatographic separation step, morphological

analysis can be performed as a function of the molecular weight of the PDMS block segments within a specific sample. This has never been possible before without difficult solvent extraction procedures.

5.2 Recommendations

More attention needs to be paid to the studying of the degradation mechanism after corona treatment. From the positron data it is clear that this is a true surface phenomenon making analysis difficult due to the small concentrations of possible degradation species compared to that of the bulk material. LC-CC coupled to FT-IR would prove invaluable in this endeavour, as the chemical compositional changes and possible shifts in molecular weights would be able to be studied. This could provide comprehensive information on the degradation mechanism. A possible way to increase the amount of degraded surface material to the bulk is to increase the surface area. This could be achieved by spinning nano-fibres of the polymer material and corona treating these new surfaces. This exponential increase in the surface area may allow an increase in the concentration of degradation products and allow the before mentioned characterisation.

Also, further studies of corona treated polymer films using confocal Raman spectroscopy, could allow characterisation of this surface degradation effect. The ability of this technique to depth profile from the very surface of sample specimens makes it ideal to study this surface specific degradation. Due to time and travel constraints, this technique could not be applied to its full potential in this project, however, as a future project this technique could yield comprehensive information.

Further applications of the new TEM coupled to chromatographic separation technique to different samples may yield interesting results. For example, the studying of block copolymers synthesised using uncontrolled methods. This non uniformity in chain segmental length, may lead to drastic changes in the morphology moving from the high molecular weight to the low molecular weight side. A direct comparison study of TEM samples prepared by chromatographic coupling to samples prepared in the conventional bulk material way, may also provide interesting data. Analysis of multiblock and star copolymers may also provide interesting results, as this technique could allow chromatographic separation of stars with different numbers of arms, molecules that can prove otherwise difficult to separate in bulk.
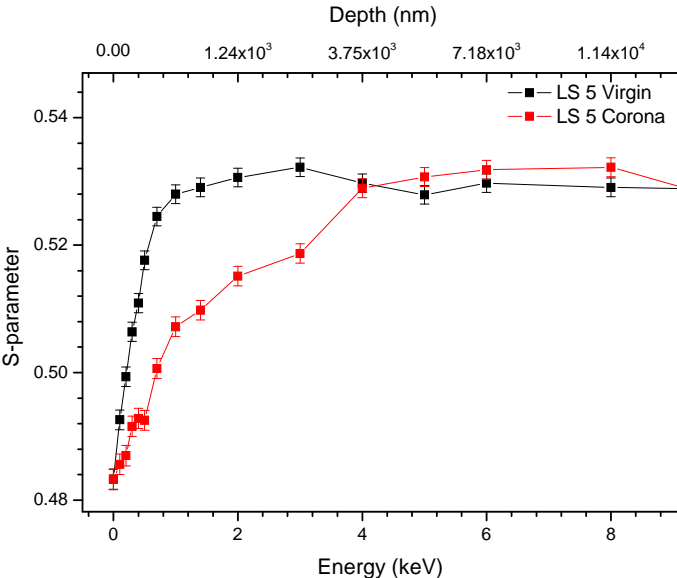
Appendix A   Slow positron beam overlays

Figure A.1   A typical S-parameter overlay of virgin and corona treated (LS5) block copolymer films.
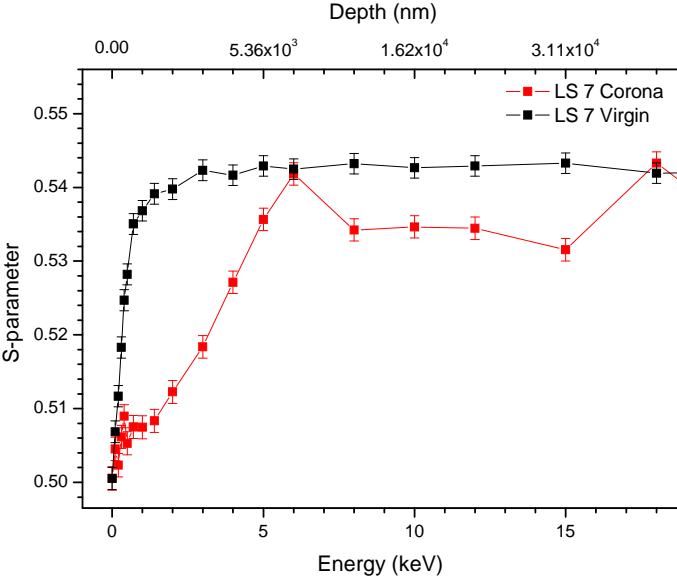

Figure A.2   A typical S-parameter overlay of virgin and corona treated (LS7) block copolymer films.
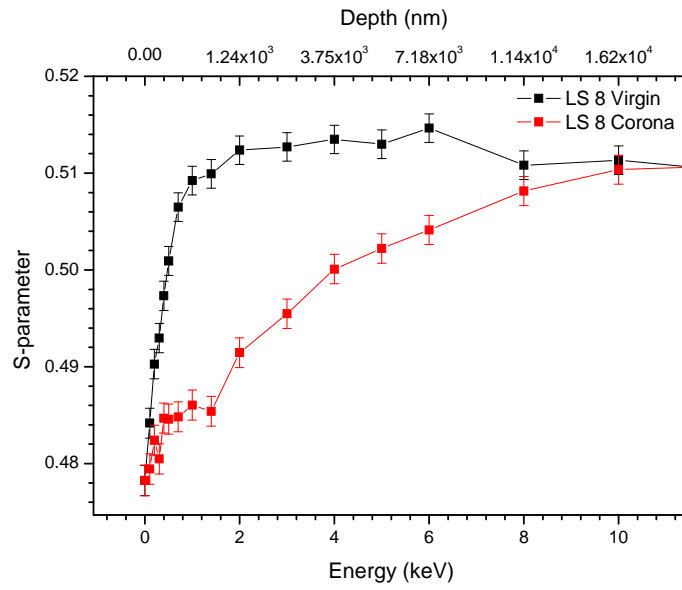
Figure A.3   A typical S-parameter overlay of virgin and corona treated (LS8) block copolymer films.
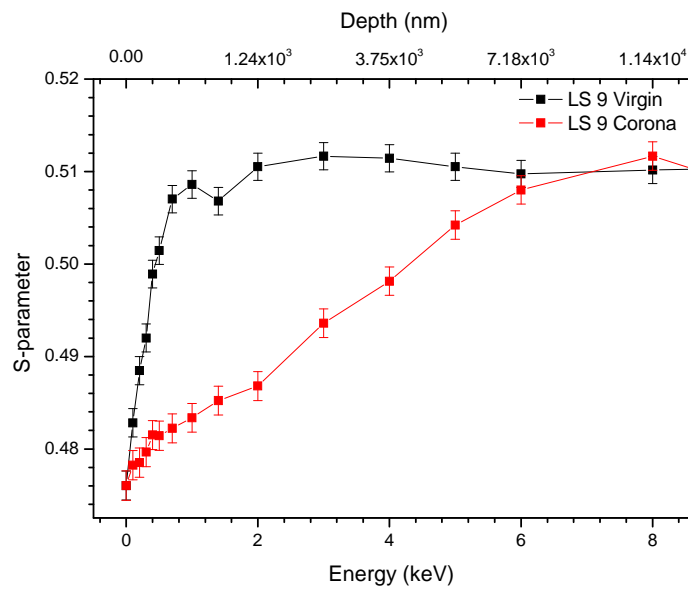

Figure A.4   A typical S-parameter overlay of virgin and corona treated (LS9) block copolymer films.